UNIVERSITY OF CALIFORNIA
RIVERSIDE

Molecular Characterization of a Novel Class of Viral DNA Binding Proteins

A Dissertation submitted in partial satisfaction
of the requirements for the degree of

Doctor of Philosophy

in

Cell, Molecular, and Developmental Biology

by

Tatsinda Verity Spears

August 2010

Dissertation Committee:
Dr. Brian A. Federici, Chairperson
Dr. Ayala L. N. Rao
Dr. Eugene Nothnagel

The Dissertation of Tatsinda Verity Spears is approved:

_____

_____

_____
Committee Chairperson

University of California, Riverside

ACKNOWLEDGEMENTS

I am grateful to my major professor, Dr. Brian A. Federici, for allowing me to be a member of his laboratory and encouraging me in the various works presented in this dissertation. Dr. Federici took a chance and offered me a great opportunity that many have never even imagined, so I have much to be thankful for. He has the kind of intelligence that I wish to emulate; it is not simply focused on his area of expertise. Dr. Federici embraces inquiry and the pursuit of knowledge of many types and it is this quality that I want to acknowledge, adopt, and spread to others.

I also thank Dr. Ayala Rao and Dr. Eugene Nothnagel for agreeing to be a part of my dissertation committee and offering the needed advice and critique of this work.

I appreciate all the members of the Federici lab who have offered their expertise, critique and friendship. Mujin Tang, Yeping Tan, Dennis Bideshi, Jeff Johnson, Mercedes Diaz-Mendoza - Thank you all so much.

Chapter 2 of this dissertation is a reprint of the material as it appears in a Journal of Virology article:

Y. Tan, T. Spears, D. Bideshi, J. Johnson, R. Hice, Y. Bigot, and B. A. Federici (2009). P64, a Novel Major Virion DNA-Binding Protein Potentially Involved in Condensing the *Spodoptera frugiperda Ascovirus* 1a Genome. J. Virol. **83:**2708-2714. DOI:10.1128/JVI.01610-08

The co-authors Y. Tan, T. Spears, and D. Bideshi were listed as equal contributors because of the experiments and ideas they performed and contributed to this publication. B. A. Federici supervised the research. J. Johnson, R. Hice, and Y. Bigot provided their

technical expertise with electron microscopy, experimental design, and bioinformatics. This research was supported in part by grant INT-9726818 from the U.S. National Science Foundation to B.A.F. and grants to Y.B. from NATO and CNRS (PICS Nu 3434), France.

The research described in Chapter 2 was supported in part by grant INT-9726818 from the U.S. National Science Foundation to B.A.F. and grants to Y. B. from NATO and CNRS (PICS Nu 3434), France. Thanks also to Dr. Ayala L. Rao, Professor of Plant Pathology and Microbiology at the University of California, Riverside, for the use of his grid discharger to prepare formvar grids for loading and analysis of samples.

DEDICATION

I am deeply grateful to my parents Gary B. and Katherine K. Spears. Without their sacrifices for my sister Charissa and myself and their commitment to their principles I would not have become the person that I am. From them I have learned a most valuable lesson, how to stay committed for the long haul, for a greater good, even when it is uncomfortable sometimes.

ABSTRACT OF THE DISSERTATION

Molecular Characterization of a Novel Class of
Viral DNA Binding Proteins

by

Tatsinda Verity Spears

Doctor of Philosophy, Graduate Program in Cell, Molecular, and Developmental Biology
University of California, Riverside, August 2010
Dr. Brian A. Federici, Chairperson

Ascovirus infection of lepidopteran larvae leads to an accumulation of virion-containing vesicles in the hemolymph turning it opaque white. The unusual feature of the formation of virion-filled vesicles by these large, complex, double-stranded DNA viruses results from a process similar to apoptosis, but one modified to rescue the developing apoptotic bodies for viral reproduction and virion dissemination. Another unusual feature of these viruses is their dependence on transmission by endoparasitic wasps that deposit their eggs in a lepidopteran host. Four species of ascoviruses have been sequenced and reveal a range of genes involved in apoptosis, RNA metabolism, and lipid metabolism. In the present dissertation, the research focuses on characterization of a novel type of DNA binding protein, P64 along with its homologs, responsible for condensing viral genomic DNA as part of the process of virion assembly.

Proteomic, electron microscopic, and biochemical studies demonstrated that P64 is a major virion protein which bound to and condensed DNA prior to virion core formation and envelopment. Mobility shift assays, bioinformatics, and additional electron microscopy data provided strong evidence that P64 and its homologs constitute a novel family of DNA condensing proteins. The combination of P64's highly basic nature, its large size relative to known viral/eukaryotic genome condensing proteins, its non-specific DNA binding activity, and the presence of two distinct and unique domains suggest that these proteins evolved in certain complex DNA viruses to condense and assist the packaging of newly synthesized viral genomes as part of the assembly of progeny virions. Preliminary data suggest that P64 might associate with other virion structural proteins once it has bound to condensed DNA.

Finally, phylogenetic analyses and results of binding studies showed that P64 is related to DNA binding proteins from viruses of the closely related *Iridoviridae* family, which provided additional evidence that the ascoviruses evolved from iridoviruses.

TABLE OF CONTENTS

Chapter 2: P64 a Novel Major Virion DNA-Binding Protein Potentially Involved in Condensing the *Spodoptera frugiperda ascovirus 1a* Genome

Chapter 3: The Ascovirus Basic Virion Protein P64 and its Homologs Comprise a Novel Family of Viral Genome Condensing Proteins

Chapter 5: Summary and Conclusions

LIST OF FIGURES

Chapter 1

Chapter 2

Chapter 3

Chapter 4

LIST OF TABLES

CHAPTER 1

Introduction to Ascoviruses

1.1 The general biology of viruses.

Viruses are obligate intracellular parasites, with the most obvious physical form being the virion, the principle infectious form. At a minimum, the virion differs from other life forms in that it consists of either RNA or DNA, never both, contained within a protein core. The virion in simple viruses consists of nucleic acid and a protein coat, the capsid, whereas in more complex viruses, one or two lipid/protein envelopes can be components of the virion.

The etymology of the term “virus” is ascribed to the Latin term for “poison, slimy liquid” (Guralnik and Friend, 1962). Viruses depend on and effectively hijack a host’s cellular machinery to be able to replicate and spread to infect other cells; they have no metabolic pathways of their own from which to derive energy or to create the basic building blocks of life (Shors, 2009). On the other hand, cellular organisms can replicate independently of another organism because they do have the machinery necessary for this and other processes. This is the primary reason viruses are considered obligate intracellular parasites. For viral infection to be successful, viruses have to complete the following five steps: (1) cell binding, (2) cell penetration, (3) uncoating of genome within the host cell, (4) replication of mature virion particles, and (5) release of mature virions (Shors, 2009). The diversity of viruses, their hosts, their gross and cytopathologies, and the mechanisms by which they spread demonstrate that viruses employ different

strategies to accomplish each of the five steps. These strategies are driven largely by genes encoded by genomes classified as single- or double-stranded DNA or RNA (Shors, 2009).

In this dissertation, my research focused on ascoviruses (family *Ascoviridae*), a small family of enveloped, double-stranded DNA (dsDNA) viruses of particular interest because they are so unique compared to other large, enveloped dsDNA viruses. In this chapter, I review the literature on ascoviruses (AVs) and close with a statement of my research objectives.

Virus-like particles with morphology similar to ascoviruses had been noted in several species of caterpillars in the late 1970's but it was not until the early 1980's (Federici, 1983) that the first species of ascoviruses were described in detail, providing the basis for the formation of a new family of viruses. Since that time several species and variants from around the world have been ascribed to the family *Ascoviridae.* This family of dsDNA viruses had gone unnoticed because infection produced few gross signs of disease in noctuid larvae (caterpillars) upon cursory field observation. After their discovery, a range of subsequent studies of AVs and their pathobiology has revealed a wealth of novelties, e.g., the modification of apoptotic bodies creating an "anucleate" environment where virions assemble, a reliance on parasitoid wasps for transmission, the presence of virus-encoded lipid metabolizing enzymes in the genome and synthesis of novel DNA condensing proteins. Further analysis of these and other novel phenomena associated with AVs could contribute substantially to our understanding of cell and

molecular biology. Below, key knowledge developed about AVs since the recognition of this novel group of viruses as a new family is reviewed.

1.2 Species.

The family *Ascoviridae* was proposed to accommodate the dsDNA virus members whose cytopathology includes the formation of virion-filled sacs (Greek *askos* = sac, bladder) that accumulate in the hemolymph (Fig. 1.2) of lepidopteran larvae turning it from translucent green to opaque white. The names of the virus species are derived from the first host that each was found in. For example, the type species *Spodoptera frugiperda* AV-1a (SfAV1a) was found in *Spodoptera frugiperda* (fall army worm) in corn and cotton fields where the larvae feed. The numeral indicates the order in which each species was recognized and the lower case letter indicates the variant of that species and the order in which the variant was recognized (Federici *et al.*, 2008). Other recognized species include *Trichoplusia ni* AV-2c (TnAV2c), *Heliothis virescens* AV-3e (HvAV3e), and *Diadromus pulchellus* AV-4a (DpAV4a). Several AV variants of the previously described species have been found (Cheng *et al.*, 2005; Federici *et al.*, 1990). Analysis of the genomes of AVs has shown that each species consists of numerous variants. None of the AVs have been plaque-purified because of the difficulties encountered in obtaining progeny virions from cell culture. The definition of a viral species and variants varies among different types of viruses. Thus far, a combination of characteristics is used to distinguish AV species and variants from one another, including restriction fragment length polymorphisms, Southern blot hybridization, and the degree of gene homology for key genes such as the DNA polymerase and major capsid protein (MCP). Differences in

virion morphology, host range, and tissue tropism also help delineate AV species (Federici *et al*., 2008).

1.3 Structure.

AV virions share a similar complex symmetry, and are typically either bacilliform or elongated ovoid shape, such as in the SfAV1a (Fig. 1.3), or allantoid, with slightly tapered ends and a flattened side, as in the case of TnAV2a. Virion dimensions range from 300-400 nm in length by 130 nm in width. Electron micrographs show an electron dense interior (nucleoprotein core) surrounded by two envelopes (Fig. 1.4B). With the exception of DpAV4a, the outer membrane has a reticulate appearance (Fig. 1.4C and D) (Federici, 1990; Bigot *et al*., 1997b) that may be due to a regular arrangement of protein complexes like the oligomeric structures in the capsid of herpes simplex virus-1 or the brome mosaic virus (Plomp *et al*., 2002; Kuznetsov *et al*., 2004). The reticulate pattern could instead be a result of the superimposition of the outer envelope over the protruding structures seen on the internal envelope immediately surrounding the core (Fig. 1.4D) (Federici *et al*., 1990). To date, the genomes of at least one isolate of each recognized AV species has been sequenced (Fig. 1.1). The genomes of AVs are large and circular (Cheng *et al*., 1999), ranging from 119 kbp (DpAV4a) to 186 kbp (HvAV3a) and have from 119 to over 200 open reading frames (Asgari *et al*., 2007; Bigot *et al*., 2009; Bideshi *et al*., 2006; Cheng *et al*., 2000; Wang *et al*., 2006). Bigot *et al.* (2005) found that the DpAV4a genome was highly methylated with up to 76% of cytosines being modified depending on which stage and host the virus was in during an infection cycle. SDS-PAGE of purified AV virions reveals that they have well over 14 structural proteins (Federici *et al*, 1990;

Cheng *et al*., 2000; Tan *et al*., 2009). The more sensitive silver-nitrate staining method applied to SfAV1a virions shows even more proteins.

1.4 Transmission and prevalence.

To further study AV infection, attempts were made to infect larvae by feeding them virion-containing vesicles or purified virions. This approach yielded inconsistent and often low rates of infection (Federici, 1983; Hamm *et al*., 1986). By contrast, inoculation of virions using virion-laced fine pins proved more successful with infection rates often at 100% in a permissive species (Hamm *et al*., 1986). This provided a clue as to how the virus might be transmitted in the field. The prevalence of AV infection in larvae populations was at times found to be 25% but usually less than 10% depending on the time of year (Cheng *et al*., 2005; Hamm *et al*., 1986). Field observations of the prevalence of AV infection in noctuid populations correlated well with the presence of endoparasitic wasps of the families *Braconidae* and *Ichneumonidae* (both of the order Hymenoptera) in a given area providing another clue as to how the virus was transmitted (Hamm *et al*., 1985). Laboratory studies confirmed that female endoparasitic wasps can serve as vectors by acquiring virions or vesicles from an infected noctuid host in which they had laid eggs and transferring virions to the next host (Tillman *et al.*, 2004). Thus, evidence from laboratory and field studies suggests that AVs have a unique dependence on parasitoid wasps for their transmission, without which the infection of lepidopteran hosts would be a dead end (Hamm *et al*., 1985). After infection of a host, most AV species cause the death of the noctuid host as well as that of the parasitoid eggs and larvae (Federici *et al*., 1991). DpAV4a infection of host larvae on the other hand, results

in successful development of the larvae of the parasitoid wasp *D. pulchellus* (Stasiak *et al*., 2005). This beneficial relationship between the parasitoid wasp and DpAV4a is an example of symbiosis.

DpAV4a differs from the AVs isolated from noctuid hosts in that it is vertically transmitted by its wasp host, but still contributes to the understanding of AV transmission via a unique mechanism. More specifically, DpAV4a is the only AV that replicates in the tissues of both the endoparasitoid wasp *Diadromus pulchellus,* and their lepidopteran host, the pupa of the leek-moth *Acrolepiopsis assectella* (order Lepidoptera, family Yponomeutidea; Bigot *et al*., 1997a, b). The DpAV4a genome occurs in the nuclei of both male and female wasps in various tissues, with the highest concentration being in the female abdomen. Within the nuclei, the DpAV4a genome exists as non integrated circle. This finding and the observation of DpAV4a virions in wasp tissues indicated that this virus is able to replicate within the wasp. It has been shown that DpAV4a suppresses the immune system of the lepidopteran larvae enabling *D. pulchellus* eggs to hatch and the wasp to survive into adulthood (Bigot *et al*., 1997a; Renault *et al*., 2002). Thus, DpAV4a is the only known AV species that is beneficial for its wasp vector.

The families Noctuidae, Braconidae and Ichneumonidae are some of the largest insect families, with each consisting of tens of thousands of species. Members of these families are found worldwide. Considering the prevalence and distribution of their hosts and vectors, it is plausible that AVs can also be found worldwide. Indeed, AVs have been identified on the East and West coasts of the U.S., in France, Indonesia and Australia (Federici *et al*., 2008). Their likely prevalence has gone unnoticed for so long because

signs of disease are not obvious in the field. One question then is how these various AVs are able to persist when it appears that they (SfAV1a, TnAV2c, and HvAV3e) lead to the death of both the noctuid host and the parasitoid wasp larvae. Two cases have been observed where HvAV3e infection of non-noctuids did not prevent parasitoid survival (Furlong *et al*., 2010; Smede *et al*., 2008). This suggests that AVs are likely to have a wider host range in nature and therefore a higher prevalence than what is currently recognized. Infection in alternative hosts could be less severe and allow parasitoid wasps to develop successfully in non-noctuid species. As long as AVs have a viable vector and semi permissive host, they can persist in nature.

1.5 Host range and tissue tropism.

The rate or extent of AV infection in host tissues is determined by the viral genome, the composition of the calyx fluid from the parasitoid wasp, and the genetic background of the lepidopteran host (Bigot *et al*., 1997a; Stasiak *et al*., 2005; Furlong *et al*., 2010). Of all AVs, SfAV1a is the most restricted in its host range and tissue tropism. SfAV1a is limited to replicating in larvae of the lepidopteran genus *Spodoptera*. Within these larvae, SfAV1a replicates more readily in the fat body (Federici and Govindarajan, 1990), a tissue comparable to the vertebrate liver, which is responsible for nutrient absorption, storage, and metabolism, as well as functions such as detoxification of plant secondary defensive compounds. Few if any SfAV1a virions can be detected in other tissues (Federici and Govindarajan, 1990). TnAV2c and HvAV3e have a more diverse host range infecting of the genera *Spodoptera, Scotogramma, Heliothis, Autographa Feltia, Helicoverpa* (order: Lepidoptera, family: *Noctuidae*) and possibly others

(Federici, 1982; Federici, 1983; Hamm *et al*., 1998). TnAV2c and HvAV3e can also replicate in fat body (HvAV3e more so than TnAV2c) as well as the epidermis, tracheal matrix, and epithelium around the testis and midgut of larvae (Carner and Hudson 1983; Federici, 1982; Hamm *et al*., 1998). Certain tissues including nerves, hemocytes, and heart muscles did not appear to be infected in different hosts infected with a variety of AVs (Hamm *et al*., 1998).

DpAV4a and its relationship to its hosts again present an interesting variation from the other AV species. Molecular analysis of DpAV4a open reading frames supports DpAV4a's uniqueness compared to other AVs, and provides a basis for considering DpAV4a as part of a subfamily separate from SfAV1a, TnAV2c, and HvAV3e(Bigot *et al*., 2009; Stasiak *et al*., 2005). DpAV4a not only replicates in species from the order Lepidoptera but also in species from the order Hymenoptera (wasps, *Diadromus* spp., *Eupelmus orientalis* and *Itoplectis tunetana*) and at different rates (Bigot *et al*., 1997a; Stasiak *et al*., 2005). DpAV4a genomic DNA has been detected in the head, thorax, and abdomen of both sexes of the wasp *D. pulchellus* and does not appear to have any adverse affects on the adult wasp (Bigot *et al*., 1997b; Renault *et al*., 2002). DpAV4a can be vertically transmitted from adult wasps to their progeny. DpAV4a virions are produced in the calyx cells in the genital tract of the female wasp and are inserted with the eggs when a female wasp oviposits into *A. assectella*. Most of the tissues of *A. assectella* pupa (hosts for the wasp *D. pulchellus*) become infected and lyse within four days (Bigot *et al*., 1997a).

1.6 Gross pathology.

The life-cycle of noctuid species begins with the laying of eggs by the adult female moth. Three to four days are spent in the egg stage. The larval stage—lasting approximately 14 days—follows, during which time the larva develops through five or more instars. When larval development is complete, the larvae pupate, and then emerge as adults about a week later (Wiseman, 1999; Pennacchio, 2006). Whereas noctuid larvae progress through the larval stage to the pupal stage in a matter of ten days to two weeks, AV infected larvae exhibit developmental defects giving rise to the chronic nature of the disease (Govindarajan and Federici, 1990; Cheng *et al*., 2000). Infected larvae are usually unable to molt, thereby halting development, leaving them unable to progress to the next instar. In the event that infected individuals reach the pupal stage, most are unable to survive to adulthood (Cheng *et al*., 2000; Hamm *et al*., 1986). Infected larvae usually remain in the larval stage one to three weeks longer than healthy noctuid larvae (Cheng *et al.*, 2000; Federici, 1983; Govindarajan and Federici, 1990). During this time, diseased larvae cease feeding and become lethargic (Federici, 1982; Federici, 1983). Field observation of infected larvae has shown that infected larvae tend to be found towards the top part of plants exposing them to easy parasitization by wasps (Cheng *et al*., 2005). In permissive infections, AV infected larvae can exhibit slight to moderate discoloration which results from the accumulation of AV virion-containing vesicles in the once translucent hemolymph, giving it the milky appearance, the signature of AV infection (Federici *et al*., 1983). In addition to inducing virion vesicle formation, DpAV4a particles block the host's immune response by preventing hemocyte-

encapsulation by the host that would otherwise lead to the destruction of wasp eggs (Renault *et al*., 2002).

1.7 Cytopathology.

Although AVs vary in their host and tissue specificity, disease progression at the cellular level appears to progress in a similar manner. Initial observations of the cytopathic effects of TnAV2c in *Trichoplusia ni* larvae were later corroborated by studies of additional isolates found in other hosts (Federici, 1983; Bigot *et al*., 1997a; Hamm *et al*., 1998; Cheng *et al*., 2000). Furthermore, AVs encode a repertoire of DNA metabolizing genes that allow them to replicate without an intact nucleus while other AV genes/proteins result in the cytopathological effects that are peculiar to AVs (Asgari *et al*., 2007; Bideshi *et al*., 2006, Bigot *et al*., 2009; Wang *et al*., 2006). Four stages of infection at the cellular level have been described: (1) nuclear hypertrophy and invagination of the nuclear envelope, (2) cellular hypertrophy to five times the normal size accompanied by nuclear enlargement and disintegration (Fig. 1.3), (3) virion assembly and the appearance of vesicles containing virions (Fig. 1.4), and (4) vesiculation of enlarged cells (Asgari, 2006; Smede *et al*., 2008) or complete division of the cell into virion-containing vesicles (Fig. 1.3) that are 4-10 µm (Carner and Hudson, 1983; Federici, 1983). During the first stage, while the nuclei become enlarged, condensed fragmented chromatin can be detected (Federici, 1983, Hamm *et al*., 1998). Apoptotic cells also exhibit chromatin condensation, but unlike AV infection, this is usually accompanied by cellular shrinkage and phagocytosis of apoptotic bodies (Fadok, 1995; Bortner and Cidlowski, 2002). During AV infection, once the nucleus is disrupted,

virions begin to appear as the plasma membrane invaginates to form vesicles. Plasma membrane blebbing and invagination is likely due to AV manipulation of actin filament activity at the cell cortex (Hussain *et al*. 2009). It also appears that *de novo* synthesis of membranes occurs in the interior of the infected cell; those membranes probably coalesce to complete the division of an infected cell into vesicles (Federici, 1982; Federici, 1983). It is not clear whether the mechanism for creating the new lipid membranes for vesicles is related to the synthesis of the viral envelope (Federici, 1982). An interesting characteristic of AV cytopathology is that mitochondria line up along the cell membrane invaginations (Federici, 1983). More vesicles accumulate in the infected tissues until the basement membrane ruptures, after which they dissociate and accumulate in the hemolymph to a concentration of 10^7-10^8/ml (Federici, 1982; Federici and Govindarajan, 1990). In vitro analysis of infected cell cultures has also shown that AVs are capable of budding (Asgari, 2006).

The virion-containing vesicles appear to have different phases of maturation. Newly formed vesicles will have what appear to be intact mitochondria. The role of mitochondria is not understood at this point but they may be maintained for some period (Cheng *et al*., 2005) perhaps to provide energy for DNA packaging, envelope formation and envelopment of the AV core (Fig. 1.6). The more mature vesicles appear to be more densely packed with mature virions and appear to have structural differences based on the AV they were induced by. In TnAV2c vesicles, virions are along the cortex of the vesicle with a stroma-like structure in the center from which immature virus particles are released (Federici, 1983). Vesicles may have virions clustered towards the center or

towards the periphery (Federici *et al.*, 1990; Hamm *et al.*, 1998). During SfAV1a maturation (Fig 1.4B), clusters of small, empty, vesiculate bodies develop adjacent to occluded virions (Federici *et al.*, 1990; Federici *et al.*, 2008). Both TnAV2c and DpAV4a produce vesicles with large empty vacuoles (Bigot *et al.*, 1997a; Cheng *et al.*, 2000; Federici *et al.*, 1990). Filament structures of unknown function are present alongside maturing virus particles in DpAV4a induced vesicles (Bigot *et al.*, 1997a).

The AV cytopathological process is unique in several respects. First, it appears that AVs modify apoptosis so that developing apoptotic bodies sufficiently resilient to resist phagocytosis, and subsequently function as virion maturation containers that can be disseminated with the aid of endoparasitic wasps (Carner and Hudson, 1983; Hamm, 1985). Indeed, virion-containing vesicles have been shown to be resistant to osmotic lysis when placed in distilled water for 15 minutes indicating significant membrane modification towards rigidness (Federici, 1982). The second unique feature of AV pathobiology is its dependence on the parasitic relationship between endoparasitic wasps and lepidopteran larvae for dissemination. Without the wasp, AV infection results in a dead end. Larvae having external contact with or feeding on infected individuals would not be enough to maintain AV in a population of noctuids (Carner and Hudson, 1983; Federici, 1983; Hamm, 1985). DpAV4a is an exception because it can be transmitted vertically from the adult wasps to their eggs (Bigot *et al.*, 1997a; 1997b). Thirdly, AVs' collection of genes associated with apoptosis and lipid metabolism provide an interesting molecular basis for the unique cytopathology described above (Bideshi *et al.*, 2006; Bigot *et al.*, 2009).

1.8 Apoptosis - convergence and divergence with this process.

Viral invasion often triggers a death response from hosts in order to minimize the amplification and spread of the virus. Nonetheless, viruses are able to employ various mechanisms to counter the apoptotic responses of their hosts. Examples of viral proteins which modulate some aspect of the apoptotic pathway include, γ-herpes virus FLICE inhibitory proteins that block caspase activity, poxvirus E3 proteins which down-regulate receptors with death domains, and adenovirus E1B-19K, which blocks mitochondrial pore formation (Shen and Shenk, 1995; Benedict *et al.*, 2002). Some viruses will ultimately allow or even induce apoptosis to enhance virion dissemination (Shen and Shenk, 1995; Kaplan and Sieg, 1998). Examples of viral cytopathologies involving apoptosis include adenovirus infection, vesicular stomatitis virus infection, HIV infection, and red sea bream iridovirus infection (Shen and Shenk, 1995; Koyama, 1995; Kaplan and Sieg, 1999; Imajoh *et al.*, 2004). While AVs may not be unique with regard to the induction of apoptosis (Fig. 1.5 and 1.6), certain novel aspects of AV pathology are apparent. Specifically, no other viruses are known to encode a caspase. The link between the AV caspase, viral vesicle formation, and viral dissemination suggests that the host's intrinsic, apoptotic, self-defense mechanism fails to prevent viral amplification. On the contrary, the apoptotic program enhances virogenesis. AV caspases are likely to participate in complex, coordinated interactions with other viral and host proteins in a modified form of apoptosis giving rise to the viral vesicles.

1.9 Bioinformatics and the molecular basis for disease.

1.9.1 Caspase genes. In vitro RNA interference analysis of several AV genes has shown that they are essential for AV cytopathology and replication. AV genomes encode a caspase. Caspases are cysteinyl aspartate-specific proteases activated upon proteolysis that cleave specific protein targets. These enzymes are crucial mediators of apoptosis, cell proliferation in T-cells, and cell differentiation macrophages (Schwerk and Schulze-Osthoff, 2003). Knockdown of SfAV1a caspase and HvAV3e caspase during their respective infections in cell cultures prevented cell blebbing and the formation of apoptotic bodies (Bideshi *et al*., 2005; Asgari, 2007). SfAV1a caspase expression in cell culture induced the hallmark events of DNA fragmentation and apoptotic body formation (Bideshi *et al*., 2005); however, HvAV3e caspase expression in cell culture did not lead to cell blebbing or fragmentation although it was still essential for virus replication (Asgari, 2007). The HvAV3e caspase appears to be non-canonical in two ways: it lacks the cysteine residue that is typically a part of the caspase enzyme active site and it lacks the aspartate residue where the immature procaspases are cleaved to become active caspase (Asgari, 2007). These studies suggest that AV caspases act in traditional and nontraditional ways, and both ways contribute to successful AV infection. It is possible that the HvAV3e caspase could still be functional and target downstream effectors of apoptosis that are derived from the AV rather than the host so you would not see an effect with the expression HvAV3e caspase alone, but in the presence of AV gene products. Lack of a proteolytic processing site in HvAV3e caspase would not preclude it from having cleavage activity. Others have noted that some procaspases have a low level of

cleavage activity when in close proximity to other procaspases and are thought to be responsible for initial activation/formation of mature caspases (Chang and Yang, 2000; Fuentes-Prior and Salvesen, 2004).

1.9.2 Additional genes associated with apoptosis. A putative cathepsin B (SfAV1a ORF114) and several putative inhibitor of apoptosis (IAP) gene sequences were also found among the AVs (SfAV1a ORF25 and ORF74, DpAV4a ORF7) (Asgari *et al*., 2007; Bideshi *et al*., 2006, Bigot *et al*., 2009; Wang *et al*., 2006). Cathepsin B is a protease with a cysteine in its catalytic site and is normally localized within lysosomes. Cathepsin B is known to play a role in immunity and apoptosis (Linder and Shoshan, 2005; Reinheckel *et al*., 2001). Apoptotic signaling can lead to the release of cathepsin B into the cytosol where it can cleave the mitochondrial-pore-forming protein Bid which localizes and oligomerizes in the outer mitochondrial membrane to make pores. Pore formation causes the loss of mitochondrial membrane integrity and results in cytochrome c release and further apoptotic signaling events (Stoka *et al*., 2007). IAPs have been shown to block various aspects of the apoptotic signaling cascade. Some IAPs bind caspases directly, thereby preventing other substrates from accessing the catalytic cleavage site. Other IAPs are able to prevent the recruitment and activation of initiator caspases to certain death-domain-containing receptors (Deveraux and Reed, 1999). Hussain and Asgari (2008) showed that in vitro expression of one of the IAP-like proteins from HvAV3e (ORF28) was not sufficient to block Actinomycin D-induced apoptosis but it was necessary for the progression of HvAV3e cytopathology and virus replication in cell culture. The presence of putative apoptotic promoting and suppressing genes in

AV genomes suggests that AVs actively encourage and control the apoptotic process (Fig 1.5 and 1.6) to produce highly modified apoptotic bodies that can be used for virion storage and transport.

1.9.3 Genes associated with lipid metabolism. AVs encode lipid metabolizing enzymes that may participate in their unique cytopathology. These include a fatty acid elongase and a phosphate acyltransferase (SfAV1a ORF87 and ORF112, respectively), both of which are found in all four AV species (Asgari *et al*., 2007; Bideshi *et al*., 2006, Bigot *et al*., 2009; Wang *et al*., 2006). SfAV1a and HvAV3e also encode a putative esterase lipase (SfAV1a ORF13) and a patatin-like phospholipase (SfAV1a ORF93). The esterase lipase-like gene in HvAV3e (ORF19) was shown to be essential for the progression of AV cytopathology and viral replication, even though it did not appear to have lipase or esterase activity (Smede *et al*, 2009). The enlargement of infected cells and their subsequent cleavage into virion vesicles requires new lipid membranes to be synthesized for the new surface area being created. Indeed, electron microscopy has shown that small, membrane-lined, empty vesicles form and coalesce along planes within infected cells (Federici 1983; Federici *et al*., 2008) suggesting that this is a mechanism for joining plasma membrane invaginations across the cytoplasm to form cleavage planes for making virion vesicles. Apparently, AVs have acquired and adapted these various lipid-processing enzymes to aid their development and transmission.

1.9.4 Additional ORFs of importance. RNase III-like sequences have also been found among the various species of AV (Bigot *et al*., 2009). RNase III enzymes are known to participate in mRNA, rRNA, and tRNA maturation. These enzymes are also

crucial to the short interfering- and microRNA mediated gene silencing pathways (Conrad and Rauhut, 2002; Hussain *et al*., 2010). The RNase-like ORF27 of HvAV3e was shown to have catalytic activity against dsRNA and be able to regulate its own expression by cleaving its own transcripts. In addition, RNAi against this gene during infection inhibited replication (Hussain *et al*., 2010). Furthermore, examination of the DpAV4a and HvAV3e genomes revealed the presence microRNA encoding sequences (Bigot *et al*., 2009, Hussain *et al*., 2010). Work done on the HvAV3e derived microRNA against the major capsid protein along with the RNase III studies demonstrates the capability of AVs to regulate viral gene expression using RNAi mechanisms (Hussain *et al*., 2008; Hussain *et al*., 2010).

1.10 Phylogeny and Evolution.

Phylogenetic analysis of a number of AV genes from the different species provided evidence of an evolutionary relationship between AVs and iridoviruses (Stasiak *et al*., 2000; Stasiak *et al*., 2003), a relationship that was not obvious based on structural features of the virions. Members of family *Iridoviridae* are icosahedral in shape and can infect a wide range of hosts that include nematodes, fish, amphibians and insects. Five genera make up this family: *Ranavirus, Lymphocystivirus, Megalocytivirus, Iridovirus,* and *Chloriridovirus*. Here, the term iridovirus will be used to refer to the family and not the specific genera. Iridovirus virions accumulate in the cytoplasm, leaving the nucleus intact, and giving the infected organism an iridescent blue-green color. Iridoviruses often induce acute, lethal infections in their permissive hosts, which has given rise to concern in the fish farming industry. These viruses have also presented an opportunity for those

interested in developing biological pest controls (Jakob and Dara, 2002). In contrast, the AV host range is limited primarily to larvae of lepidopteran species in which they cause a chronic but fatal disease that involves in the production of virion-containing vesicles after the destruction of the nucleus.

Modes of transmission are also different for these two families of viruses. Iridoviruses have been known to transfer between wounded fish and between females and the eggs they lay, whereas AV transmission from host to host is dependent on an endoparasitic wasp vector (Stasiak *et al.*, 2003). Despite these differences, initial phylogenetic comparisons of four genes (δ DNA polymerase, major capsid protein, thymidine kinase and ATPase III) from the different AV species, vertebrate and invertebrate iridoviruses, phycodnaviruses (host: algae), an asfarvirus (host: swine) and others showed that AVs were most closely related to invertebrate iridoviruses (Stasiak *et al.*, 2000; Stasiak *et al.*, 2003). Phylogenetic comparisons also confirmed the delineation of AV species and various strains that had been previously based on observations of mode of transmission, host range, tissue tropism and Southern hybridizations. DpAV4a was always in a lineage separate from the others (Stasiak *et al.*, 2003). Recent genomic comparisons of DpAV4a with the other AVs and iridoviruses has revealed that DpAV4a has 63 genes in common with the *Chilo* iridescent virus (CIV) and only 40 to 42 genes in common with the other sequenced AVs. Comparison of SfAV1a, TnAV2c, HvAV3e, DpAV4a and two iridovirus genomes led to the conclusion that these viruses share 28 core genes (Bigot *et al.*, 2009). The difference in homologous gene numbers (63 homologs with CIV and 43 homologs with other AVs) suggests that DpAV4a is a part of

a separate subfamily of AVs or at the very least, of a different viral genus (Bigot *et al*., 2009). It is possible that an ancestor of DpAV4a was also a precursor that gave rise to the other different AV species.

An evolutionary pathway has been proposed to explain how AVs arose. Based on the sequences of the four genes mentioned above as well as others (Fig. 1.1), and the presence or absence of several "marker" genes in viral genomes, AVs appear to have evolved from the invertebrate lineage of iridoviruses. In turn, both vertebrate and invertebrate iridoviruses were derived from a phycodnavirus lineage that diverged from asfarviruses (Stasiak *et al*., 2003; Bigot *et al*., 2009). At the root of this lineage is an ancestor virus described as having an icosahedral capsid and linear genome (Stasiak *et al*., 2003). On the other hand, it is also possible that such comparisons lack validity because viruses tend to be polyphyletic. Some of these viral families could have arisen independently of other viruses and experienced convergent evolution due to similar selective pressures within the eukaryotic cellular system of the hosts. In the case of AVs, the number (28 ORFs) and extent of gene similarity with iridoviruses makes a strong case for AV evolution from iridoviruses (Bigot *et al*., 2009).

1.11 Virion structural proteins.

Analysis of AV virion structural proteins confirmed their uniqueness among large dsDNA viruses and in addition verified their close relationship to iridoviruses (Tan *et al*., 2009; Bigot *et al*., 2009). Twenty-one structural proteins ranging from 5 - 120 kDa from purified SfAV1a virions were identified by MALDI-TOF mass spectrometry (Tan *et al*., 2009). Alternatively, only seven proteins ranging from 45-180 kDa were identified in

TnAV2c virions using the same technique (Cui *et al*., 2007; Tan *et al*., 2009). Four of the latter proteins had homologs present in SfAV1a virions. Of the 21 structural proteins identified in SfAV1a, nine have no recognizable domain that would indicate a possible function for that protein, 11 have homologs in all AVs, and ten of these also occur in invertebrate iridoviruses (Tan *et al*., 2009; Bigot *et al*., 2009). The occurrence of similar virion structural proteins in these two taxa provides further support for the concept that AVs and iridoviruses arose from a common ancestor.

1.12 Virion protein P64 and dissertation objectives.

A crucial aspect of AV biology not understood is how their large genomes are condensed and packaged into the virion during assembly. Analysis of AV genomes has shown that small, basic histone-like and protamine-like proteins known to condense genomes of eukaryotes and many large dsDNA viruses are absent (Tan *et al*., 2009; Bigot *et al*., 2009). SDS-PAGE and mass spectrometric analyses revealed P64 (SfAV1a ORF48) to be the second most abundant structural protein after the major capsid protein (Tan *et al*., 2009). The abundance of P64 raised questions about its role and importance in virion assembly and structure. Electron microscopy of infected noctuid tissues demonstrated the general sequence in which the major structural components of the virion assembled, e.g., the dense nucleoprotein core, outer layer of the inner particle that surrounded the core, and envelope (Fig. 1.4). However, these studies did not identify the protein components involved at each step in the process. As noted above, many viruses contain small, DNA-condensing proteins but no such proteins were identified in AV virions (Tan *et al*., 2009). Thus, for my research, I decided to focus on the function of the

SfAV1a P64 protein in virion assembly and structure, and the phylogenetic relatedness of this protein to those in other AVs and related iridoviruses. The following were my specific objectives:

Objective 1: Determine the cellular location of P64 during SfAV1a replication and virion assembly.

Objective 2: Characterize the function of P64 and its two major domains.

Objective 3: Identify homologs of P64 in other AVs and iridoviruses and compare AV and iridovirus virion structural proteins that participate in DNA binding.

Objective 4: Identify the location of other structural proteins within the virion and determine which of these interact with P64.

My progress in accomplishing these objectives is reported in the following chapters. The next chapter, Chapter 2, reports the experiments and results of Objective 1 and 2 on the localization of P64 in infected tissues during SfAV1a infection and initial results on the identification of two domains of this protein and their functions. Chapter 3 reports experiments and results that significantly expand our understanding of the biochemical functions of P64 (Objective 2), and goes beyond this by identifying P64 homologs in other AVs as well as iridoviruses, the latter which make up a separate family (*Iridoviridae*) from which AVs evolved. Chapter 4 reports preliminary data the location of other structural proteins in the SfAV1a virion and virion-containing vesicles (Objective 4). In addition to these chapters, I have included Appendix A, which is a review paper on AV pathobiology and includes some of my unpublished results.

1.13 References

Asgari, S. 2006. Replication of *Heliothis virescens ascovirus* in insect cell lines. Arch. Virol. **151:**1689-1699.

Asgari, S., J. Davis, D. Wood, P. Wilson, and A. McGrath. 2007. Sequence and organization of the *Heliothis virescens ascovirus* genome. J. Gen. Virol. **88:**1120-1132.

Benedict, C. A., P. S. Norris, and C. F. Ware. 2002. To kill or be killed: viral evasion of apoptosis. Nat. Immunol. **3:**1013-1018.

Bideshi, D. K., M. V. Demattei, F. Rouleux-Bonnin, K. Stasiak, Y. Tan, S. Bigot, Y. Bigot, and B. A. Federici. 2006. Genomic sequence of *Spodoptera frugiperda ascovirus* 1a, an enveloped, double-stranded DNA insect virus that manipulates apoptosis for viral reproduction. J. Virol. **80:**11791-11805.

Bideshi, D. K., Y. Tan, Y. Bigot, and B. A. Federici. 2005. A viral caspase contributes to modified apoptosis for virus transmission. Genes Dev. **19:**1416-1421.

Bigot, Y., A. Rabouille, G. Doury, P. Y. Sizaret, F. Delbost, M. H. Hamelin, and G. Periquet. 1997. Biological and molecular features of the relationships between *Diadromus pulchellus ascovirus*, a parasitoid hymenopteran wasp (*Diadromus pulchellus*) and its lepidopteran host, *Acrolepiopsis assectella*. J. Gen. Virol. **78:**1149-1163.

Bigot, Y., A. Rabouille, P. Y. Sizaret, M. H. Hamelin, and G. Periquet. 1997. Particle and genomic characteristics of a new member of the Ascoviridae: *Diadromus pulchellus ascovirus*. J. Gen. Virol. **78:**1139-1147.

Bigot, Y., S. Renault, J. Nicolas, C. Moundras, M. V. Demattei, S. Samain, D. K. Bideshi, and B. A. Federici. 2009. Symbiotic virus at the evolutionary intersection of three types of large DNA viruses; iridoviruses, ascoviruses, and ichnoviruses. PLoS One. **4:**e6397.

Bortner, C. D., and J. A. Cidlowski. 2002. Apoptotic volume decrease and the incredible shrinking cell. Cell Death Differ. **9:**1307-1310.

Carner, G. R. and J. S. Hudson. 1983. Histopathology of virus-like particles in *Heliothis* spp. J. Invertebr. Pathol. **41:**238-249.

Chang, H. Y., Yang, X. 2000. Proteases for cell suicide: functions and regulation of caspases. Microb. Mol. Biol. Rev. **64:**821-846.

Cheng, X. W., G. R. Carner, and B. M. Arif. 2000. A new ascovirus from *Spodoptera exigua* and its relatedness to the isolate from *Spodoptera frugiperda*. J. Gen. Virol. **81:**3083-3092.

Cheng, X. W., G. R. Carner, and T. M. Brown. 1999. Circular configuration of the genome of ascoviruses. J. Gen. Virol. **80:**1537-1540.

Cheng, X. W., L. Wang, G. R. Carner, and B. M. Arif. 2005. Characterization of three ascovirus isolates from cotton insects. J. Invertebr. Pathol. **89:**193-202.

Conrad, C., and R. Rauhut. 2002. Ribonuclease III: new sense from nuisance. Int. J. Biochem. Cell Biol. **34:**116-129.

Cui, L., X. Cheng, L. Li, and J. Li. 2007. Identification of *Trichoplusia ni ascovirus* 2c virion structural proteins. J. Gen. Virol. **88:**2194-7.

Deveraux, Q. L., and J. C. Reed. 1999. IAP family proteins--suppressors of apoptosis. Genes Dev. **13:**239-52.

Fadok, V. A. 1999. Clearance: the last and often forgotten stage of apoptosis. J Mammary Gland Biol. Neoplasia. **4:**203-211.

Federici, B. A. 1982. A new type of insect pathogen in larvae of the clover cutworm, *Scotogramma trifolii*. J. Invertebr. Pathol. **40:**41-54.

Federici, B. A. 1983. Enveloped double-stranded DNA insect virus with novel structure and cytopathology. Proc. Natl. Acad. Sci. USA. **80:**7664-7668.

Federici, B. A., D. K. Bideshi, Y. Tan, T. Spears, and Y. Bigot. 2009. Ascoviruses: superb manipulators of apoptosis for viral replication and transmission. Curr. Top Microbiol. Immunol. **328:**171-196.

Federici, B. A., and R. Govindarajan. 1990. Comparative histopathology of three ascovirus isolates in larval noctuids. J. Invertebr. Pathol. **56:**300-311.

Federici, B. A., J. M. Vlak, and J. J. Hamm. 1990. Comparative study of virion structure, protein composition and genomic DNA of three ascovirus isolates. J. Gen. Virol. **71:**1661-1668.

Fuentes-Prior, P., and G. S. Salvesen. 2004. The protein structures that shape caspase activity, specificity, activation and inhibition. Biochem. J. **384:**201-232.

Furlong, M. J., and S. Asgari. 2010. Effects of an ascovirus (HvAV-3e) on diamondback moth, *Plutella xylostella*, and evidence for virus transmission by a larval parasitoid. J. Invertebr. Pathol. **103:**89-95.

Govindarajan, R., and B. A. Federici. 1990. Ascovirus infectivity and effects of infection on the growth and development of noctuid larvae. J. Invertebr. Pathol. **56:**291-299.

Guralnik, D. B., and J. H. Friend (Ed.). 1962. Webster's new world dictionary of the American language. College edition. Cleveland: World Publishing Co.

Hamm, J. J., Nordlund, D. A., Marti, O. G. 1985. Effects of a nonoccluded virus of *Spodoptera frugiperda* (Lepidoptera: Noctuidae) on the development of *Cotesia marginiventris* (Hymenoptera: Braconidae). Environ. Ent. **14:**258-261.

Hamm, J. J., Pair, S. D., Marti, O. G. 1986. Incidence and host range of a new ascovirus isolated from fall armyworm, *Spodoptera frugiperda* (Lepidoptera: Noctuidae). Fla. Entomol. **69:**524-531.

Hamm, J. J., E. L. Styer, and B. A. Federici. 1998. Comparison of field-collected ascovirus isolates by DNA hybridization, host range, and histopathology. J. Invertebr. Pathol. **72:**138-146.

Hussain, M., A. M. Abraham, and S. Asgari. 2010. An Ascovirus-encoded RNase III autoregulates its expression and suppresses RNA interference-mediated gene silencing. J. Virol. **84:**3624-3630.

Hussain, M., and S. Asgari. 2008. Inhibition of apoptosis by *Heliothis virescens ascovirus* (HvAV-3e): characterization of orf28 with structural similarity to inhibitor of apoptosis proteins. Apoptosis. **13:**1417-1426.

Hussain, M., S. Garrad, and S. Asgari. 2009. The role of actin filaments in ascovirus replication and pathology. Arch. Virol. **154:**1737-1743.

Hussain, M., R. J. Taft, and S. Asgari. 2008. An insect virus-encoded microRNA regulates viral replication. J. Virol. **82:**9164-9170.

Imajoh, M., H. Sugiura, and S. Oshima. 2004. Morphological changes contribute to apoptotic cell death and are affected by caspase-3 and caspase-6 inhibitors during red sea bream iridovirus permissive replication. Virology. **322:**220-230.

Jakob, N. J., and G. Darai. 2002. Molecular anatomy of *Chilo* iridescent virus genome and the evolution of viral genes. Virus Genes. **25:**299-316.

Kaplan, D., and S. Sieg. 1998. Role of the Fas/Fas ligand apoptotic pathway in human immunodeficiency virus type 1 disease. J. Virol. **72:**6279-6282.

Koyama, A. H. 1995. Induction of apoptotic DNA fragmentation by the infection of vesicular stomatitis virus. Virus Res. **37:**285-290.

Kuznetsov, Y. G., J. G. Victoria, A. Low, W. E. Robinson, Jr., H. Fan, and A. McPherson. 2004. Atomic force microscopy imaging of retroviruses: human immunodeficiency virus and murine leukemia virus. Scanning. **26:**209-216.

Linder, S., and M. C. Shoshan. 2005. Lysosomes and endoplasmic reticulum: targets for improved, selective anticancer therapy. Drug Resist. Updat. **8:**199-204.

Pennacchio, F., and M. R. Strand. 2006. Evolution of developmental strategies in parasitic hymenoptera. Annu. Rev. Entomol. **51:**233-258.

Plomp, M., M. K. Rice, E. K. Wagner, A. McPherson, and A. J. Malkin. 2002. Rapid visualization at high resolution of pathogens by atomic force microscopy: structural studies of herpes simplex virus-1. Am. J. Pathol. **160:**1959-1966.

Reinheckel, T., Deussing, J., Roth, W., Peters, C. 2001. Towards specific functions of lysosomal cysteine peptidases: phenotypes of mice deficient for cathepsin B or cathepsin L. Biol. Chem. **382:**735-741.

Renault, S., A. Petit, F. Benedet, S. Bigot, and Y. Bigot. 2002. Effects of the *Diadromus pulchellus ascovirus*, DpAV-4, on the hemocytic encapsulation response and capsule melanization of the leek-moth pupa, Acrolepiopsis assectella. J. Insect Physiol. **48:**297-302.

Shen, Y., and T. E. Shenk. 1995. Viruses and apoptosis. Curr. Opin. Genet. Dev. **5:**105-111.

Shors, T. 2009. Understanding viruses. Sudbury: Jones and Bartlett Publishers. pp. 31-69.

Schwerk, C., **and K. Schulze-Osthoff.** 2003. Non-apoptotic functions of caspase in cellular proliferation and differentiation. Biochem. Pharmacol. **66:**1453-1458.

Smede, M., M. J. Furlong, and S. Asgari. 2008. Effects of *Heliothis virescens ascovirus* (HvAV-3e) on a novel host, *Crocidolomia pavonana* (Lepidoptera: Crambidae). J. Invertebr. Pathol. **99:**281-285.

Smede, M., M. Hussain, and S. Asgari. 2009. A lipase-like gene from *Heliothis virescens ascovirus* (HvAV-3e) is essential for virus replication and cell cleavage. Virus Genes. **39:**409-417.

Stasiak, K., M. V. Demattei, B. A. Federici, and Y. Bigot. 2000. Phylogenetic position of the *Diadromus pulchellus ascovirus* DNA polymerase among viruses with large double-stranded DNA genomes. J. Gen. Virol. **81:**3059-3072.

Stasiak, K., S. Renault, M. V. Demattei, Y. Bigot, and B. A. Federici. 2003. Evidence for the evolution of ascoviruses from iridoviruses. J. Gen. Virol. **84:**2999-3009.

Stasiak, K., S. Renault, B. A. Federici, and Y. Bigot. 2005. Characteristics of pathogenic and mutualistic relationships of ascoviruses in field populations of parasitoid wasps. J. Insect. Physiol. **51:**103-115.

Stoka, V., V. Turk, and B. Turk. 2007. Lysosomal cysteine cathepsins: signaling pathways in apoptosis. Biol. Chem. **388:**555-560.

Tan, Y., D. K. Bideshi, J. J. Johnson, Y. Bigot, and B. A. Federici. 2009. Proteomic analysis of the *Spodoptera frugiperda ascovirus* 1a virion reveals 21 proteins. J. Gen. Virol. **90:**359-365.

Tillman, P. G., Styer, E. I., Hamm, J. J. 2004. Transmission of Ascovirus from *Heliothis virescens* (Lepidoptera: Noctuidae) by three parasitoids and effects of virus on survival of parasitoid *Cardiochiles nigriceps* (Hymenoptera: Braconidae). Environ. Entomol. **33:**633-643.

Wang, L., J. Xue, C. P. Seaborn, B. M. Arif, and X. W. Cheng. 2006. Sequence and organization of the *Trichoplusia ni ascovirus* 2c (Ascoviridae) genome. Virology. **354:**167-177.

Wiseman, B. R. 1999. Cumulative effects of antibiosis on five biological parameters of the fall armyworm. Fla. Entomol. **82:**277-283.

1.14 Figures

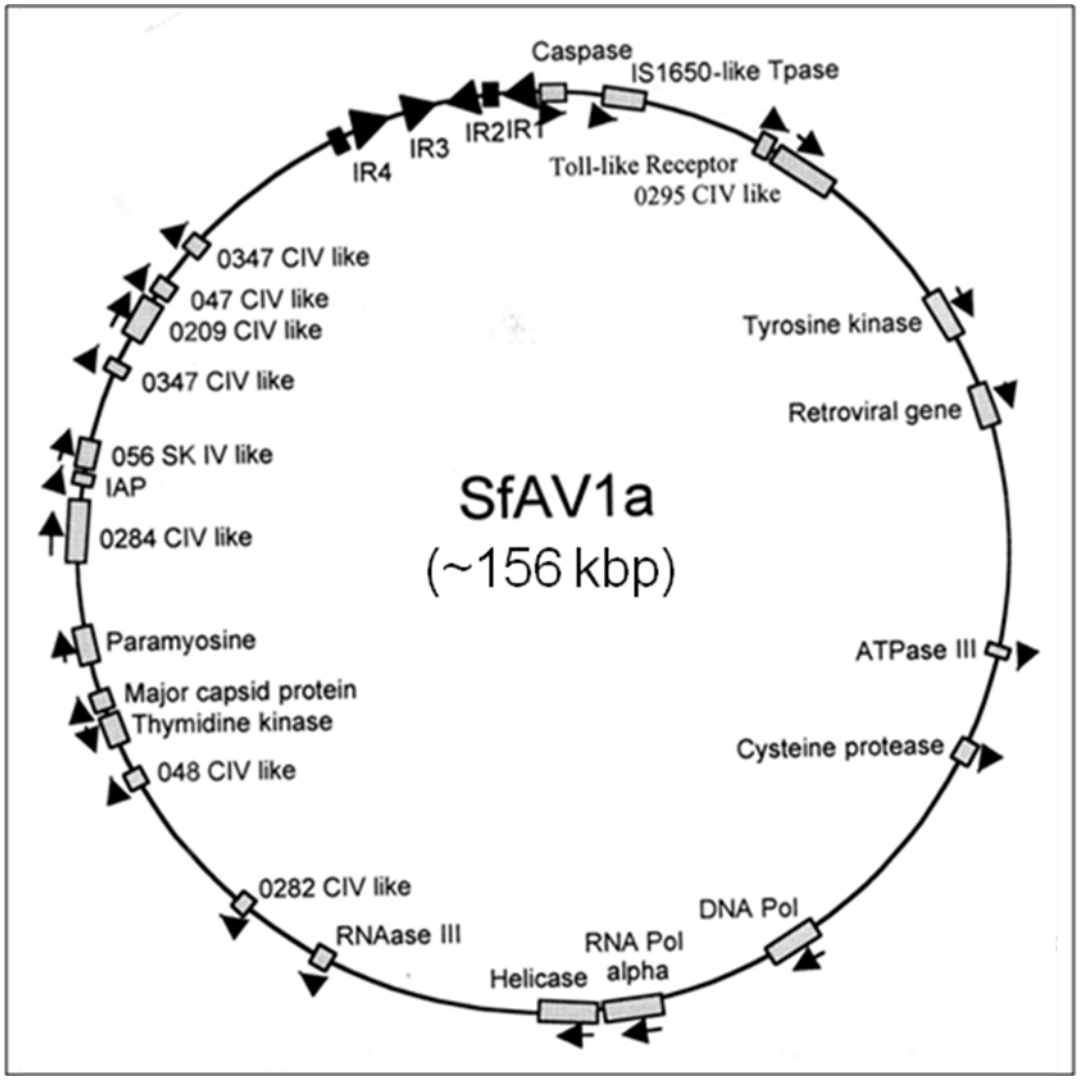

Figure 1.1 Map of key genes in the SfAV1a genome. Ascovirus genomic DNA is circular and double-stranded. DNA polymerase, indicated near the bottom right of the figure, corresponds to open reading frame 1. Ascovirus genomes bear many homologs to proteins of the *Chilo iridescent virus 6* (CIV), which suggests a close phylogenetic relationship to iridescent viruses.

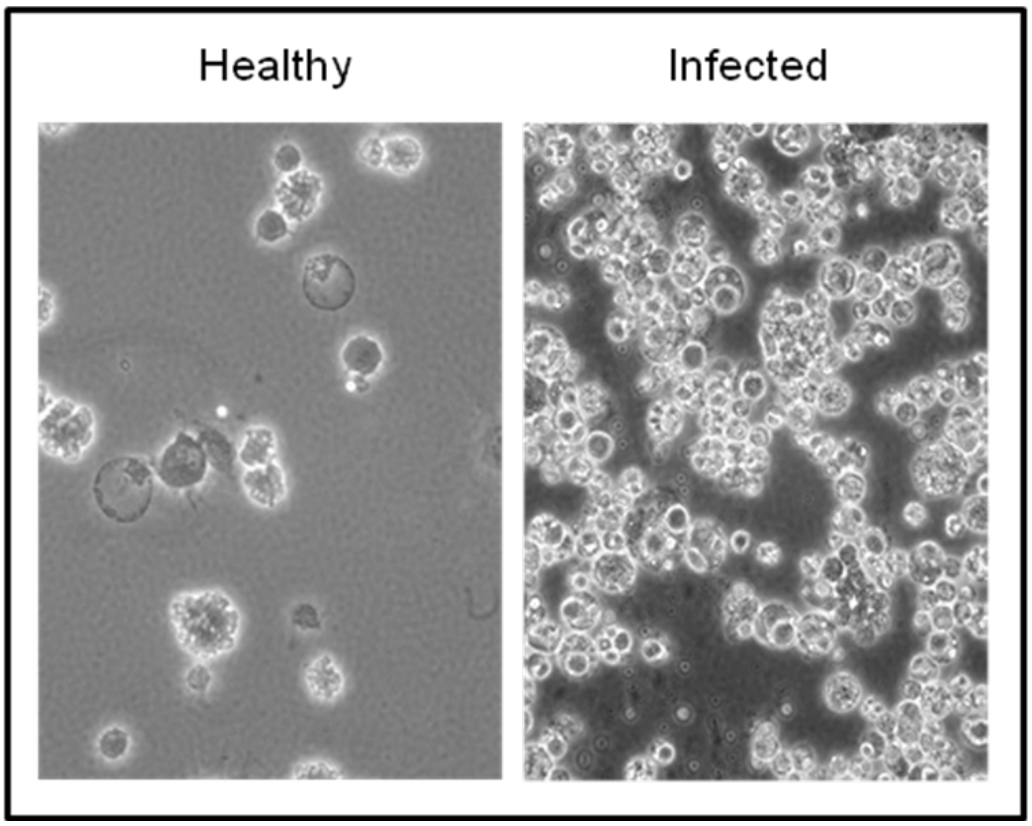

Figure 1.2 Ascovirus infection results in the accumulation of virion-filled vesicles in the hemolymph. The above panels show wet mount preparations of healthy and SfAV1a-infected hemolymph from the noctuid larvae of *Spodoptera exigua*. Infected hemolymph has a high concentration of light refracting virion-containing vesicles, also referred to as viral vesicles, whereas healthy hemolymph has a low concentration of blood cells (hemocytes). Infection by ascoviruses results in a chronic disease in caterpillars that halts their development thereby extending the larval stage. Ascoviruses are mechanically vectored from one caterpillar to another via wasp oviposition with a contaminated ovipositor. Within a few days, viral amplification results in the virion-containing vesicles illustrated above that will break away from tissues into the hemolymph where they can be acquired by another wasp. Micrographs were taken using the SPOT-RT Color camera (Diagnostic Instruments) and a Leica DMRE microscope, magnification 400X.

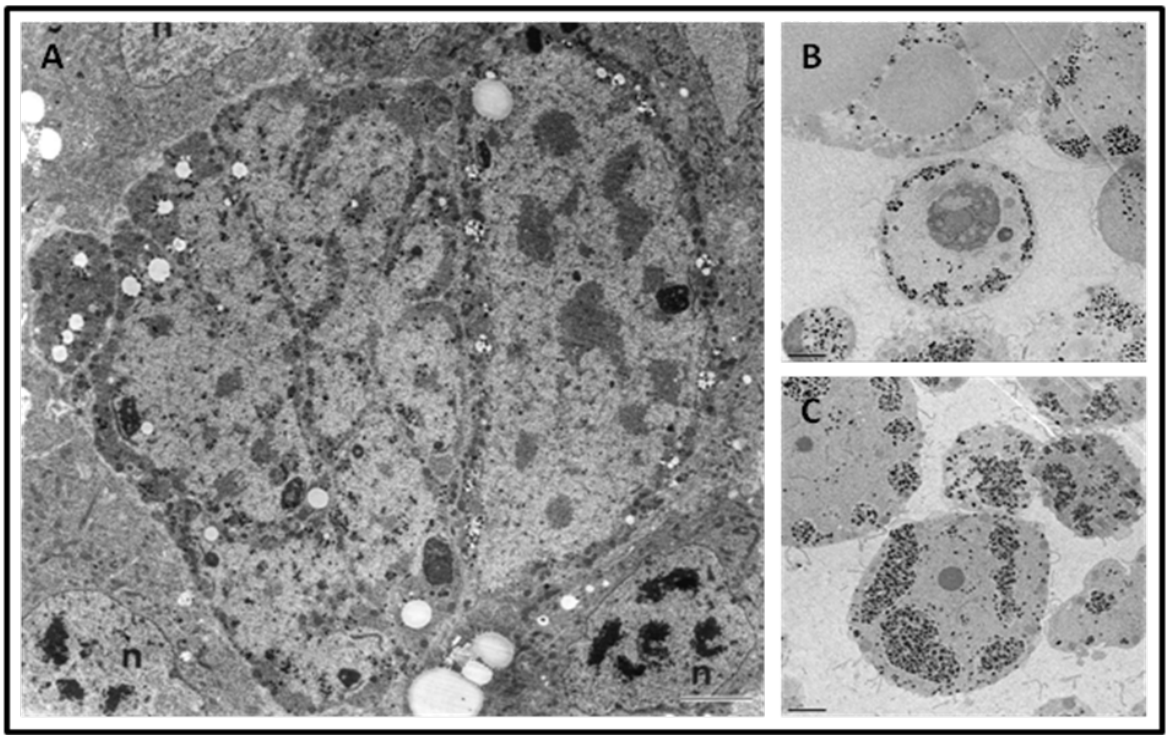

Figure 1.3 Ascovirus infection and virogenesis. (A) An electron micrograph of a cross section through SfAV1a infected fat body tissue in a *Spodoptera* larva. The nuclei (n) indicated at the bottom are in healthy cells, whereas the three infected cells above are in various stages of infection. The infected cells exhibit some of the following stages of infection: enlargement of the cell, an enlarged or fragmented nucleus, and plasma membrane invagination. (B and C) Ascovirus infected cells are eventually cleaved into virion-containing vesicles that change over time due to the assembly and accumulation of additional virions. Scale bars (A) 2 µm, (B and C) 1 µm.

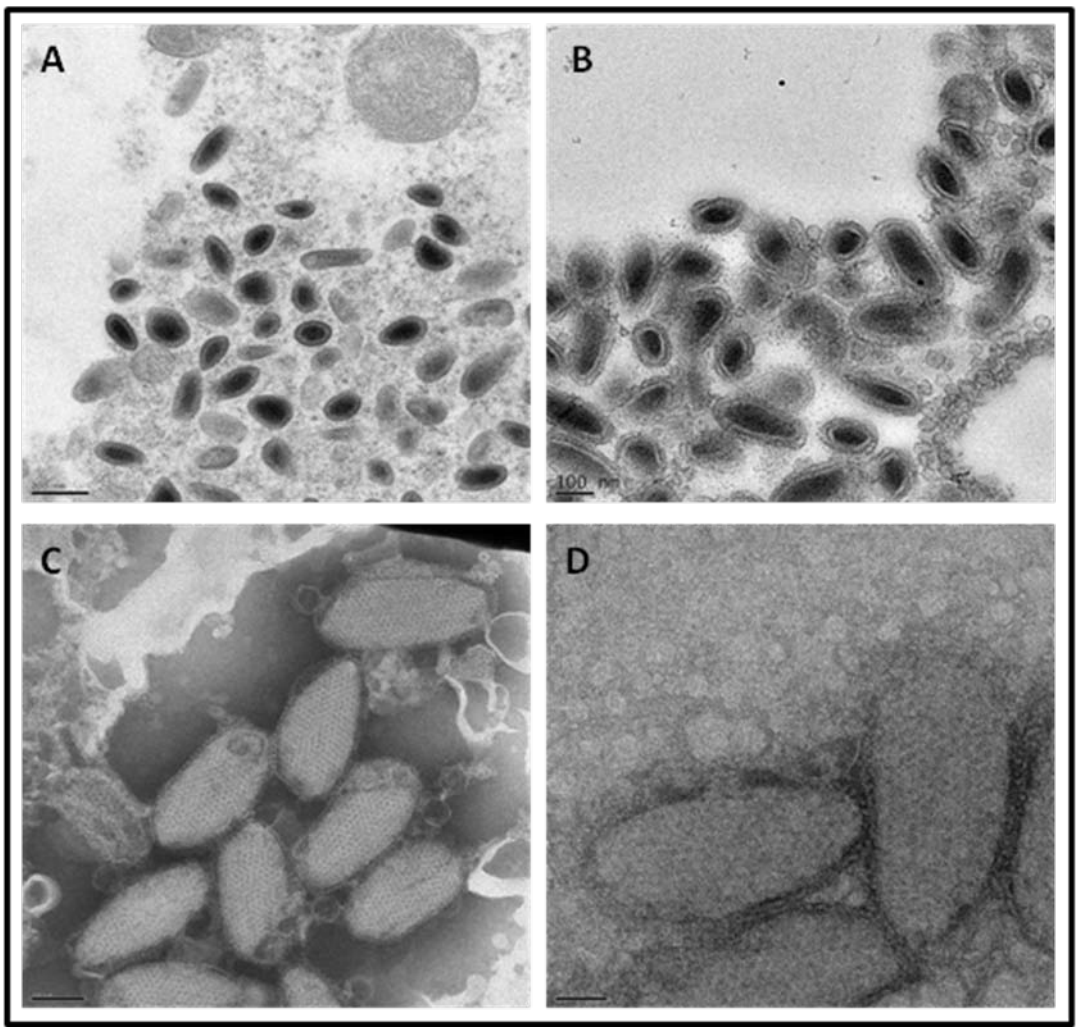

Figure 1.4 Ascovirus virogenesis. Viriogenesis takes place within infected cells and virion-containing vesicles. It begins with the formation of the nucleoprotein core, which then is encapsidated (A). Later, these nucleocapsid structures become envelope (B). (C and D). A reticulate pattern can be clearly seen on SfAV1a virions purified using sucrose gradients and negatively stained with uranyl acetate. Electron micrographs were obtained using a FEI Tecnai12 microscope and photographed with a Gatan US 1000 camera. Scale bars (A) 200 nm, (B and C) 100 nm, (D) 50 nm.

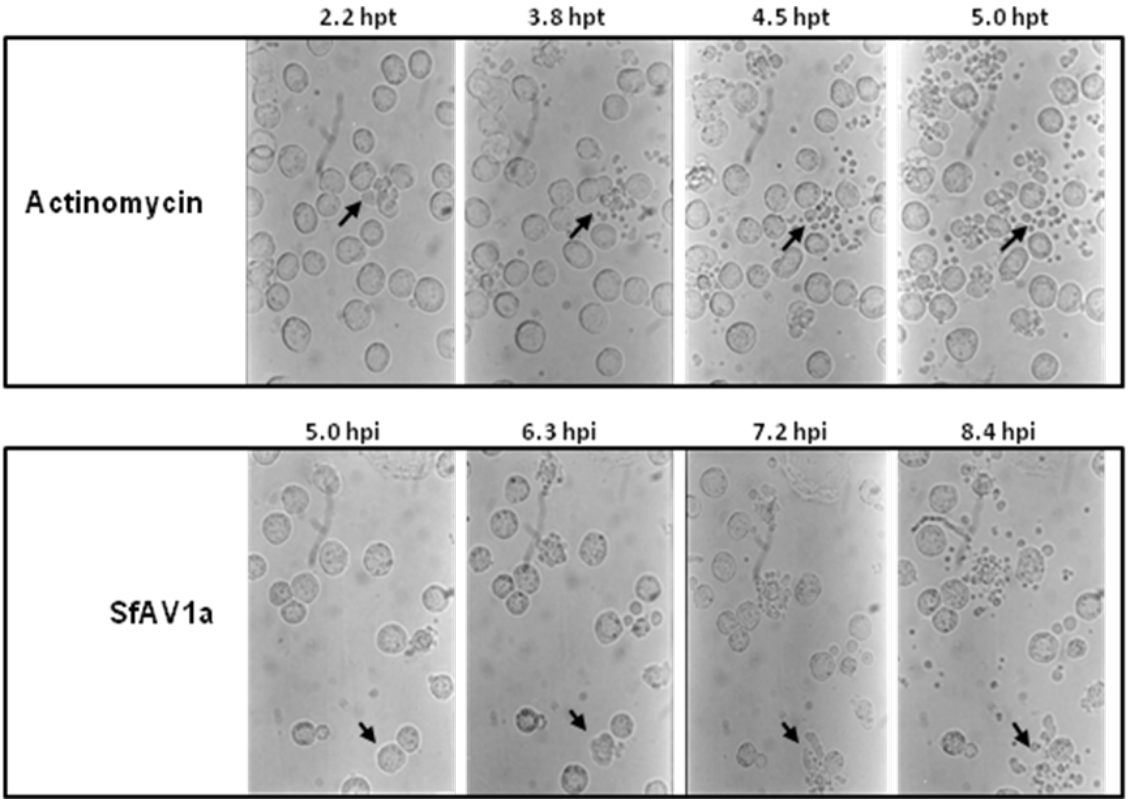

Figure 1.5 SfAV1a infection resembles apoptosis. Sf21 cell lines were seeded and grown to 60-70% confluence in wells of a 24-well culture plate (Costar, Corning). A time course of cytopathic changes due to apoptosis or infection was recorded at 400-fold magnification using an Olympic 35mm camera connected to a Zeiss standard UPL inverted mircroscope. For each treatment (Actinomycin or SfAV1a), the arrow points to the same position within the field of view. Actinomycin D is a cyclic peptide compound that intercalates into GC rich regions of DNA duplexes; this interferes with polymerase activity and induces apoptosis.

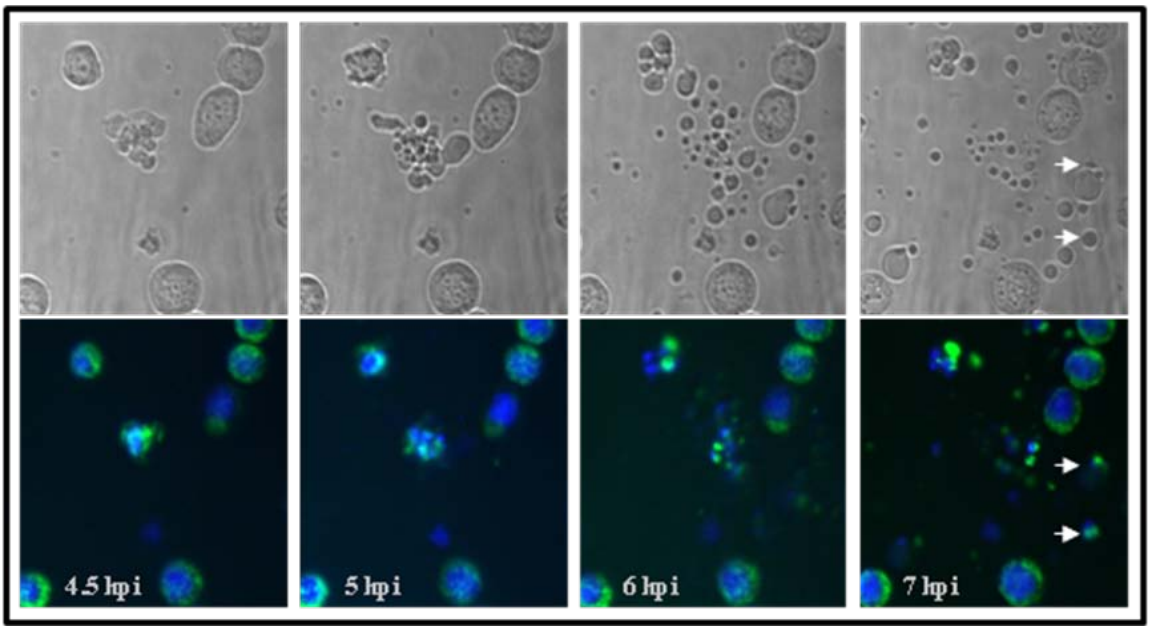

Figure 1.6 Confocal fluorescence microscopy of cells progressing through SfAV1a infection. Sf21 cells were inoculated with SfAV1a for 1 hr then washed and incubated with stain for the duration of observation. DNA (blue) was visualized using Hoechst 33342 and mitochondria (green) were visualized using Rhodamine 123. Fluorescent images are composites of separate micrographs of green and blue fluorescent emissions. Mitochondrial stain was still detected after vesicles were formed (arrows). Pictures were taken of the same field of view over time using the Atto Pathway HT confocal microscope at 400-fold magnification in the Core Instrumentation Facility of University of California, Riverside.

CHAPTER 2

P64, a Novel Major Virion DNA-Binding Protein Potentially Involved in Condensing the *Spodoptera frugiperda ascovirus 1a* Genome

2.1 Abstract

Previously, 21 structural proteins had been identified in the virion of *Spodoptera frugiperda ascovirus* 1a (SfAV1a), a virus with a large, double-stranded DNA genome of 157 kbp, which attacks species of the lepidopteran family Noctuidae. The two most abundant virion proteins were the major capsid protein and a novel protein (P64) of 64 kDa that contained two distinct domains not known previously to occur together. The amino-terminal half of P64 (residues 1 to 263) contained four repeats (a recently recognized motif with an unknown function) of a virus-specific two-cysteine adaptor. Adjoined to this, the carboxy-terminal half of P64 (residues 279 to 455) contained 14 copies of a highly basic, tandemly repeated motif rich in arginine and serine, having an 11- to 13-amino-acid consensus sequence, SPSQRRSTS(V/K)(A/S)RR, yielding a predicted isoelectric point of 12.2 for this protein. In the present study, we demonstrate by Southwestern analysis that SfAV1a P64 was the only virion structural protein that bound DNA. Additional electrophoretic mobility shift assays showed that P64 bound SfAV1a as well as non-SfAV1a DNA. Furthermore, we show through immunogold labeling of ultrathin sections that P64 is a component of virogenic stroma and appears to be progressively incorporated into the SfAV1a DNA core during virion assembly. As no other virion structural protein bound DNA and no basic DNA-binding proteins of lower

mass are encoded by the SfAV1a genome or were identified by proteomic analysis, our results suggest that P64's function is to condense the large genome of this virus and assist in packaging this genome into its virion.

2.2 Introduction

Following nucleic acid synthesis, viral genomes are condensed and packaged into virions by a variety of mechanisms (Guo and Lee, 2007; Lieberman, 2008; Locker *et al.*, 2007; Roos *et al.*, 2007). Essential to this process is neutralization of the negative electrostatic charge on phosphate groups of the nucleotide backbone by positively charged ions. The negative charge of the phosphates groups in the DNA would otherwise resist condensation of viral genomes during encapsidation. Viruses typically accomplish this by sequestering positive charges in the form of divalent cations, such as Mg^{2+}, or through polyvalent polyamine cations, such as spermine and spermidine or other small, basic cationic proteins that bind and condense nucleic acids with high affinity (Brewer *et al.*, 1999; Fuller *et al.*, 2007; Koltover *et al.*, 2000; Lanzer and Holowszak, 1975). An example of the latter group is histones, which are abundant in the nucleus and high in arginine and lysine content, their primary role being to condense host chromosomal DNA and package it into nucleosomes (Bartova *et al.*, 2008). During virion assembly, histones are involved in condensation of viral genomes by several DNA viruses, including polyomaviruses, papovaviruses (Chestier and Yaniv, 1979; Coco-Prados *et al.*, 1980; La Bella and Vesco, 1980; Milavetz, 2004), and herpes viruses (Maxwell and Frappier, 2007), and by RNA retroviruses (Segura *et al.*, 2008).

Despite their ubiquity in the nucleus, histones do not appear to be involved in genome condensation and packaging of most viruses. For example, viruses as diverse as hepatitis B virus (HBV), baculoviruses, and other DNA viruses that replicate in the nucleus encode cationic proteins rich in arginine and lysine, a characteristic they share with histones and protamines. The latter are small, arginine-rich proteins that replace histones on chromosomal DNA during the late stages of spermatogenesis (Andrabi, 2007). Similar proteins have been found in viruses. The carboxy terminus of the HBV core antigen (Gallina *et al.*, 1989), for example and the small P6.9 (6.9-kDa) proteins of baculoviruses (Wilson *et al.*, 1987; Wilson and Price, 1988) are protamine-like virion components known to bind and condense viral DNA for encapsidation.

Viruses of the family *Ascoviridae* are highly pathogenic to larvae of the lepidopteran family Noctuidae. The virions typically are large (130 to 150 nm by 200 to 400 nm) and have complex symmetry and organization consisting of an inner particle containing a protein/DNA core that after assembly is enveloped to form the virion (Federici, 1983; Federici *et al.*, 2005). Although the ultrastructure of ascoviruses is markedly different from those of baculoviruses, iridoviruses, and entomopoxviruses (Slack and Arif, 2007), all of these viruses have large, double-stranded DNA (dsDNA) genomes, typically >100 kbp, that must be condensed for packaging. However, whereas the protaminelike P6.9 protein of baculoviruses is known to be a key protein involved in condensing genomic DNA and packaging it into the virion, the proteins responsible for this function in the other DNA viruses that attack insects remain unknown. Sequence analysis of the *Spodoptera frugiperda ascovirus 1a* (SfAV1a) genome (Bideshi *et al.*,

2006), the type species, revealed no genes coding for small, protaminelike peptides that could facilitate condensation and packaging of its large genome (157 kbp). Moreover, of 21 proteins revealed by our recent proteomic analysis of the SfAV1a virion (Tan *et al.*, 2009), no small, cellular histones or histone-like protamines were detected. The two most abundant proteins in the SfAV1a virion were the major capsid protein (MCP) and a protein with a mass of 64 kDa (ORF048 or P64) (Bideshi *et al.*, 2006; Tan *et al.*, 2009). As MCPs and core DNA-condensing and -packaging proteins generally occur in amounts proportionally greater than those of other structural proteins, the relative abundance of P64, and its high pI of 12.2, suggested that it might be a key protein involved in condensing and packaging the SfAV1a genome. In the present study, we characterized P64 and show that it is a novel protein containing two distinct domains with two distinct motifs. The amino-terminal portion contains four repeats of a well-conserved virus-specific two-cysteine adaptor motif (pfam08793.1) (Iyer *et al.*, 2006), whereas the carboxy-terminal portion contains 14 copies of a previously uncharacterized motif rich in arginine and serine residues (SPSQRRSTS[V/K][A/S]RR) and, to a lesser extent, several lysine residues. Through a combination of DNA-binding and gel shift assays, along with immunogold labeling electron microscopy, we demonstrate that P64 is a major virion protein in the SfAV1a DNA/protein core and may be involved in packaging this virus' genome into the virion.

2.3 Materials and methods.

2.3.1 Virion purification. Early fourth-instar *Spodoptera exigua* larvae were inoculated with SfAV1a as described previously (Federici *et al.*, 1990). The hemolymph

of morbid, diseased larvae were collected after 6 to 7 days and suspended in ice-cold phosphate-buffered saline (pH 7.4) containing 1% glutathione. The suspension was centrifuged at 2,000 x *g* for 10 min, and the supernatant was collected and centrifuged at 4°C for 1 h in a Beckman SW28 rotor at 105,000 x *g*. The pellet was resuspended in 1 ml ice-cold phosphate-buffered saline. SfAV1a virions were purified by isopycnic centrifugation in a CsCl gradient (30%, wt/wt) as described previously (Tan *et al.*, 2009).

2.3.2 Analysis of SfAV1a ORF48 (P64). The predicted amino acid sequence of P64 was analyzed using various online programs, including BLAST at the NCBI website (http://www.ncbi.nlm.nih.gov/) and the Scratch protein predictor (http://www.ics.uci.edu/~baldig/scratch/), to identify gene homologs, orthologs, conserved domains, motifs, and secondary structure.

2.3.3 Recombinant six-His-tagged P64 and anti-six-His-tagged P64 antibody. The Bac-To-Bac *Autographa californica* multicapsid nucleopolyhedrovirus baculovirus expression (Bacmid) system (Invitrogen) was used for over expression of *p64* under the polyhedron promoter. The sequence containing the open reading frame of the *p64* gene (ORF48) (4) was amplified by PCR using the primer pair comprising P64Foward (5'-CGCGGATCCATGGCGTCAAAACGTAAA-3') and P64Reverse (5'-CCGCTCGAGATCCTTCGACGATCAGG-3'), with BamHI and XhoI sites added to the primers (underlined). The amplicon was digested with BamHI and XhoI and ligated to the same sites in pFastBac HTb (Invitrogen) for production of recombinant six-histidine-tagged P64 (hereafter referred to as rP64). BTI-TN-5B1-4 (Tn*5*) cells (Invitrogen) were transfected with recombinant Bacmid, using TransIT-LT1 transfection reagent (Mirus

Corp.), and rP64 was purified by affinity chromatography using nitrilotriacetic acid resin under denaturing and native conditions (Qiagen), according to the manufacturers' protocols. Antiserum against purified rP64 was raised in rats (Josman, LLC, Napa, CA).

2.3.4 Virion protein fractionation and Western blotting. Protein concentrations were determined using a Micro BCA kit (Pierce). For various assays, 20 to 70 µg of SfAV1a virion proteins and 1 to 3 µg of purified rP64 were solubilized in 2x Laemmli buffer (Laemmli, 1970), fractionated in a 12% gel by sodium dodecyl sulfate-polyacrylamide gel electrophoresis (SDS-PAGE), and stained with Coomassie brilliant blue R-250 or transferred to a polyvinylidene difluoride-plus membrane (Osmonics, Inc.) by using a Semiphor Transphor unit (GE Healthcare) set at 8 V for 1 h. Western blot analysis with primary rat anti-rP64 antibody and secondary anti-rat immunoglobulin G (IgG)-alkaline phosphatase conjugate (Sigma) was performed as described by Park *et al.* (2000).

2.3.5 Southwestern blotting. A modified Southwestern blotting technique (Bowen *et al.*, 1980, Siu *et al.*, 2008) was used to investigate SfAV1a virion protein-DNA interactions. Proteins in the purified SfAV1a virion were fractionated in a 12% gel by SDS-PAGE and electroblotted onto a polyvinylidene difluoride-plus membrane as described above. After transfer, virion proteins were fixed by drying the membrane at room temperature. Transfer of proteins onto the membrane was subsequently confirmed by staining the membrane with Ponceau S (Moore and Viseli, 2000) and the polyacrylamide gel with Coomassie blue. To renature virion proteins, the membrane was soaked in absolute methanol for 5 s, rinsed once in Western transfer buffer (25 mM Tris,

192 mM glycine, 15% methanol [pH 8.4]) and renaturation buffer (50 mM Tris, 1% Triton X-100, 100 mM KCl, 10% glycerol, 1 mM ZnCl, 0.2% bovine serum albumin [BSA] [pH 7.5]), and then incubated in fresh renaturing buffer overnight at 4°C with gentle shaking (~30 rpm). The membrane was soaked in 50 ml DNA-binding buffer (DBB) (50 mM Tris [pH 7.5], 0.1% Triton X-100, 100 mM KCl, 10% glycerol, 0.1 mM ZnCl, and 2% BSA) for 2 h at room temperature. After incubation, the buffer was removed and replaced with 25 ml of fresh DBB containing 7.5 x 10^6 cpm of ^{32}P-labeled SfAV1a genomic DNA prepared by randomly primed labeling with hexameric nucleotides (Roche) and [α-^{32}P]dATP (Perkin-Elmer), according to the manufacturers' protocols. The DNA-binding reaction mixture was incubated at room temperature for 30 min, and the membrane was washed four times in 200 ml of fresh DBB at room temperature before autoradiography using Blue Lite Autorad Film (ISC BioExpress) was performed.

2.3.6 EMSAs. Nonviral covalently closed circular dsDNA (pGEM-T Easy, 3 kb; Promega) or a 0.2-kb SfAV1a-specific linear dsDNA originating from the ORF048 (*p64*) gene obtained by PCR with the primer pair comprising TS64CentF and TS64CentR (5'-CCATCGACATGTTTAAGCACGAGTCGTTCCAA-3' and 5'-GATGATCTCGAGCATGCTTGGACGCATG-3', respectively) was used in electrophoretic mobility shift assays (EMSAs). Fifty nanograms of pGEM-T Easy plasmid DNA or 100 ng of the linear amplicon was used in each assay. Substrate dsDNAs and various quantities of rP64 (1.5 µg to 9 µg) in a total of 15 µl of 0.5x DBB (see above) were incubated at 25°C for 20 min, followed by incubation at 4°C for an additional 20

min. In addition, to release DNA from stable rP64-DNA complexes in reaction mixtures containing 9 µg of rP64 or 50 ng of pGEM-T Easy, 5 µg or 10 µg of proteinase K (Invitrogen), respectively, was added after complex formation. Proteolytic digestion was performed at 25°C for 30 min. The controls contained all of the components of the standard reactions except that rP64 was replaced with 9 µg of BSA. After incubation, 2 µl of 50% glycerol was added, reaction tubes were stored on ice, and products were fractionated in a 0.7% agarose gel containing ethidium bromide (0.5 µg/ml) by electrophoresis in 1x Tris-borate-EDTA buffer (Fisher Scientific).

2.3.7 Immunogold labeling electron microscopy. Purified virions and virion-containing vesicles were embedded in 2% agar and fixed with 0.1% glutaraldehyde and 2% formaldehyde in 0.05 M $NaPO_4$ (pH 7.4) for 1 h. The specimen was dehydrated through an ethanol series and embedded in LR-White (Polysciences). Ultrathin sections were cut with a Sorvall MT 5000 ultramicrotome, stained with lead citrate and uranyl acetate, and examined and photographed with an FEI Tecnai 12 electron microscope and a Gatan US 1000 camera. Ultrathin sections of inner particles and sectioned virions were observed and quantified as described by Wills *et al.* (Will *et al.*, 2006). Immunogold labeling was performed as described previously (Snigirevskaya *et al.*, 1997; Will *et al.*, 2006), using gold-labeled rabbit anti-rat IgG (Ted Pella, Inc., CA) against the primary rat anti-rP64 antibody.

2.3.8 Phosphorylation of P64. Different amounts of SfAV1a virion proteins (10 µg, 15 µg, and 20 µg) and purified rP64 (0.7 µg, 1.5 µg, and 3 µg) were fractionated by SDS-PAGE in a 12% gel and stained with Pro-Q Diamond phosphoprotein gel stain

(Invitrogen). Destaining with Pro-Q Diamond phosphoprotein destaining solution (Invitrogen), detection with UV transillumination (300 nm), and calibration with ovalbumin and β-casein phosphoprotein markers in PeppermintStick phosphoprotein standards (Invitrogen) were performed according to the manufacturer's protocols, using an Alpha imager (Alpha Innotech Corp.). After detection by UV spectroscopy, the gel was stained with Coomassie blue to confirm the identities and locations of corresponding phosphoproteins.

2.4 Results

2.4.1 SfAV1a P64 (ORF048) is rich in arginine and serine and contains two distinct motifs. P64 is composed of 565 amino acid residues (Fig. 2.1). Analysis of its primary sequence showed that it is an unusual highly basic protein, with a predicted isoelectric point (pI) of 12.2. The high pI is primarily due to abundances of arginine and lysine (112 and 26 residues, respectively), which accounted for 26.2% of this protein's amino acids. P64 is also rich in serine (107 residues) and threonine (31 residues), which accounted for an additional 24.4% of its amino acids.

Two domains, comprising residues spanning from positions 1 to 263 (the amino-terminal portion) and 264 to 565 (the carboxy-terminal portion), were predicted based on the Scratch protein predictor program. The P64 amino-terminal portion contained four well-conserved repeats of the virus-specific two-cysteine adaptor motif (pfam08793.1) (Iyer *et al.*, 2006), at positions 13 to 50, 58 to 94, 141 to 177, and 182 to 218. This adaptor motif is known to be fused to ovarian tumor/A20-like peptidases and serine-threonine protein kinases. Although the biochemical function of this motif is unknown, its

occurrence in P64 suggests that it could function as an adaptor domain that facilitates intermolecular interactions among P64 molecules or other virion structural components (Iyer *et al.*, 2006).

The carboxy-terminal portion of P64 (Fig. 2.1) shares similarities with 16 viral proteins, 1 from the ascovirus HvAV3e (YP_001110913; E [expect] value of 2^{e-38}) and 15 from two vertebrate iridoviruses, a group of viruses phylogenetically related to ascoviruses (35). These were the *Regina ranavirus* virus (AAK54495; E value of 1^{e-9}) and the *Ambystoma tigrinum* virus (ACB11439, ACB11427, ACB11428, ACB11429, ACB11432, ACB11433, ACB11434, ACB11438, ACB11439, ACB11440, ACB11442, ACB11446, ACB11447, and YP_003846, with E values ranging from 4^{e-12} to 9^{e-8}). Several mammalian and invertebrate proteins with various degrees of homology to sequences in the sperm nuclear basic protein PL-1 isoform (AAT45385) of the mollusk *Spisula solidassina* showed lower levels of identity (34 to 37%) and similarity (46 to 56%) (BAE00421, AAT453384, AAT45385, and AAH34980, with E values ranging from 3^{e-4} to 0.005). An unusual feature in the carboxy terminus, not known to occur in other protein families, is the presence of 14 copies of a basic tandemly repeated motif (residues 279 to 455) rich in arginine and serine and having an 11- to 13-amino-acid consensus sequence, SPSQRRSTS[V/K][A/S]RR. Predicted extended β strands were found in both domains, but notably, it appeared that this secondary structure overlapped and connected each of the 14 basic tandem repeats (Fig. 2.1).

2.4.2 rP64 binds covalently closed circular plasmid and linear DNAs. The marked abundance of P64 (Tan *et al.*, 2009) in the SfAV1a virion (Fig. 2.2 and 2.3),

together with its high arginine and lysine content (26.2%) and basic pI of 12.2, suggested that P64 is the major protein component that interacted directly with viral DNA to neutralize the large negative electrostatic charge for genome packaging. To determine whether P64 could potentially play a role in condensing SfAV1a DNA for packaging of the genome in virions, an anti-rP64 antibody was raised in rats against the rP64 antigen produced with a Bacmid expression vector (Fig. 2.2A) and used for Western and immunogold labeling studies.

Western blot analysis showed that the anti-rP64 antibody bound specifically to purified rP64 and the P64 band observed in the profile of the purified SfAV1a virion protein (Fig. 2.2B). Nonspecific binding of the antibody to other virion proteins was not observed, thus confirming the identity of P64 based on previous proteomic and gene sequence analyses and its presence as a structural component in the SfAV1a virion (Bideshi *et al.*, 2006; Tan *et al.*, 2009).

Southwestern blot analysis using radiolabeled SfAV1a sequence-specific viral DNA showed that of all the virion proteins, only P64 bound the DNA substrate (Fig. 2.3A). To determine whether other SfAV1a virion structural proteins, particularly those with low molecular masses in the range typical for histones, protamines, and baculovirus P6.9 protein, bound DNA, the autoradiographic film was overexposed for 17 h. Even after prolonged exposure, no protein other than P64 was observed to bind viral DNA. In addition, in a similar Southwestern analysis, rP64 and native P64 were shown to bind digoxigenin-labeled pBR328 DNA (Roche) (Fig. 2.3, A and B), suggesting that this protein has a non-sequence-specific mode of DNA-binding activity.

To provide additional evidence that P64 has intrinsic DNA-binding activity, EMSAs were performed to demonstrate that rP64 bound covalently closed circular plasmid dsDNA (pGEM-T Easy, 3 kb) and linear SfAV1a-specific dsDNA (0.2 kb) (Fig. 2.4). Increased shifts in pGEM-T Easy DNA mobility were observed with increasing amounts of rP64 (Fig. 2.4A, lanes 4 to 9). In these assays, stable DNA-protein complexes were also observed based on their presence in the gel close to the wells. DNA in these complexes was liberated following proteolytic cleavage with proteinase K (Fig. 2.4A, lanes 10 and 11). Shifts in DNA mobility were not observed in controls with BSA (Fig. 2.4A, lanes 2 and 3). A similar shift in the mobility of the linear dsDNA substrate was also observed (Fig. 2.4B).

2.4.3 Localization of P64 by immunogold labeling of SfAV1a virions. Immunogold labeling electron microscopy of SfAV1a virion-containing vesicles and purified virions showed that the secondary gold-tagged antibody against the rat anti-rP64 antibody localized in virogenic stroma (Fig. 2.5, A and B) and was also incorporated into maturing virions (Fig. 2.5, C and D). In the eight sections examined, 109 of 126 (86%) gold particles (dots) were observed within the dense virogenic stroma network (Fig. 2.5, A and B), whereas only 17 (14%) appeared to be loosely attached to or outside its periphery. The apparent progressive incorporation of the label from the virogenic stroma into developing virions suggested that P64 is packaged inside the SfAV1a virion.

In this regard, counts of immunogold dots on eight micrographs of purified virions chosen randomly showed that for 508 virions, 70 (73%; ~1 dot per 7.3 virions) of 95 dots observed were located inside SfAV1a virions, whereas only 25 (27%; 1 dot per 20.3

virions) were located in close proximity to virions (Fig. 2.5, E-G). Labeled particles clearly attached to the external surfaces of SfAV1a virions were not apparent in these micrographs, suggesting that P64 was not associated with peripheral structures in the SfAV1a virion. This is supported by observations that the gold-labeled antibody did not localize with high affinity to the surfaces of intact virions in assays performed under identical conditions (Fig. 2.5H). In five negatively stained samples containing 1,236 intact SfAV1a virus particles, a total of 29 dots were observed (1 dot per 42.6 virions), and of these, only 5 (1 dot per 247.2 virions) appeared to be loosely attached to the virion surface. Thus, it is likely that these were random associations, as suggested by comparison to the results showing high affinities of the labeled antibody for virogenic stroma and internal structures of the SfAV1a virion (Fig. 2.5 A-G). The general methods and results described for the localization of P64 are similar to those that demonstrated the internal localization of the ICP35 scaffolding virion protein of herpes simplex virus 1 (Wills *et al.*, 2006).

2.4.4 Phosphorylation of P64. Phosphoprotein analysis of the SfAV1a virion showed that P64 was not modified by phosphorylation or, if phosphorylated, was undetectable by the method used (Fig. 2.6). Of the other virion proteins, only the capsid protein was phosphorylated. Interestingly, rP64 produced in insect cells in vitro was modified by phosphorylation, suggesting that P64 could be differentially phosphorylated during SfAV1a virogenesis. Treatment of rP64 with calf intestinal phosphatase (Biolabs) to dephosphorylate the recombinant protein was unsuccessful (data not shown).

2.5 Discussion

Ascoviruses are insect viruses that have unique structural and biological characteristics that distinguish them from other viruses (Federici, 1983; Federici *et al.*, 2005). The genome sequences of three ascoviruses, including SfAV1a, have been reported over the past 2 years (Asgari *et al.*, 2007; Bideshi *et al.*, 2006; Wang et al, 2006), but despite genomic sequence data, only a few proteins coded for by these viruses were identified as virion structural proteins (Cui *et al.*, 2007; Tan *et al.*, 2009). An interesting aspect of ascovirus structure is how the large genomes of these viruses are condensed and packaged into virions. Here, we have provided evidence suggesting that one of P64's functions is to condense SfAV1a genomic DNA for packaging during virion assembly. In addition to the sequence data showing that P64 contains a highly basic protaminelike, arginine-rich domain in the carboxy-terminal domain (Fig. 2.1), we show that P64 (i) is a major virion protein (Fig. 2.2), (ii) binds SfAV1a genomic DNA in vitro (Fig. 2.3 and 2.4), and (iii) is initially localized within virogenic stroma, followed by progressive packaging of what appears to be SfAV1a genomic DNA into the virion core, as observed by immunogold labeling (Fig. 2.5). This combination of data lends strong support to our conclusion that P64 is a novel DNA-binding protein involved in packaging of viral DNA into the virion during assembly. Of course, this does not exclude other proteins from participating in binding and packaging of the SfAV1a genome in the virion, and this occurrence is even likely. However, whether nuclear cations, histones, and/or protamine-like peptides participate in this process during early stages of SfAV1a virion assembly is unknown, but as the last two were not identified in proteomic analyses (Tan *et al.*, 2009)

and are not encoded by the SfAV1a genome (Bideshi *et al.*, 2006), it is unlikely that these play a role in virion assembly, as has been observed with other viruses (Brewer *et al.*, 1999; Fuller *et al.*, 2007; Koltover *et al.*, 2000; Lanzer and Holowszak, 1975; Lieberman, 2008). However, it must be noted that although DNA-binding proteins other than P64 were not observed, we cannot rule out the possibility that the SfAV1a virion contains other genome-sequestering-virus-encoded or nuclear proteins, as their activity potentially could have been abolished or suppressed by the experimental conditions used in the Southwestern assays described here.

Taken together with its abundance and location in the virion core, the modular organization of P64 into the two distinct domains, i.e., the virus-specific two-cysteine adaptor domain (pfam08793.1) (Iyer *et al.*, 2006) at the amino-terminus and the protaminelike domain at the carboxy terminus, suggests that P64 is a multifunctional protein that participates in the assembly and structure of the SfAV1a virion. In particular, its association with SfAV1a DNA in the stroma (Fig. 2.5) also suggests that P64 functions in early stages of virogenesis, not only in organizing and configuring DNA for virion assembly but also in recruiting or being recruited to other virion structural components during this process. In this regard, the amino-terminal virus-specific two-cysteine adaptor motif could play a role in virion assembly via protein-protein interactions. The specific role of this domain in virion structure and biology is not known at present. However, through comparative sequence analyses, Iyer *et al.* (Iyer *et al.*, 2006) have shown that the virus-specific two-cysteine adaptor motif is known to be fused to

ovarian tumor/A20-like peptidases and serine-threonine protein kinases, suggesting both structural and regulatory roles for this motif through protein-protein interactions.

Nevertheless, the modular arrangement of P64 is not unlike that of the hepatitis B core antigen (HBcAg) protein (Galibert *et al.*, 2007). The virion of HBV is composed of an outer envelope containing lipids and virally encoded surface proteins that form a lipoprotein shell that encloses the nucleocapsid, or HBcAg, which contains the RNA genome of this virus. Interestingly, the capsid consists of dimers of a 183-residue protein that contains two domains with distinct functions, an amino-terminal assembly domain (residues 1 to 149) and a protaminelike carboxy-terminal domain (residues 150 to 183), responsible for polymerization into virion particles and RNA packaging, respectively (Gallina *et al.*, 1989). The protaminelike domain is dispensable for HBV capsid assembly (Gallina *et al.*, 1989), and though a nucleic acid binding motif appears to be present in the amino-terminal domain, the basic motif is required for RNA packaging (Birnbaum and Nassal, 1990; Wizemann and Brunn, 1999). Therefore, the HBcAg core protein has dual functions in HBV virion maturation. By analogy, similar roles are anticipated for P64 in genome packaging, assembly, and maturation of the SfAV1a virion.

Finally, the proportionally high level of serine and threonine residues, collectively 25% (Fig. 2.1), in P64 suggests that these amino acids potentially play crucial roles in its putative function, similar to those of histones and protamines. In the nuclei of host cells, modification of histones by acylation, phosphorylation, and methylation of serine and threonine residues is known to influence processes such as chromatin structure remodeling and organization, gene transcription and silencing, and DNA replication and

repair, thereby elaborating epigenetic effects on virus nucleic acid structure and metabolism (Andrabi, 2007; Bartova *et al.*, 2008; Lieberman, 2008; Mikesh *et al.*, 2006; Milavetz, 2004). In this regard, the potential for P64 to be modified by phosphorylation/dephosphorylation (Fig. 2.6) suggests that it could play a role in diverse epigenetic processes related to SfAV1a virogenesis, including gene transcription and genome packaging and release. Whether nascent P64 is phosphorylated is unknown, but it is not surprising that it is unphosphorylated in the mature SfAV1a virion, where it presumably assists in neutralizing negative electrostatic charges conferred by phosphate groups in DNA to facilitate efficient packaging of viral genomic DNA, which otherwise would resist condensation during its encapsidation. Indeed, if P64 functions as proposed here, the mechanism(s) related to its phosphorylation during disassembly of the SfAV1a virion and release of genomic DNA during infection is of interest and could involve both host and virus-encoded kinases. Further studies are required to determine whether nascent P64 is phosphorylated after cellular invasion and to determine the mechanism(s) that results in its dephosphorylation during SfAV1a virion assembly.

2.6 References

Andrabi, S. M. H. 2008. Mammalian sperm chromatin structure and assessment for DNA fragmentation. J. Assist. Reprod. Genet. **24:**561-569.

Asgari, S., J. Davis, D. Wood, P. Wilson, and A. McGrath. 2007. Sequence and organization of the *Heliothis virescens* ascovirus genome. J. Gen. Virol. **88:**1120-1132.

Bartova, E., J. Krejci, A. Harnicarova, G. Galiova, and S. Kozubek. 2008. Histone modifications and nuclear architecture: A review. J. Histochem. Cytochem. **56:**711-721.

Bideshi, D. K., M. V. Demattei, F. Rouleux-Bonnin, K. Stasiak, Y. Tan, S. Bigot, Y. Bigot, and B. A. Federici. 2006. Genomic sequence of the *Spodoptera frugiperda ascovirus 1a*, an enveloped, double-stranded DNA insect virus that manipulates apoptosis for viral reproduction. J. Virol. **80:**11791–11805.

Birnbaum, F., and M. Nassal. 1990. Hepatitis B virus nucleocapsid assembly: primary structure requirements in the core protein. J. Virol. **64:**3319-3330.

Bowen, B., J. Steinberg, U. K. Laemmli, and H. Weintraub. 1980. The detection of DNA-binding proteins by protein blotting. Nucleic Acids Res. **8:**10-20.

Brewer,L. R., M. Corzett, and R. Balhorn. 1999. Protamine-induced condensation and decondensation of small DNA molecules. Science **286:**120-123.

Chestier, A., and M. Yaniv. 1979. Rapid turnover of acetyl groups in the four core histones of simian virus 40 minichromosomes. Proc. Natl. Acad. Sci. USA. **76:**46-50.

Coca-Prados, M. G. Vidali, and M. T. Hsu. 1980. Intracellular forms of simian virus 40 nucleoprotein complexes. III. Study of histone modifications. J. Virol. **36:**353-360.

Cui, L., X. Cheng, L. Li, and J. Li. 2007. Identification of *Trichoplusia ni ascovirus* 2c virion structural proteins. J. Gen. Virol. **88:**2194-2197.

Federici, B. A. 1983. Enveloped double stranded DNA insect virus with novel structure and cytopathology. Proc. Natl. Acad. Sci. USA. **80:**7664-7668.

Federici, B. A., Y. Bigot, R. R. Granados, J. J. Hamm, L. K. Miller, I. Newton, K. Stasiak, and J. M. Vlak. 2005. Family *Ascoviridae*. In *Virus Taxonomy: Eighth*

Report of the International Committee on Taxonomy of Viruses, pp. 269–274. Edited by C. M. Fauquet, M. A. Mayo, J. Maniloff, U. Desselberger & L. A. Ball. San Diego: Elsevier Academic Press.

Federici, B. A., J. M. Vlak, and J. J. Hamm. 1990. Comparative study of virion structure, protein composition and genomic DNA of three ascovirus isolates. J. Gen. Virol. **71:**1661-1668.

Fuller, D. N., J. P. Rickgauer, P. J. Hardine, S. Grimes, D.L. Anderson, and D. E. Smith. 2007. Ion effects on viral DNA packaging and portal motor function in bacteriophage phi 29. Proc. Natl. Acad. Sci. USA. **104:**11245-11250.

Galibert, F., E. Mandart, F. Fitoussi, P. Tiollais, and P. Charnay. 1979. Nucleotide sequence of the hepatitis B virus genome (subtype ayw) cloned in *E. coli*. Nature **281:**646-650.

Gallina, A., F. Bonelli, L. Zentilin, G. Rindi, M. Muttini, and M. Milanesi. 1989. A recombinant hepatitis B core antigen polypeptide with the protamine-like domain deleted self-assembly into capsid particles but fails to bind nucleic acids. J. Virol. **63:**4645-4652.

Guo, P., and T. J. Lee. 2007. Viral nanomotors for packaging of dsDNA and dsRNA. Mol. Microbiol. **64:**886-903.

Iyer, L. M., S. Balaji, E. V. Koonin, and L. Aravind. 2006. Evolutionary genomics of nucleo-cytoplamsmic viruses. Virus Res. **111:**156-184.

Koltover, I., K. Wagner, and C. R. Safinya. 2000. DNA condensation in two dimension. Proc. Natl. Acad. Sci. USA. **97:**14046-14051.

LaBella, F., and C. Vesco. 1980. Late modifications of simian virus 40 chromatin during the lytic cycle occur in an immature form of virion. J. Virol. **33:**1138-1150.

Laemmli, U. K. 1970. Cleavage of structural proteins during the assembly of the head of bacteriophage T4. Nature **227:**680-685.

Lanzer, W., and J. A. Holowszak. 1975. Polyamines of vaccinia virions and polypeptides released from viral cores by acid extraction. J. Virol. **16:**1254-1264.

Lieberman, P. M. 2008. Chromatin organization and virus gene expression. J. Cell Physiol. **216:**295-302.

Locker, R. C., S. D. Fuller, and S. C. Harvey. 2007. DNA organization and thermodynamics during viral packing. Biophys. J. **93:**2861-2869.

Maxwell, K. L., and L. Frappier. 2007. Viral proteomics. Microbiol. Mol. Biol. Rev. **71;**398-411.

Mikesh, L. M., B. Ueberheide, A. Chi, J. H. Coon, J. E. P. Syka, J. Shabanowitz, and D. F. Hunt. 2006. The utility of ETD mass spectrometry in proteomic analysis. Biochem. Biophys. Acta. **1764:**1811-1822.

Milavetz, B. 2004. Hyperacetylation and differential deacetylation of histones H4 and H3 define two distinct classes of acetylated SV40 chromosomes early in infection. Virology **319:**324-336.

Moore, M. K., and S. M. Viseli. 2000. Staining and quantification of proteins transferred to polyvinylidine fluoride membranes. Anal. Biochem**. 279**:241–242.

Park, H. -W., D. K. Bideshi, and B. A. Federici. 2000. Molecular genetic manipulation of truncated Cry1C protein synthesis in *Bacillus thuringiensis* to improve stability and yield. Appl. Environ. Microbiol. **66:**4449–4455.

Roos, W. H., I. L. Ivanovska, A. Evilevitch, and G. J. L. Wuite. 2007. Viral capsids: Mechanical characteristics, genome packaging and delivery mechanisms. Cell. Mol. Life Sci. **64:**1484-1497.

Segura, M. M., A. Garnier, M. R. Di Falco, G. Whisell, A. Meneses-Acosta, N. Archand, and A. Kamen. 2007. Identification of host proteins associated with retroviral vector particles by proteonomic analysis of highly purified vector preparations. J. Virol. **82:**1107-1117.

Siu, F. K. Y, L. T. O. Lee, and B. K. C. Chow. 2008. Southwestern blotting in investigating transcriptional regulation. Nat. Protocols **3:**51-58.

Slack, J., and B. M. Arif. 2006. The baculoviruses occlusion-derived virus: Virion structure and function. Adv. Virus Res. **69:**99-165.

Snigirevskaya, E. S., A. R. Hays, and A. S. Raikhel. 1997. Secretory and internalization pathways of mosquito yolk protein precursors. Cell Tissue Res. **290:**129-142.

Stasiak, K., S. Renault, M. V. Demattei, Y. Bigot, and B. A. Federici. 2003. Evidence for the evolution of ascoviruses from iridoviruses. J. Gen. Virol. **84:**2999-3009.

Tan, Y., D. K. Bideshi, J. J. Johnson, Y. Bigot, and B. A. Federici. 2009. Proteomic analysis of the Spodoptera frugiperda ascovirus 1a virion reveals 21 proteins. J. Gen. Virol. **90:**359-365.

Wang, L., J. Xue, C. P. Seaborn, B. M. Arif, and X. -W. Cheng. 2006. Sequence and organization of the *Trichoplusia ni* ascovirus 2c (*Ascoviridae*) genome. Virology **354:**167–177.

Wills, E., L. Scholtes, and J. D. Baines. 2006. Herpes simplex virus 1 DNA packaging proteins encoded by U_L6, U_L15, U_L17, U_L28, and U_L33 are located on the external surface of the viral capsid. J. Virol. **80:**10894-10899.

Wilson, M. E., T. H. Mainprizw, P. D. Friesen, and L. K. Miller. 1987. Location, transcription, and sequence of a baculovirus gene encoding a small arginine-rich polypeptide. J. Virol. **61:**661-666.

Wilson, M. E., and K. H. Price. 1988. Association of *Autographa californica* nuclear polyhedrosis virus with nuclear matrix. Virology **167:**233-341.

Wizemann, H., and A. von Brunn. 1999. Purification of *E. coli*-expressed HIS-tagged hepatitis B core antigen by Ni^{2+}-chelate affinity chromatography. J. Virol. Methods **77:**189-197.

2.7 Figures

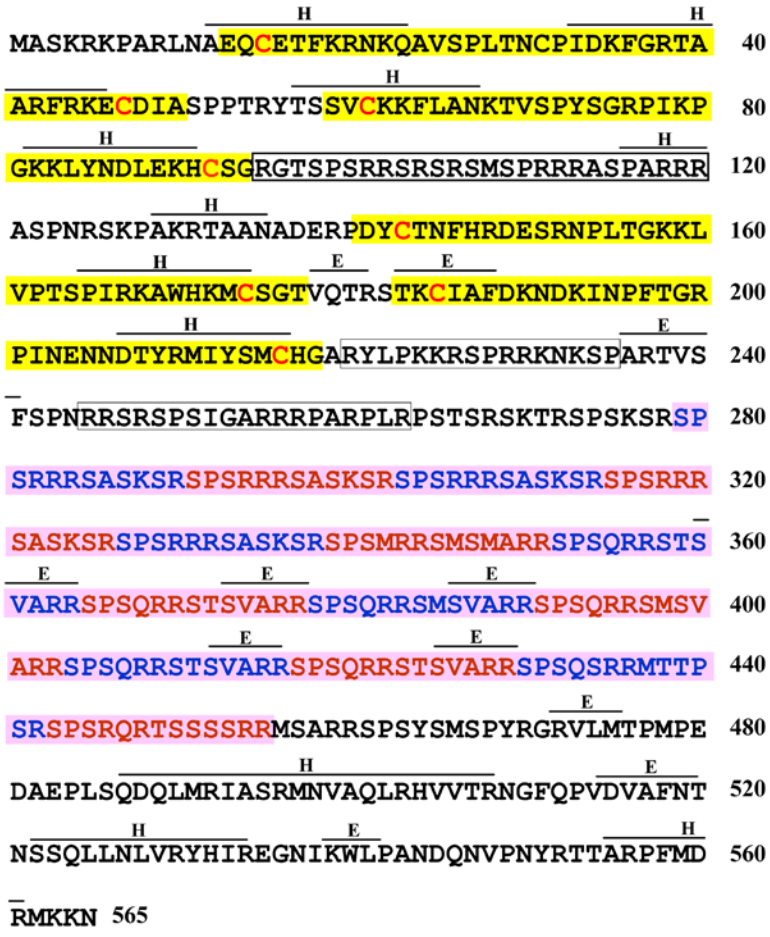

Figure 2.1. Domains and sequence motifs in the P64 structural protein of the *Spodoptera frugiperda ascovirus 1a* virion. Two domains were identified with the Scratch protein predictor program, the amino-terminal domain spanning residues 1 to 263 and the carboxy-terminal domain spanning residues 264 to 565. The four virus-specific two-cysteine adaptor motifs (highlighted in yellow) with conserved cysteines (bright red) are present in the amino-terminal domain. The 14 copies of the basic tandemly repeated motif (SPSQRRSTS[V/K][A/S]RR) composed of 11 to 13 amino acids and rich in serine and arginine (residues 279 to 455; alternating blue and dark red letters highlighted in pink) are present in the carboxy-terminal portion of P64. Amino-terminal sequences rich in arginine and/or lysine that do not conform to the basic repeat motif in the carboxy terminus are boxed. Predicted helices (H) and extended beta strands (E) are also shown.

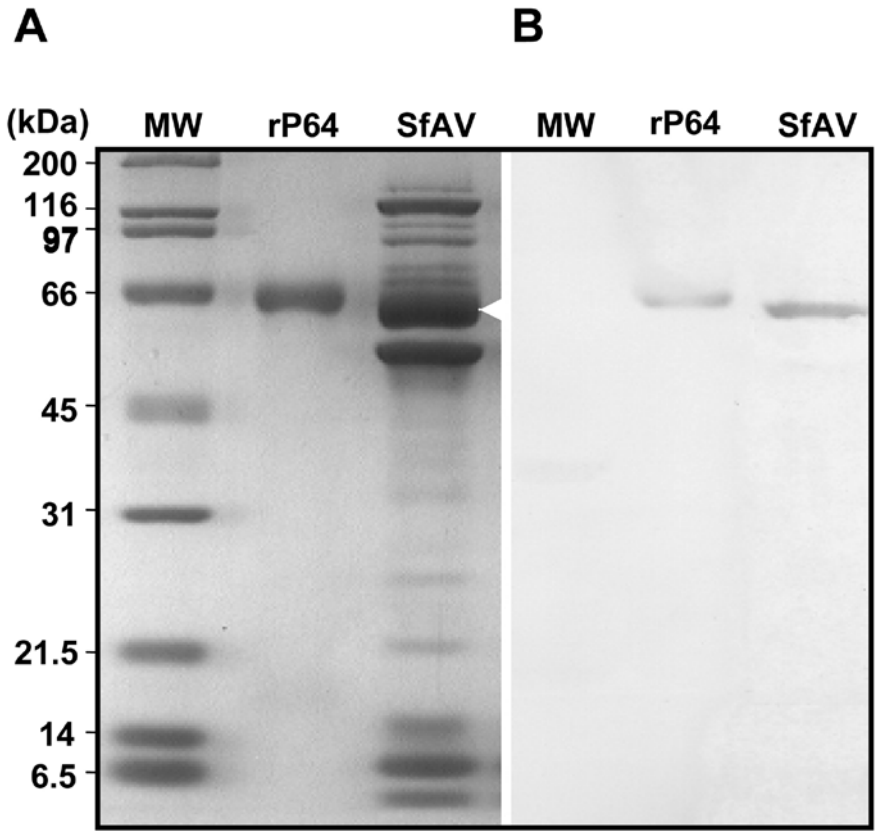

Figure 2.2. Western blot analysis showing the position of P64 among proteins of the SfAV1a virion. (A) 12% SDS-PAGE showing recombinant six-His-tagged P64 (rP64) protein produced and purified from insect (Tn*5*) cells and used for raising rat anti-rP64 antibody and protein profile of purified SfAV1a virions. (B) Western blot showing the specificity of the rat anti-rP64 antibody against purified rP64 and P64 (white arrowhead) in the virion protein profile. MW, molecular mass standards; kDa, kilodaltons.

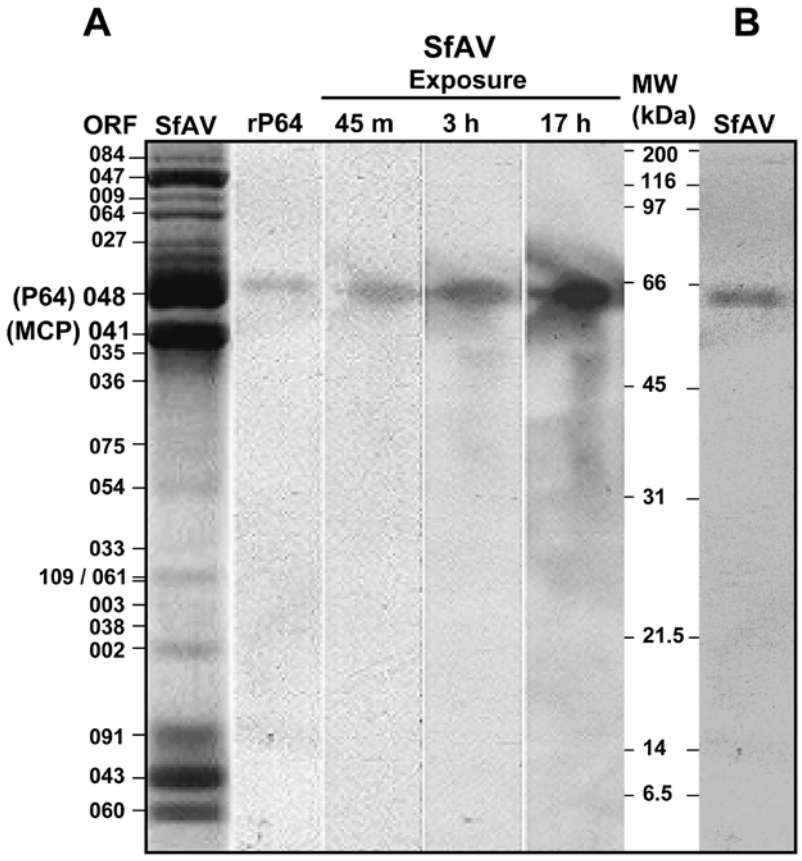

Figure 2.3. Southwestern blot showing that the *Spodoptera frugiperda ascovirus 1a* P64 virion protein binds DNA. Purified recombinant six-His-tagged P64 (rP64) and SfAV1a virion proteins were fractioned by SDS-PAGE in a 12% gel, electroblotted, and incubated with ^{32}P-labeled SfAV1a DNA (A) or pBR328 DNA (B). The autoradiographic film was exposed for 45 min (m) and 3 h (h) and overexposed for 17 h to rule out DNA-binding activities of SfAV1a virion proteins other than P64. SfAV1a open reading frames (ORFs) encoding virion proteins (4, 36), including the positions of P64 and MCP, are shown. MW, molecular mass standards; kDa, kilodaltons.

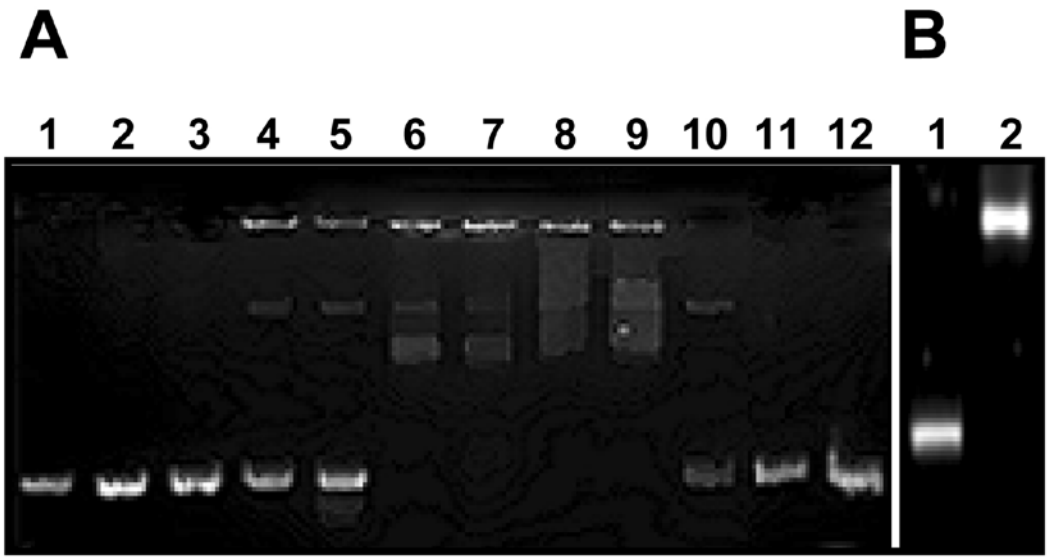

Figure 2.4. EMSAs demonstrating that *Spodoptera frugiperda ascovirus 1a* P64 is a DNA-binding protein. (A, B) EMSAs demonstrating that six-His-tagged P64 (rP64) binds covalently closed plasmid dsDNA (pGEM-T Easy, 3 kbp, 50 ng per reaction) and linear dsDNA (0.2 kbp, 100 ng per reaction); DNA was incubated with rP64 for 40 min, and products were fractionated by electrophoresis in a 0.7% agarose gel and stained with ethidium bromide. (A) pGEM-T Easy control DNA at 25 ng (lane 1) and 50 ng (lane 12) without protein; with 9 µg BSA (lanes 2 and 3); or with 1.5 µg, 6 µg, and 9 µg of P64 (replicates; lanes 4 and 5, 6 and 7, and 8 and 9, respectively). Following incubation, reaction mixtures containing 6 µg (lane 10) or 9 µg (lane 11) of rP64 were also treated with proteinase K at 5 µg and 10 µg, respectively, resulting in the release of rP64-bound dsDNA complexes. (B) EMSA using the 0.2-kb linear dsDNA, without (lane 1) and with (lane 2) rP64.

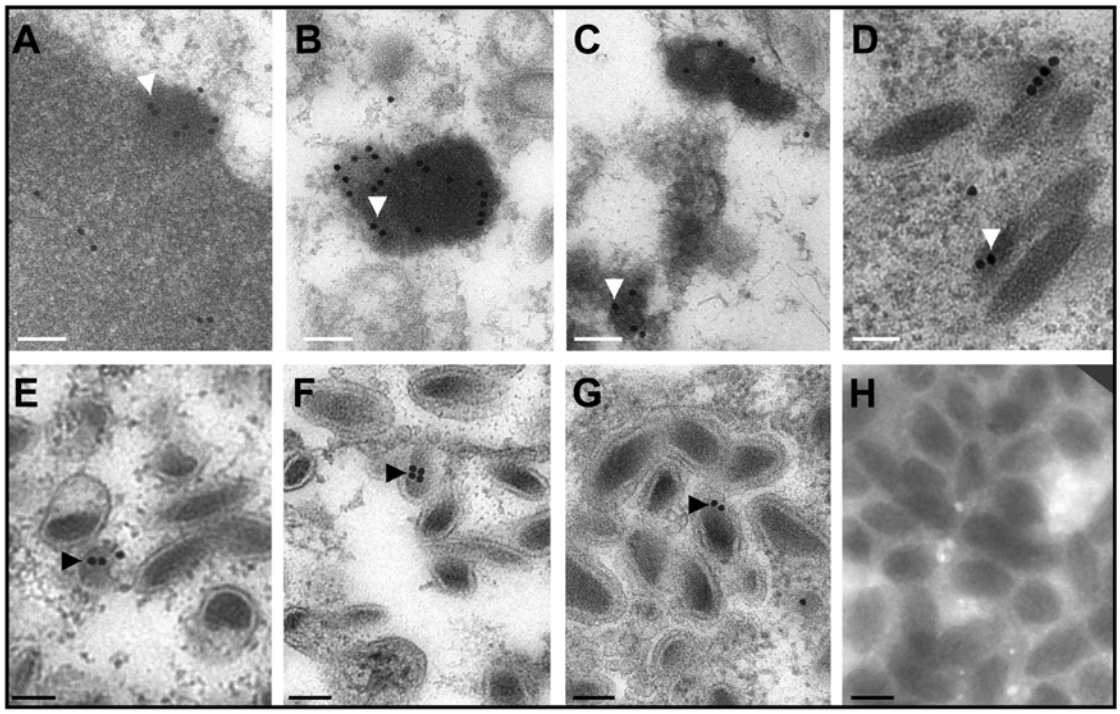

Figure 2.5. Representative electron micrographs of the *Spodoptera frugiperda ascovirus 1a* virion-containing vesicles showing the location of P64 in virogenic stroma, developing virions, and SfAV1a mature virions. (A to D) Sections of virion-containing vesicle were reacted with primary rat anti-rP64 antibody, followed by detection with gold-labeled rabbit anti-rat IgG. Arrowheads indicate the presence of gold beads within virogenic stroma (A, B) and maturing SfAV1a virions (C, D). Bar, 100 nm. (E to G) Representative electron micrographs showing internal location of P64 in purified SfAV1a virion. Sections were reacted with primary rat anti-rP64 antibody, followed by detection with gold-labeled rabbit anti-rat IgG. Arrowheads indicate the presence of gold beads inside mature sectioned SfAV1a virions (E, F, G). Specific association of gold beads with the peripheries of intact SfAV1a virions was not observed (H). Bar, 200 nm.

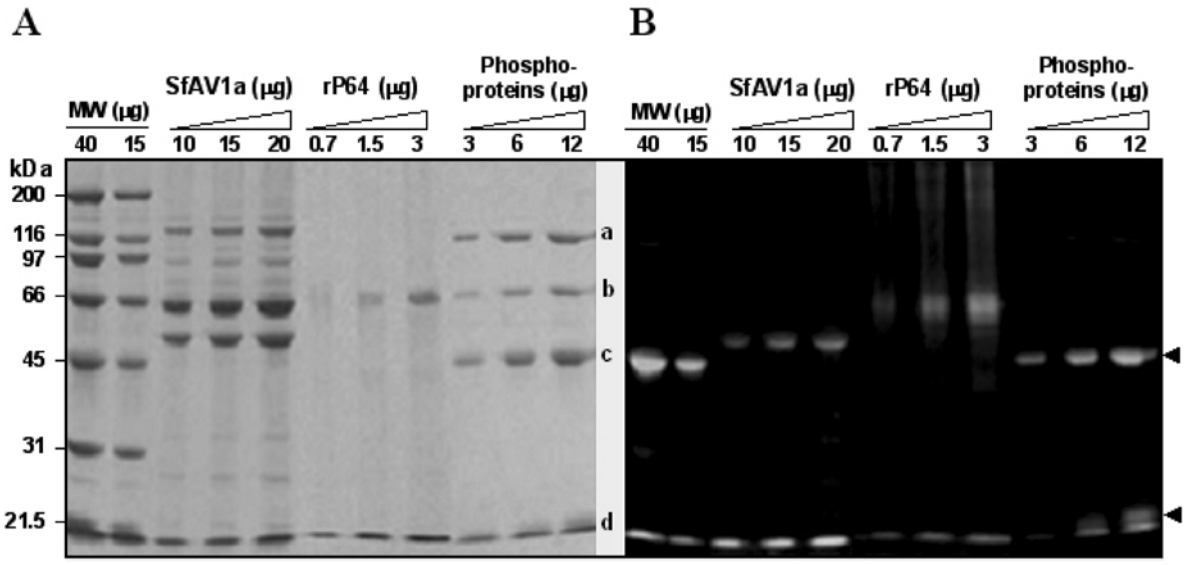

Figure 2.6. P64 is unphosphorylated in *Spodoptera frugiperda ascovirus 1a* virions. Different amounts of protein standards, purified SfAV1a virions, and recombinant six-His-tagged P64 (rP64) produced in insect cells were fractionated by SDS-PAGE in a 13% gel (A) and stained with Pro-Q Diamond phosphoprotein gel stain (Invitrogen) to detect the presence of phosphorylated proteins, which were visualized by UV transillumination at a wavelength of ~300 nm (B). The protein standards included unphosphorylated β-galactosidase and BSA at 116.3 kDa (a) and 66.3 kDa (b), respectively, and the phosphoproteins ovalbumin and β-casein (arrowheads) at 45 kDa (c) and 23.6 kDa (d), respectively. After UV transillumination, the gel was stained with Coomassie blue to confirm the locations and identities of phosphoproteins. MW, molecular mass standards; kDa, kilodaltons.

CHAPTER 3

The Ascovirus Basic Virion Protein P64 and its Homologs Comprise a Novel Family of Viral Genome Condensing Proteins

3.1 Abstract

Recent molecular and biochemical studies of virion proteins synthesized by the *Spodoptera frugiperda ascovirus 1a* virus (SfAV1a) identified a novel highly basic DNA-binding protein of 64 kDa (P64) abundant in the virion. This protein initially localized at sites of DNA synthesis in the virogenic stroma and later became progressively associated with the dense core of the virion as it assembled. Here I show that P64 condenses SfAV1a genomic (g) DNA, supporting the hypothesis that it functions in condensing gDNA for encapsidation. The results of biochemical studies of function and sequence analyses suggest similar roles for other ascovirus P64 homologs. This group of proteins is characterized by the presence of two major domains, one with one or more 2-cysteine adaptor (vs2C-ad) motifs, and the other containing arginine-rich, repetitive motifs. Each domain can bind and condense double-stranded DNA. Differences in the structural and biochemical characteristics of these two domains together with phylogenetic studies suggest the combination of the two domains was selected for during evolution to condense viral genomic DNA and associate it with the virion core. Iridoviruses (family *Iridoviridae*) are closely related to ascoviruses and also encode proteins with similar vs2C-ad motifs and arginine rich repetitive motifs. These results

show that ascovirus P64 proteins and homologs in other viruses comprise a novel family of viral gDNA condensing proteins.

3.2 Introduction

Virions of ascoviruses have a complex structural symmetry, with an ovoid shape that is typically 130 nm by 300-400 nm. They are large enveloped double-stranded DNA viruses with a genome ranging from 119-180 kbp (Federici *et al*., 2005, 2009). Aside from their size and complexity, they are unusual in several other respects, including their transmission and cytopathology. Specifically, virions are transmitted from one lepidopteran larval host to another on the ovipositors of endoparasitic wasps. Once cells are infected, they undergo a process resembling apoptosis, in which the apparent developing apoptotic bodies are converted in virion-containing vesicles. This results in a chronic, fatal disease. After formation, vesicle-bound and free progeny virions circulate in the hemolymph where they contaminate wasp ovipositors during egg-laying. (Federici *et al.*, 2005, 2009).

Within the vesicles, virions continue to assemble and mature. For all ascovirus species, the virions contain a dense nucleoprotein core comprised of circular dsDNA surrounded by a capsid layer and an outer membrane that has a reticulate pattern (Cheng *et al.*, 1999; Federici, 1983; Federici *et al.*, 2009). An important aspect of ascovirus biology that is not well understood is how their large genomes are condensed and packaged during virion assembly. In other viruses, several mechanisms have evolved for packaging viral DNA into virions. For example, in Hepatitis B virus, host-derived histones (14-30 kDa) are used to create nucleosomal structures and package DNA into

virions (Bock *et al.*, 2001). More often, viruses encode their own basic, DNA-condensing proteins that generally are smaller than eukaryotic histones. Typically, these are small basic proteins, e.g., small histone-like proteins as well as protamine-like proteins that condense genomes of dsDNA viruses such as adenoviruses, baculoviruses, and poxviruses (Andrabi, 2008; Bartova *et al.*, 2008; Lieberman 2008; Roos *et al.*, 2007; Sato and Hosokawa, 1984; Wilson *et al.*, 1987; Wilson *et al.*, 1988). However, analysis of the SfAV1a genome revealed that no genes coding for proteins similar to these were present, nor did any small, basic, DNA-binding proteins appear in the SfAV1a virion protein profile (Bideshi *et al.*, 2006; Tan *et al.*, 2009a). Nonetheless, genomic, SDS-PAGE, and MALDI-TOF studies did reveal a novel, large, basic, DNA-binding protein of 64 kDa that was abundant in the SfAV1a virion (P64, SfAV1a ORF048; GenBank CAL44648). This protein was observed by immunogold-labeling transmission electron microscopy (TEM) to progressively localize from the virogenic stroma into the SfAV1a virion core (Tan *et al.*, 2009b). These results suggested that P64 functioned in condensing SfAV1a genomic (g) DNA for encapsidation, but provided no direct evidence to support that conclusion.

Using a combination of centrifugation and transmission electron microscopy, I show that double-stranded (ds) DNA is condensed by P64 as well as by the two domains identified in P64. The N-terminus domain (referred to N-term hereafter) lies in the amino-terminal portion of P64 and has four virus-specific 2-cysteine adaptor motifs (vs2C-ad, Iyer *et al.*, 2006, Tan *et al.*, 2009b) specific to proteins from only three families of viruses (*Phycodnaviridae*, *Iridoviridae* and *Ascoviridae*). The vs2C-ad motif

(pfam08793.1) is characterized by two cysteines that are 30 to 31 amino acids apart and a proline that is 11 or 12 amino acids downstream of the first cysteine. The C-terminus basic domain (referred to as C-term hereafter) of P64 contains a tandem series of 14 arginine-rich motifs. Neither of the two types of motifs found in P64 has been characterized previously. Through parallel analyses of each of the domains and whole P64, I show that both domains have the capacity to bind and condense dsDNA. Furthermore, by Western and Southwestern analyses along with sequence analysis of genes from other ascovirus species, a major protein was identified in virions of TnAV2c, HvAV3e, and *Spodoptera exigua* AV 5a (SeAV5a, Federici *et al.*, 2009) and was confirmed as being antigenically and functionally related to P64. Proteins with motif arrangement similar to P64 were found in proteins from the genera Iridovirus, Chloriridovirus, and Ranavirus (family *Iridoviridae*). These viruses infect vertebrates and invertebrates in moist or aquatic environments and will also be discussed. These data strongly support the hypothesis that among large dsDNA viruses, P64 and its homologs comprise a novel family of proteins that sequester viral gDNA in virogenic stroma for condensation and packing into virions.

3.3 Materials and Methods

3.3.1 Virion purification. To prepare a stock of SfAV1a virions, *Spodoptera exigua* larvae were infected by puncturing late third-early fourth instars with virion laced needles. Nine days post infection, the hemolymph of infected larvae was collected in ice cold PBS (pH 7.4) with 1% glutathione. Infected hemolymph was sonicated 30 sec at 50% duty cycle using the Ultrasonic Homogenizer 4710 series (Cole-Parmer Instruments

Inc.) then spun at 1,200 x g using the TS-5.1-500 rotor in the Allegra 25R centrifuge (Beckman-Coulter Inc) for 10 min at ˚4C. The supernatant was layered on top of a smooth sucrose gradient (20-55%) at 4°C and centrifuged for 1 h using a Beckman SW28 rotor at 104,000 x g. The band of virus was collected and washed in ice cold PBS, spinning at 104,000 x g for 1 h at 4˚ C. SfAV1a virion pellet was resuspended in PBS and stored at -80˚ C.

Chilo iridescent virus 6 virions were a gift from Dr. Shan Bilimoria of Texas Tech University, Lubbock, Texas. A procedure described previously (Federici, 1980) was modified to purify iridovirus virions from purple colored pill bugs (*Armadillidium vulgare*), assumed to be infected, collected from the University of California, Riverside campus. Pill bugs were ground with a glass tube and pestle (Kontes) 12 bugs at a time in 4 ml 0.1 M phosphate buffer. The volume was brought to 15 ml and poured through three layers of cheese cloth. An additional 5 ml phosphate buffer was added to filtrate and the total mix was poured through four layers of fresh cheese cloth. Using vacuum filtration, the second filtrate was passed through a 0.8 µm nucleopore membrane (Millipore). To collect suspended iridovirus, the filtrate was centrifuged at 21,000 x g for 35 min at ˚4C. To purify iridovirus, the pellet was suspended in 2 ml of phosphate buffer and loaded onto a smooth sucrose gradient (25-55%) and centrifuged at 65,300 x g for 1 h at 4˚ C. The band of virions (at approximately 45% sucrose) was collected, washed, and reloaded on another smooth sucrose gradient. Virions were collected, washed, and stored at -70˚ C in 0.1 M phosphate buffer.

3.3.2 SDS-PAGE, Western and Southwestern blotting. Proteins were fractionated by SDS-PAGE, blotted on PVDF membranes (GE Osmonics) and analyzed with Western and Southwestern methods described previously (Federici *et al.* 1990; Tan *et al.* 2009b).

3.3.3 Recombinant 6-histidine-tagged proteins. Recombinant 6-histidine-tagged P64 (rP64) was produced using the Bac-to-Bac (Invitrogen) expression kit as previously described (Tan *et al.* 2009b). Recombinants of the vs2C-ad domain in the amino-terminal (rN-term) and the basic repeats in carboxy-terminal (rC-term) were expressed with the histidine tag on the amino-terminus of each recombinant and purified in a similar manner as rP64 (Fig. 3.1A). SfAV1a genomic (g) DNA was purified with DNAzol (Invitrogen) according to the manufacturer's instructions and used for PCR. The rN-term included the first 219 amino acids of P64 (SfAV1a048) and was amplified by PCR using the primer pair P64forward 5'-CGCGGATCCATGGCGTCAAAACGTAAA-3' and N1reverse 5'-ATACTCGAGGGCGCCGTGACACATGCT-3'. Amino acids 265 to 565 of P64 were included in the rC-term and amplified by PCR using the primer pair Cforward 5'-AGAGGATCCAGCACGAGTCGTTCCAAG-3' and P64reverse 5'-CCGCTCGAGATCCTTCGACGATCAGGT-3'.

3.3.4 Electrophoretic mobility shift assay (EMSA) using radiolabeled DNA. An oligonucleotide (5'-TAAAGGTTTAAATAACAGTTTAAATTTAAGTT TAACTTTCAGTTTACA-3') and its complement were labeled with [^{32}P]-ATP by T4 polynucleotide kinase (New England Biolabs) according to the manufacturer's instructions and the protocol described in Tang *et al.* (2007). The reaction was stopped by

adding EDTA up to 5 mM. Free [^{32}P]-ATP was removed by using Micro Bio-Spin 30 chromatography columns (Bio-Rad) according to the manufacturer's instructions. The level of radioactivity was determined by scintillation counting. Water or increasing amounts of protein (25, 50, 100 and 150 ng) were combined with approximately 11,000 CPM of 65 nt radiolabeled probe per reaction in DNA binding buffer (DBB) (25 mM Tris pH 7.5, 0.05% Triton X-100, 50 mM KCl, 5% glycerol, 0.05 mM ZnCl) in a volume of 15 µl and incubated overnight at 4° C. Reactions were resolved on 4% polyacrylamide gels prepared from a recipe modified from Tang *et al.* (2007) and Current Protocols in Molecular Biology (ed. Ausubel *et al.*, 1994). Gels included 10% acrylamide (bis-acrylamide 40%, 37.5:1, Fisher), 40% 1X TBE, 37% ddH_2O, 0.5% ammonium persulfate (10% w/v solution), and 0.07% TEMED (EMD Chemicals). Electrophoresis was done at 120V for 2 h. Gels were dried on blotting paper (Ahlstrom) and exposed to X-ray film.

3.3.5 EMSA using plasmid DNA. Observation of purified recombinant proteins in 0.7% agarose gels showed that DNA was present and bound to the proteins (data not shown), therefore, where indicated, rP64, rN-term, and rC-term in DBB were pretreated with micrococcal nuclease (MNase) with MNase buffer (New England Biolabs) for 1.5 h at 37° C then with 5 mM EGTA before adding 4 ng of plasmid DNA (linearized pIZT/V5-His; Invitrogen). The same was done for controls with no protein, BSA, and cytochrome c (cyt c; Sigma). The DNA-protein mixtures were then heated at 60° C for two minutes to encourage the release of endogenous DNA (DNA that co-purified with protein under denaturing conditions) and its replacement with plasmid and then incubated at 4° C overnight. Plasmid DNA was incubated with increasing amounts of protein: 0.5-

2.0 μg of rP64, 0.5-1.5 μg of rN-term, 0.13-0.5 μg of rC-term, 4.0 μg BSA, and 0.4-2.0 μg cyt c. Total reaction volumes were kept below 40 μl. Reactions were resolved in 0.7% agarose gels containing the nucleic acid stain GelRed (Phenix).

3.3.6 DNA-protein complex aggregation. Additional reactions were prepared as described in the EMSA method using plasmid DNA except for two changes: (1) 15 ng SfAV1a gDNA was used instead of plasmid, (2) proteins were not pre-treated with MNase but were still heated to increase the likelihood of SfAV1a gDNA replacement of endogenous nucleic acids (similar reactions were done using plasmid DNA and MNase treated protein but not shown here). After incubation, protein-DNA complexes were pelleted at 16,300 x g for 30 min at 25 ^{o}C. Supernatants were transferred to new tubes and mixed with 1.5 μl glycerol. The remaining pellets were dissolved in 10 μl of 0.1 X TE and 1 μl glycerol. Supernatant and pellet fractions for each protein-DNA combination were resolved by electrophoresis (100 volts, 1 h) in a 0.7% agarose gel containing GelRed.

3.3.7 Transmission electron microscopy. SfAV1a gDNA-protein complexes were prepared according to the DNA-protein complex aggregation method described above. After centrifugation and separation of supernatant and pellet fractions, resuspended pellets were adsorbed onto discharged carbon-coated formvar grids according to a method adapted from Black and Center (1979). For SfAV1a gDNA only and BSA-gDNA (negative) controls, the suspension were not centrifuged but simply adsorbed onto grids. Samples were first placed on parafilm. A grid was touched to the surface of the droplet of sample for 1 min and 30 sec. The grids were lifted and touched

to the surface of a drop of 0.25 M ammonium acetate for 40 sec then lifted and touched to the surface of a drop of 4% uranyl acetate in 50% ethanol. Grids were touched to a drop of 95% ethanol twice and flicked to remove the excess ethanol each time then allowed to dry. Samples were examined by TEM (FEI Tecnai) and photographed with a Gatan US 1000 camera.

3.3.8 MALDI-TOF and bioinformatics. Iridovirus virion structural proteins were prepared and submitted for matrix assisted laser desorption ionization-time of flight (MALDI-TOF) mass spectrometry analysis as described in Tan *et al*. (2009a). BLAST analyses of ascovirus and iridovirus ORFs were performed using NCBI's protein database (http://www.ncbi.nlm.nih.gov). The ScanProsite and ProtParam programs in the Expasy proteomics server from Swiss Institute of Bioinformatics (http://expasy.org/tools/#proteome) were used to analyze various proteins for amino acid composition and the presence of repeats. Sequence alignment and phylogenetic analyses were carried out through Biology WorkBench from the Sand Diego supercomputer center (http://workbench.sdsc.edu/) using the CLUSTALW (Thompson *et al*., 1994) and PHYLIP (Felsenstein, 1989) programs.

3.4 Results

3.4.1 Electrophoretic mobility shift assays. The recombinant proteins (Fig. 3.1A) were first analyzed for their correct size and antigenic relatedness to P64 by Western blotting (Fig. 3.1B). Analysis of P64's ability to bind DNA revealed that rP64 is versatile in its capacity to bind various types of dsDNA. Parallel analysis of the rN-term and the rC-term showed that these domains were also able to bind DNA independently of

each other. All recombinant proteins (rP64, rN-term, and rC-term, Fig. 3.1B) were able to bind a 65nt DNA oligonucleotide radiolabeled probe (Fig. 3.2). All recombinant proteins were able to prevent the migration of plasmid DNA from the wells of agarose gels (Fig. 3.3). Analysis of the purified recombinant proteins showed that a small amount of DNA, which probably originated from the Bacmid infected TN5 cell lysate, adhered to these proteins, even though denaturing conditions were used (data not shown). To reduce the amount of this contaminating rP64, rN-term, and rC-term were treated with a MNase-EGTA-plasmid addition-heat shock series. This treatment did not interfere with the recombinant proteins' ability to bind DNA (Fig. 3.3), as was evident from their capacity to bind plasmid DNA. The DNA alone or BSA-DNA reactions did not show a shift in DNA migration (Fig. 3.2 and 3.3). Cytochrome c (cyt c)-DNA reactions, the positive control, did demonstrate a shift in DNA ~~as~~ compared to the negative controls (Fig. 3.2).

3.4.2 DNA Aggregation. The ability of rP64, rN-term, and rC-term to aggregate different types of DNA was determined using an incubation-centrifugation technique. Recombinant P64, rN-term, and rC-term were incubated overnight with plasmid DNA (data not shown) or SfAV1a gDNA (Fig. 3.4) in parallel with BSA and cyt c controls, and then pelleted by centrifugation. Supernatant fractions were compared with their corresponding pellet fractions from DNA-recombinant protein preparations that were put through the MNase-EGTA-plasmid addition-heat shock series (data not shown), as well as to those that had only been heat shocked (Fig. 3.4). The rP64, rN-term, and rC-term caused aggregation of SfAV1a gDNA, which was primarily observed in the well of the pellet fractions (Fig. 3.4, arrow). The gDNA only and BSA-gDNA controls did not

induce aggregation of DNA since all the DNA remained in the supernatant fraction and migrated into the agarose gel (Fig. 3.4). The cyt c-gDNA fractions showed bound and unbound gDNA in both the supernatant and the pellet. The cyt c-gDNA sample shown has the strongest signal coming from gDNA in the well of the supernatant fraction (Fig. 3.4). This results from the cyt c-gDNA complex being more sensitive to heat disruption than recombinant protein-gDNA interactions. If the cyt c-gDNA mixture had not been heated, all gDNA would have gone to the pellet fraction and stayed in the well (data not shown). Twice as much cyt c will also cause more gDNA to go to the pellet (data not shown).

Cyt c does not function as a DNA associating protein in normal cellular processes but it has been used in methods for preparing DNA for electron microscopy. The basic nature of cyt c (pI 9.59) allows it to bind DNA and in electron microscopy procedures it has been noted to "spread" rather than condense DNA (Bock and Zentgraf, 1993; Brack, 1981; Serwer, 1978). Cyt c was used as a positive control to distinguish its binding/spreading character from P64's proposed condensing character. In this analysis, cyt c did bind (Fig. 3.2) and precipitate DNA (Fig. 3.4).

3.4.3 Transmission Electron Microscopy. To determine the effect of each protein on DNA conformation, samples were prepared and negatively stained for observation by TEM. For SfAV1a gDNA and BSA-gDNA preparations, suspensions that were not centrifuged were examined by TEM (Fig. 3.5, A-D). For SfAV1a gDNA mixtures with cyt c, rP64, rN-term, or rC-term (Fig. 3.5, E-L) the pellet fractions were used to determine the DNA conformation. SfAV1a gDNA only (Fig. 3.5, A and B) and

BSA-gDNA (Fig. 3.5, C and D) preparations had tangled and individual strands of SfAV1a DNA, but no dense aggregates of DNA. The cyt c-gDNA pellet also showed no condensed DNA, just individual linear strands (Fig. 3.5, E and F). Condensed foci of DNA complexes of various sizes were observed in the presence of rP64, rN-term, and rC-term (Fig. 3.5, K-L). The formation of condensed SfAV1a gDNA with the recombinant proteins resembled DNA-protein complexes observed in similar studies with the adenovirus major core protein (Black and Center, 1979) and the amyloid β-peptide (Yu *et al.*, 2007).

3.4.4 Homologs of P64. Among ascoviruses, apparent P64 homologs are encoded by the HvAV3e (*orf061*, 67.7 kDa; GenBank AB037247.1) (Asgari *et al.*, 2007) and TnAV (*orf141*, 72.7 kDa; GenBank ABF706581) (Wang *et al.*, 2006). Although it is known that TnAV ORF141 is a major component of the TnAV virion (Cui *et al.*, 2007), data related to proposed function(s) of this and other ascovirus P64 homologs have not been reported. Examination of putative amino acid sequences of these proteins showed that they have a structural architecture similar to P64 (Fig. 3.6). The amino-terminal domain of each of the P64 homologs in ascoviruses contains four copies of the vs2C-ad motif (Iyer *et al.* 2006) (Fig. 3.6A). Each of the ascovirus vs2C-ad is composed of two cysteines separated by 30-31 amino acids and a conserved proline residue 11-12 amino acids downstream from the first cysteine. In database searches (www.ncbi.nlm.nih.gov/sites/gquery), few proteins encoded by members of large dsDNA virus families with significant homology to the vs2C-ad in ascovirus P64 homologs were identified. These included a putative protein from the DpAV that contained one copy of

the vs2C-ad in its amino-terminal region (Bigot *et al.*, 2009) and proteins from several members of the family *Iridoviridae*, including the Chilo iridescent virus type 6 (CIV6) ORF232R (GenBank AAK82093, Iridovirus) and the Frog virus 3 ORF019R (GenBank AAT09678.1, Ranavirus), that contained, respectively, two and five vs2C-ad motifs (Fig. 3.6A). Among other virus families, one putative protein (ORF676R, GenBank AAC96984.1, *Phycodnaviridae*: Chlorovirus) encoded by the *Paramecium bursaria* chlorella virus (PBCV) was identified (Fig. 3.6A).

Not all of the proteins having the vs2C-ad motif have the accompanying basic, tandem motifs found in SfAV1a P64, but several do have both types of motifs. The SfAV1a P64 protein has 15 copies of the basic motif (Fig. 3.6B). HvAV3e ORF061 contains 14 basic motifs, whereas 12 basic motifs are present in TnAV6a ORF141. In addition to arginine, each of the basic motifs is also rich in serine residues. BLAST searches revealed a few proteins of iridoviruses that have both the vs2C-ad and basic repetitive motifs. CIV6 ORF232R contains 13 repeats, P(S/T)RRSS(P)R, divided into three separate blocks of tandem motifs in addition to the two vs2C-ad motifs (Fig. 3.6B). Two of those repeats in CIV6 ORF232R occur within the first vs2C-ad motif (Fig. 3.6A). The mosquito iridescent virus 3 (MIV3, Chloriridovirus) ORF100L (GenBank ABF82130) also has two vs2C-ad motifs (Fig. 3.6A) along with four SPSRRTTRS repeats in tandem (Fig. 3.6B) and is less than half the size of P64 or CIV6 ORF232. Another uncharacterized protein (not shown, GenBank ACO25279) that was found in the Epizootic hematopoietic necrosis virus (Ranavirus) having four vs2C-ad motifs and 13 SPAR[K/R/S] repeats.

Western analysis using an anti-P64 antibody helped determine whether any protein species in the complete virion protein profiles of HvAV3e, TnAV2c, and SeAV5 (Fig. 3.7A) were antigenically related to SfAV1a P64 (Fig. 3.7B). The antibody recognized similar major virion proteins and these homologs were the only species that bound DNA in Southwestern assays (Fig. 3.7C). As with SfAV1a, I cannot conclude whether the method used in the assay suppressed or abolished DNA-binding activity of other AV virion proteins. However, based on complete genomic sequence data for the SfAV1a, HvAV3e and TnAV2c (Bideshi *et al.*, 2006; Bigot *et al.*, 2009; Asgari *et al.*, 2007; Wang *et al.*, 2006), it is known that these AVs do not encode additional cationic proteins suggestive of this function.

3.4.5 Iridovirus DNA-binding proteins. Since ascoviruses have many homologous genes in common with iridoviruses, virions of SfAV1a, CIV6 and an iridovirus purified from *Armadillidium vulgare* (AIV) were analyzed for similarities. Specifically, Western and Southwestern procedures were used to determine if DNA binding proteins antigenically similar to P64 were present in CIV6 and AIV. Western blotting indicated that CIV6 had two at least two proteins with some antigenic similarity to P64 (Fig 3.8B). AIV appeared to have at least one small protein with antigenic similarity to P64 which matched the migration of the smaller band in CIV6 that was recognized by the anti-P64 antibody. The result of the Southwestern procedure was more pronounced and showed large and small DNA binding proteins in iridoviruses as compared to only one large DNA binding protein (P64) in SfAV1a (Fig 3.8C).

Several of the proteins (a 60 kDa and a 20 kDa protein from AIV, and 10 kDa proteins from AIV and CIV6) corresponding to the location of DNA binding proteins in the Southwestern were sent for mass spectrometric analysis (MALDI-TOF) for identification (Table 3.1). Peptides resulting from cleavage during mass spectrometry were compared to a protein database containing viral protein sequences. Several genomes of different iridoviruses have been sequenced and annotated including CIV6 (also known as IIV6), but the one for AIV (also known as IIV31) has not been sequenced. For this reason, proteins from AIV were correlated to the closest matches in CIV6 (Table 3.1). The majority of the MALDI-TOF proposed matches were not basic, nor did they have basic stretches or domains that might indicate they bound DNA. Only three small proteins in the lower DNA binding band of the CIV6 protein profile contained a basic stretch of amino acids but no identifiable function (Table 3.1): CIV6 ORF84L [LRATLAAKKKELKTLRTARKK], CIV6 ORF312R [RRRRUMWGRWRK], and CIV6 ORF466 (pI 9.1).

3.4.6 Phylogeny. Seven protein sequences were noted that contained one or more vs2C-ad motifs and tandem repeats of basic motifs (Fig 3.9A). Except for two, these proteins were identified in previous analyses (Bigot *et al.*, 2009). Three were from the family *Iridoviridae* (ORF232 *Chilo* iridescent virus 6; MIV100L *Aedes taeniorhynchus* iridescent virus; and ORF89L Epizootic haematopoietic necrosis virus) and four were from *Ascoviridae* (ORF48 SfAV1a, ORF61 HvAV3e, ORF141 TnAV2c, and ORF8 DpAV4a). Sequence alignment and phylogenetic analyses indicated that the P64 homologs in SfAV1a, HvAV3e, and TnAV2c were closely related (Fig. 3.9A). The

homolog in DpAV4a, however, grouped with the IIV6 homolog in a separate clade (Fig. 3.9A) which confirmed previous findings and supports the hypothesis that DpAV4a is of separate origin or in a separate subfamily apart from the other ascoviruses (Bigot *et al.*, 2009). BLAST searches using the N-terminal domain of P64 showed a number of proteins from different genera of *Iridoviridae* and *Phycodnaviridae* that had one to ten vs2C-ad motifs and zero to three pentapeptide basic repeats; representative proteins of the vs2C-ad type were aligned and used to create a phylogenetic tree (Fig. 3.9B). Results from C-terminal BLAST searches revealed three types of putative protein sequences containing an extensive amount of basic repeats in *Iridoviridae* and *Phycodnaviridae*. Representative proteins of the tandem-basic-repeat-type were also used to create a phylogenetic tree (Fig 3.9C). One type included large (over 630 amino acids) proteins (Fig 3.9C, highlighted) having basic, tandem repeats and having a motif reminiscent of the vs2C-ad: two cysteines were 32-33 amino acids apart with many conserved residues in between (not shown). Another type of basic protein in the *Iridoviridae* included smaller putative proteins (less than 300 amino acids, Fig 3.9C asterisks) with the first 30 amino acids (not shown) having significant similarity with a region of the larger basic proteins including a region that was not basic or repetitive. The third type of basic repetitive protein found with BLAST searches of the P64 C-terminal domain was also small but held no noticeable similarity to the other basic proteins besides their basic repeats.

3.5 Discussion

Collectively, the results reported here and in a previous report (Tan *et al.*, 2009b) lend strong support to the hypothesis that P64 plays a vital role in nucleating the SfAV1a gDNA for condensation and packaging it into mature virions. My latest results show that rP64 has non-specific, DNA-binding activity and is able to induce DNA condensation. The amino-terminal domain of P64 containing the vs2C-ad's (rN-term) and the carboxy-terminal domain containing a series of arginine rich tandem repeats (rC-term) were able to bind and aggregate DNA also. The combination of the two domains in P64 makes it a novel type of DNA-condensing protein relative to histones, protamines, or other virus-derived, DNA-condensing proteins. There are other DNA condensing proteins with multiple domains. For example, the DNA-interacting domain accompanies an oligomerization domain in the bacterial H-NS protein (Esposito *et al.*, 2002) and a globular domain in histones (Tanaka *et al.*, 2005). Basic (aginine/lysine rich), repetitive motifs in DNA condensing proteins have, until now, only been seen in the transition protein HANP1 (Tanaka *et al.*, 2005) and sperm basic nuclear protein PL-1 (Lewis *et al.*, 2004) and contributes their DNA binding function. However, none of these contain vs2C-ad motifs.

The ability of rN-term to bind DNA is likely due to the presence of a short, arginine-rich stretch located in between the second and third vs2C-ad motif, see Fig. 3.1A (Tan *et al.*, 2009b). The ability of rN-term to aggregate DNA could be due to the formation of homomeric complexes when bound to DNA because of their closer proximity. This would not be outside the realm of possibilities since eukaryotic histones,

bacterial H-NS proteins, human adenovirus major core protein VII, and shrimp white spot syndrome virus VP15 form oligomers when complexing with DNA (Pusarla and Bhargava, 2005; Sato and Hosokawa, 1984; Esposito *et al.*, 2002; Witteveldt *et al.*, 2005). I hypothesize that the vs2C-ad functions differently from the repetitive basic domain by allowing P64 to form homo- or heteromeric protein-protein complexes. Further studies are required to determine whether such protein-protein interactions take place.

Although P64 and the recombinant domains were co-purified (under denaturing conditions) with DNA from Bacmid infected TN5 cells, they were still able to bind and aggregate the DNA that was added in the experiments. This reflects a remarkable stability in the P64-DNA interaction.

As with the ascovirus P64 homologs, the basic motif occurring in the carboxy-terminal of CIV6 ORF232R suggests a function in nucleic-acid binding, and perhaps a role in condensation and packing of the viral genome. At present, such activities have not been characterized for ORF232R or any of the other iridovirus homologs of P64. There is evidence to suggest that this protein is part of mature CIV6 virion structure (Ince *et al.*, 2010). Proteins containing the vs2C-ad have also been identified as virion structural proteins in species of the genus megalocytivirus, family *Iridoviridae* (Dong *et al.*, 2010). In addition, Southwestern blotting of CIV6 virion proteins reveals a DNA binding protein at the predicted size of CIV6 ORF232R along with much smaller DNA binding proteins (Fig. 3.8C). Phylogenetic analysis of P64 and CIV6 ORF232 along with other ascovirus and iridovirus proteins by Bigot *et al.* (2009) suggested an interesting relationship among these viruses. The invertebrate iridovirus CIV6 ORF232 occurs in the clade with

ascoviruses, completely separate from vertebrate iridovirus proteins (Bigot *et al.*, 2009). This is likely because the vertebrate iridovirus proteins chosen as homologs of P64 had few to no basic repeats, whereas the CIV6 ORF323R had both the vs2C-ad motifs and a longer extension of basic motifs, similar to the ascovirus P64 homologs. Phylogenetic analysis using a set of proteins only having both the vs2C-ad and basic motifs confirmed the divergent relationship (Fig. 3.9A) between DpAV4a and the other ascoviruses noted in Bigot *et al*. (2009) but put P64 homolog from the Epizootic haematopoietic necrosis virus in a clade closer to SfAV1a, HvAV3e and TnAV2c rather than with the other *Iridoviridae* P64 homologs (Fig. 3.9A). This would also support the idea of a separate origin for AVs and DpAV but both would still be derived from viruses similar to iridoviruses. The proteins having mainly vs2C-ad are from the families *Iridoviridae* and *Phycodnaviridae* and suggest a possible source for the vs2C-ad motifs in AVs. The phylogeny of the basic types of proteins tells more about how the various sequences are related to each other than about possible origins. The concern is that repetitive sequences in all of these proteins could simply represent homoplasy or convergent evolution rather than a true evolutionary relationship. Nonetheless, the presence of a motif similar to the vs2C-ad in some of those basic proteins is of compelling interest because it could represent another kind of 2C-ad or a precursor to the one in P64. It is likely that these motifs (the vs2C-ad and basic repeat) are able to function separately but became joined in ascoviruses and certain iridoviruses, to function specifically as dsDNA condensing and packaging proteins able to assemble virion cores.

Tan *et al.* (2009b) demonstrated that P64 is phosphorylated in the purified recombinant form. In these studies, phosphorylated, rP64 was still able to bind and condense dsDNA. It seems that the negatively charged phosphates on serine and threonine residues in the positively charged P64 should prevent DNA binding; however, phosphorylation does not have to be a zero sum situation. There are examples of phosphorylation of a DNA binding protein leading to the disruption of DNA-binding, e.g. the hepadnavirus HBV capsid protein p21.5 (Machida *et al.*, 1991; Hatton *et al.*, 1992). On the other hand, histones H1 and H3 are phosporylated during mitosis when DNA is condensed (Spencer and Davie, 1999; He and Lehming, 2003) and protamine-2 must be phosphorylated in order to replace the transition proteins for the repackaging of DNA in proper spermatid maturation (Wu *et al.*, 2000). It may be that phosphorylation of P64 is not meant to completely abolish DNA-binding but loosen the association to varying degrees to allow the replication and translation machinery access to viral DNA. The NetPhosK 1.0 server (http://www.cbs.dtu.dk/services/NetPhosK/, Blom *et al.*, 2004) predicts over 50 phosphorylation sites in P64 for protein kinase C alone, the majority of those sites being located among the basic repeats in P64. Varying levels of phosphorylation could provide the ascovirus with an intricate means of controlling viral DNA condensation, gene expression and protein-protein interactions.

The ability of the rN-term and the rC-term to precipitate DNA and the variation in repetitive sequences among P64 homologs could provide a clue as to what kind of arginine-rich sequence could be useful in peptide-mediated gene delivery (amino acids 95-120 of P64, SfAV1a ORF 48). Martin and Rice (2007) noted many lysine-rich

peptides that have been examined for their ability to deliver DNA to the nucleus *in vivo* and *in vitro* in efforts to find novel gene therapy approaches. Virus-derived peptides have been used to aid gene delivery: nuclear localizing sequences from simian virus 40 and adenovirus peptides have been used in conjunction with cationic peptides to increase nuclear uptake of DNA (Martin and Rice, 2003). In addition, a cationic peptide, mu, from the adenovirus has been shown to significantly improve the delivery of a plasmid by cationic lipids in vivo (Murray *et al.*, 2001). Histones have also been analyzed for their effectiveness in mediating the transfection of genes (Kaouass *et al.*, 2006). With peptide-mediated gene transfection there are concerns about immunogenicity and stability of the DNA peptide complex once inside a patient. These concerns could be mitigated with the use of sequences from P64 because it behaves similarly to histones and protamines in its ability to tightly bind DNA, yet the sequence would be different from those found in vertebrate systems. P64 appears to be stable and can be manipulated in various ways and still maintain its DNA binding capacity as demonstrated in this body of work and previously (Tan *et al.*, 2009b), it could, therefore, provide a viable alternative for use of peptides in non-viral gene transfer.

Finally, P64, and by extension other viral P64 homologs, functions in condensing SfAV1a gDNA through interactions with its basic carboxy-terminal while the amino-terminal is likely to mediate DNA binding and association with other virion structural proteins for virus assembly. P64 has features found in several types of DNA condensing proteins from various sources. These shared features support the classification of P64 as a DNA condensing protein that may oligomerize during assembly and envelopment of the

virion core. However, these various features do not allow for P64 to be classified as a histone or protamine like those in eukaryotes, or a small basic protein like those in bacteria and viruses. Due to the large size of the P64 protein and its homologs, their unique combination of the vs2C-ad and basic repetitive domains, and the data reported here and elsewhere (Tan *et al.*, 2009b), P64 should be considered the first in a novel family of proteins that nucleate and condense ascovirus gDNA beginning in virogenic stroma and continuing as the core is transported, encapsidated, and enveloped.

3.6 References

Andrabi, S. M. H. 2008. Mammalian sperm chromatin structure and assessment for DNA fragmentation. J. Assist. Reprod. Genet. **24:**561-569.

Asgari, S., J. Davis, D. Wood, P. Wilson, and A. McGrath. 2007. Sequence and organization of the *Heliothis virescens* ascovirus genome. J. Gen. Virol. **88:**1120-1132.

Ausubel, F. M., R. Brent, R. E. Kingston, D. D. Moore, J. G. Seidman, J. A. Smith, and K. Struhl. 1994. Current Protocols in Molecular Biology. Wiley, New York, NY. 12.2.1-12.2.7**.**

Bartova, E., J. Krejci, A. Harnicarova, G. Galiova, and S. Kozubek. 2008. Histone modifications and nuclear architecture: a review. J. Histochem. Cytochem. **56:**711-721.

Bideshi, D. K., M. V. Demattei, F. Rouleux-Bonnin, K. Stasiak, T. Tan, S. Bigot, Y. Bigot, and B. A. Federici. 2006. Genomic sequence of the *Spodoptera frugiperda ascovirus 1a*, an enveloped, double-stranded DNA insect virus that manipulates apoptosis for viral reproduction. J. Virol. **80:**11791–11805.

Bigot, Y., S. Asgari, D. Bideshi, X. W. Cheng, B. A. Federici, and S. Renault. 2008. http://gicc.univ-tours.fr/recherche/projets/pics.php?connect=0&dang=en

Bigot, Y., A. Rabouille, P. Y. Sizaret, M. H. Hamelin, and G. Periquet. 1997. Particle and genomic characteristics of a new member of the *Ascoviridae*: *Diadromus pulchellus* ascovirus. J Gen. Virol. **78:**1139-1147.

Bigot, Y., S. Renault, J. Nicolas, C. Moundras, M. V. Demattei, S. Samain, D. K. Bideshi, and B. A. Federici. 2009. Symbiotic virus at the evolutionary intersection of three types of large DNA viruses; iridoviruses, ascoviruses, and ichnoviruses. PLoS One **4:**e6397.

Black, B. C., and M. S. Center. 1979. DNA-binding properties of the major core protein of adenovirus 2. Nucleic Acids Res. **6:**2339-2353.

Blom, N., T. Sicheritz-Ponten, R. Gupta, S. Gammeltoft, S. Brunak. 2004. Prediction of post-translational glycosylation and phosphorylation of proteins from the amino acid sequence. Proteomics **4**:1633-49.

Bock, T., S. Schwinn, S. Locarnini, J. Fyfe, M. P. Manns, C. Trautwein, and H. Zentgraf. 2001. Structural organization of the Hepatitis B virus minichromosome. J. Mol. Biol. **307:**183-196.

Bock, C. T. and H. Zentgraf. 1993. Detection of minimal amounts of DNA by electron microscopy using simplified spreading procedures. Chromosoma. **102:**249-252.

Brack, C. 1981. DNA electron microscopy. CRC Crit. Rev. Biochem. **10:**113-169.

Bradford, M. M. 1976. A rapid and sensitive method for the quantitation of microgram quantities utilizing the principle of protein dye binding. Anal. Biochem. **72:**248-254.

Brewer, L. R., M. Corzett, and R. Balhorn. 1999. Protamine-induced condensation and decondensation of small DNA molecules. Science **286:**120-123.

Carner, G. R. and J. S. Hudson. 1983. Histopathology of virus-like particles in *Heliothis* spp. J. Invertebr. Pathol. **41:**238-249.

Cheng, X. W., G. R. Carner, and T. M. Brown. 1999. Circular configuration of the genome of ascoviruses. J. Gen. Virol. **80:**1537-1540.

Cui, L., X. Cheng, L. Li, and J. Li. 2007. Identification of *Trichoplusia ni ascovirus* 2c virion structural proteins. J. Gen. Virol. **88:**2194-2197.

Dong, C., S. Weng, Y. Luo, M. Huang, H. Ai, Z. Yin, and J. He. 2010. A new marine megalocytivirus from spotted knifejaw, *Oplegnathus punctatus*, and its pathogenicity to freshwater mandarinfish, *Siniperca chuatsi*. Vir. Res. **147:**98-106.

Esposito, D., A. Petrovic, R. Harris, S. Ono, J. F. Eccleston, A. Mbabaali, I. Haq, C. F. Higgins, J. C. D. Hinton, P. C. Driscoll, and J. E. Ladbury. 2002. H-NS oligomerization domain structure reveals the mechanism for high order self-association of the intact protein. J. Mol. Biol. **324:**841-850.

Federici, B. A. 1982. A new type of insect pathogen in larvae of the clover cutworm, *Scotogramma trifolii*. J. Invertebr. Pathol. **40:**41-54.

Federici, B. A. and R. Govindarajan. 1990. Comparative histopathology of three Ascovirus isolates in larval noctuids. J. Invertebr. Pathol. **56:**300-311.

Federici, B. A. 1983. Enveloped double stranded DNA insect virus with novel structure and cytopathology. Proc. Natl. Acad. Sci. USA. **80:**7664-7668.

Federici, B. A., D. K. Bideshi, Y. Tan, T. Spears, and Y. Bigot. 2009. Ascoviruses: Superb manipulators of apoptosis for viral replication and transmission. Curr. Topics Microbiol. Immunol. **328:**171-196.

Federici, B. A., Y. Bigot, R. R. Granados, J. J. Hamm, L. K. Miller, I. Newton, K. Stasiak, and J. M. Vlak. 2005. Family *Ascoviridae*, p. 269–274. *In* C. M. Fauquet, M. A. Mayo, J. Maniloff, U. Desselberger, and L. A. Ball (ed.), Virus Taxonomy: Eighth Report of the International Committee on Taxonomy of Viruses. Academic Press, San Diego.

Federici, B. A., J. M. Vlak, and J. J. Hamm. 1990. Comparative study of virion structure, protein composition and genomic DNA of three ascovirus isolates. J. Gen. Virol. **71:**1661-1668.

Felsenstein, J. 1989. PHYLIP-Phylogeny Inference Package (Version 3.2). Cladistics **5**: 164-166.

Galibert, F., E. Mandart, F. Fitoussi, P. Tiollais, and P. Charnay. 1979. Nucleotide sequence of the hepatitis B virus genome (subtype ayw) cloned in *E. coli*. Nature **281:**646-650.

Gallina, A., F. Bonelli, L. Zentilin, G. Rindi, M. Muttini, and M. Milanesi. 1989. A recombinant hepatitis B core antigen polypeptide with the protamine-like domain deleted self-assembly into capsid particles but fails to bind nucleic acids. J. Virol. **63:**4645-4652.

Hamm, J. J., E. L. Styer, B. A. Federici. 1998. Comparison of field-collected ascovirus isolates by DNA hybridization, host range, and histopathology. J. Invertebr. Pathol. **72:**138-146.

Hatton, T., S. Zhou, and D. N. Strandring. 1992. RNA- and DNA-binding activities in Hepatitis B virus capsid protein: a model for their roles in viral replication. J. Virol. **66:**5232-5241.

He, H. and N. Lehming. 2003. Global effects of histone modification. Brief. Funct. Genomic Proteomic. **2**:234-243.

Ince, I. A., S. A. Boeren, M. M. van Oers, J. J. M. Vervoot, and J. M. Vlak. 2010. Proteomic analysis of Chilo iridescent virus. Virology. In press. doi:10.1016/j.virol.2010.05.038

Iyer, L. M., S. Balaji, E. V. Koonin, and L. Aravind. 2006. Evolutionary genomics of nucleo-cytoplasmic viruses. Virus Res. **111:**156-184.

Kaouass, M., R. Beaulieu, and D. Balicki. 2006. Histonefection: novel and potent non-viral gene delivery. J. Control Release **113:**245-254.

Lewis, J. D., R. McParland, J. Ausio. 2004. PL-I of *Spisula solidissima*, a highly elongated sperm-specific histone H1. Biochem. **43:**7766-7775

Lieberman, P. M. 2008. Chromatin organization and virus gene expression. J. Cell Physiol. **216:** 295-302.

Machida, A., H. Ohnuma, F. Tsuda, A. Yoshikawa, Y. Hoshi, T. Tanaka, S. Kishimoto, Y. Akahane, Y. Miyakawa, and M. Mayumi. 1991. Phosphorylation in the carboxyl-terminal domain of the capsid protein of Hepatitis B virus: evaluation with a monoclonal antibody. J. Virol. **65:**6024-6030.

Martin, M. E., and K. Rice. 2007. Peptide-guided gene delivery. AAPS J. **9:**E18-E29.

Murray, K. D., C. J. Etheridge, S. I. Shah, D. A. Matthews, W. Russell, H. M. D. Gurling, and A. D. Miller. 2001. Enhanced cationic liposome-mediated transfection using the DNA-binding peptide μ (mu) from the adenovirus core. Gene Ther. **8:**453-460.

Nalçacıoğlu, R., I. A. Ince, and Z. Demirbağ. 2009. The biology of Chilo iridescent virus. Virologica Sinica **24:**285-294.

Pusarla, R. H. and P. Bhargava. 2005. Histones in functional diversification: core histone variants. FEBS J. **20:**5149-5168.

Roos, W. H., I. L. Ivanovska, A. Evilevitch, and G. J. L. Wuite. 2007. Viral capsids: Mechanical characteristics, genome packaging and delivery mechanisms. Cell. Mol. Life Sci. **64:**1484-1497.

Sato, K. and K. Hosokawa. 1984. Analysis of the interaction between DNA and major core protein in adenovirus chromatin by circular dichroism and ultraviolet light induced cross-linking. J. Biochem. **4:**1031-1039.

Sato K. and K. Hosokawa. 1983. DNA-binding domain in adenovirus core protein VII. Biochem. Int. **4:**443-448.

Serwer, P. 1978. A technique for observing extended DNA in negatively stained specimens: observation of bacteriophage T7 capsid-DNA complexes. J. Ultrastruct. Res. **65:**112-118.

Siu, F. K. Y, L. T. O. Lee, and B. K. C. Chow. 2008. Southwestern blotting in investigating transcriptional regulation. Nat. Protocols **3:**51-58.

Spencer, V.A. and J. R. Davie. 1999. Role of covalent modifications of histones in regulating gene expression. Gene **240**:1-12.

Tan, Y., D. K. B. Bideshi, J. J. Johnson, Y. Bigot, and B. A. Federici. 2009(a). Proteomic analysis of the *Spodoptera frugiperda ascovirus 1a* virion reveals 21 proteins. J. Gen. Virol. **90:**359-365.

Tan, Y., T. Spears, D. K. Bideshi, J. J. Johnson, R. Hice, Y. Bigot, and B. A. Federici. 2009(b). P64, a novel major virion structural protein potentially involved in condensing the *Spodoptera frugiperda ascovirus 1a* genome. J. Virol. **83:**2708-2714.

Tanaka, H., N. Iguchi, A. Isotani, K. Kitamura, Y. Toyama, Y. Matsuoka, M. Onishi, K. Masai, M. Maekawa, K. Toshimori, M. Okabe, and Y. Nishimune. 2005. HANP1/H1T2, a novel histone H1-like protein involved in nuclear formation and sperm fertility. Mol. Cell Biol. **16:**7107-7119.

Tang, M., D. K. Bideshi, H. W. Park, and B. A. Federici. 2007. Iteron-binding ORF157 and FtsZ-like ORF156 proteins encoded by pBtoxis play a role in its replication in *Bacillus thuringiensis* subsp. *israelensis*. J. Bacteriol. **22:**8053-8058.

Thompson J.D., Higgins D.G., Gibson T.J. 1994. CLUSTAL W: improving the sensitivity of progressive multiple sequence alignment through sequence weighting, position-specific gap penalties and weight matrix choice. Nucleic Acids Res. **22**:4673-4680.

Vollenweider, J., J. M. Sogo, and T. Koller. 1975. A routine method for protein-free spreading of double and single-stranded nucleic acid molecules. Pro. Nat. Acad. Sci. USA **72:**83-87.

Wang, L., J. Xue, C. P. Seaborn, B. M. Arif, and X. W. Cheng. 2006. Sequence and organization of the *Trichoplusia ni ascovirus 2c* (*Ascoviridae*) genome. Virology **354:**167–177.

Wilson, M. E., T. H. Mainprizw, P. D. Friesen, and L. K. Miller. 1987. Location, transcription, and sequence of a baculovirus gene encoding a small arginine-rich polypeptide. J. Virol. **61:** 661-666.

Wilson, M. E., and K. H. Price. 1988. Association of *Autographa californica* nuclear polyhedrosis virus with nuclear matrix. Virology **167:**233-341.

Witteveldt, J., A. M. G. Vermeesch, M. Langenhof, A. de Lang, J. M. Vlak, and M. C. W. van Hulten. 2005. Nucleocapsid protein VP15 is the basic DNA binding protein of white spot syndrome virus of shrimp. Arch. Virol. **150:**1121-1133.

Wu, J. Y., T. J. Ribar, D. E. Cummings, K. A. Burton, G. S. McKnight, and A. R. Means. 2000. Spermiogenesis and exchange of basic nuclear proteins are impaired in male germ cells lacking Camk4. Nat. Genet. **25**:448-452.

Yu, H., Ren J, & Qu, X. 2007. Time-dependent DNA condensation induced by amyloid β-peptide. Biophys. J. **92:**185-191.

3.7 Figures

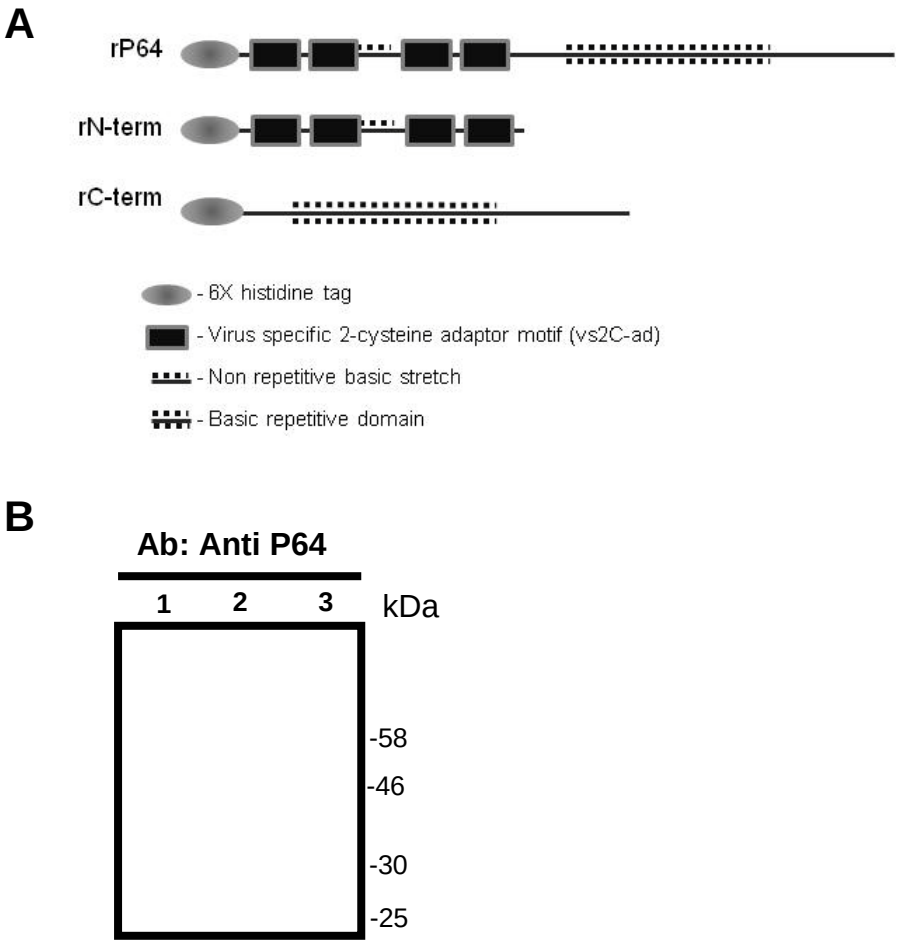

Figure 3.1 Diagram and Western blot verification of the identity of recombinant P64 and domains. (A) Histidine-tagged recombinant proteins derived from SfAV1a ORF48 were constructed with the histidine tag at the amino terminus. Each construct was expressed using the Bac-to-Bac expression system and included the entire sequence for P64 (rP64), the sequence encompassing the four virus specific 2-cysteine adaptor motifs (rN-term), or that encompassing the basic repetitive domain (rC-term). (B) Recombinant proteins were purified using Ni-NTA agarose beads. Recombinant proteins rP64 (lane 1), rN-term (lane 2), and rC-term (lane 3) were resolved by SDS-PAGE and their identity was verified by Western Blotting using a rat-derived anti-P64 antibody.

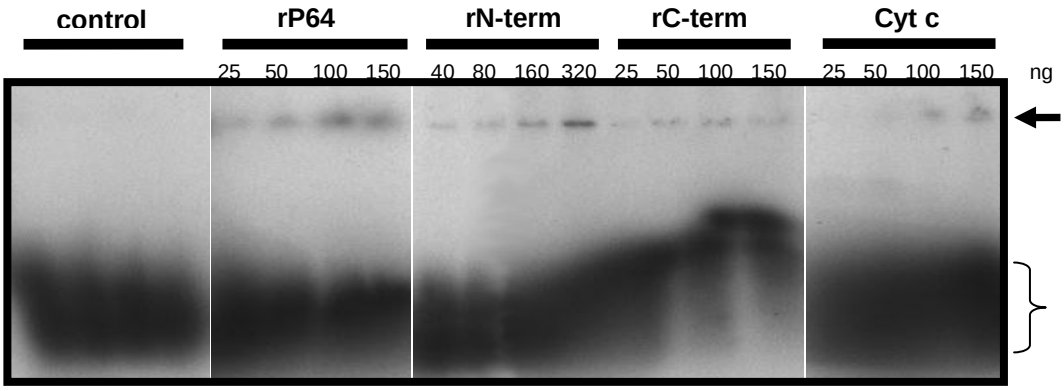

Figure 3.2 Recombinant P64 and domains can bind short oligonucleotides. A 65 nt radiolabeled DNA probe was incubated alone (control) or with increasing amounts of protein (indicated in nanograms) overnight in DNA binding buffer, final volume 15 µl. All recombinant proteins were able to bind the probe but rC-term induced a significant upward shift of the probe just above the front. Approximately 11,000 CPM worth of labeled probe was used for each reaction. Reactions were loaded onto 10% acrylamide gels and run at 120 V for 1 hr. Acrylamide gels were dried on blotting paper before exposing to film for 19 hr. Single arrow indicates the bottom of the loading wells in the acrylamide gels. The bracket indicates the migrating front of free 65 nt radiolabeled probe.

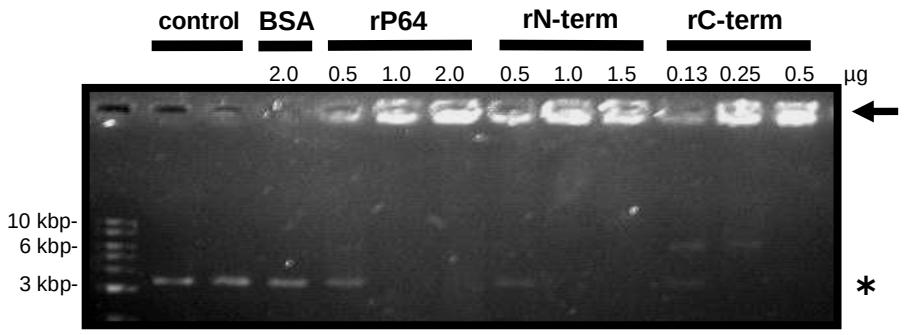

Figure 3.3 Recombinant P64 and each of its domains can bind plasmid DNA. The plasmid pIZT/V5-His, linearized by *Hind* III, was incubated alone or with protein (indicated in micrograms) overnight in DNA binding buffer â€.4 Prior to the addition of 4.5 ng of pIZT/V5-His to protein suspensions and controls, an effort was made to remove some of the DNA that had been co purified with the recombinant proteins. This was done by treating all the protein suspensions and the controls, prepared with DNA binding buffer, with MNase followed by deactivation with EGTA. Plasmid was added to the nuclease treated suspensions followed by heating at 60 ˚C to release any DNA that had been protected from the nuclease and to increase the likelihood of plasmid uptake. Reactions were resolved on 0.7% agarose gels stained with GelRed. Arrow indicates the loading wells of the agarose gel. Asterisk indicates position of unbound plasmid.

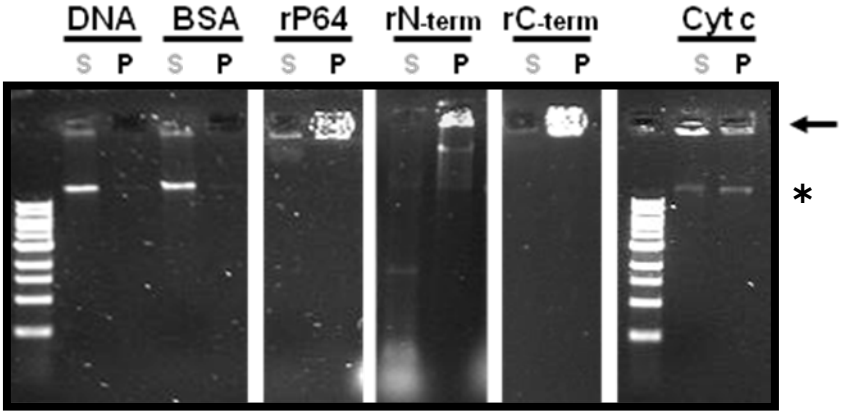

Figure 3.4 The SfAV1a encoded P64 protein and derived recombinant proteins are able to aggregate DNA. SfAV1a gDNA (15 ng) was incubated alone or with each of the proteins BSA (1.2 µg), rP64 (2.4 µg), rN-term (2 µg), rC-term (2.8 µg), cytochrome c (Cyt c, 1.2 µg). Before placing at 4º C overnight, DNA-protein mixtures were heated for 2 min at 60º C in order to increase the likelihood of SfAV1a gDNA replacing the nucleic acids that had been co-purified with recombinant proteins. To separate any bound DNA from unbound DNA, mixtures were spun at 16,300g, 30 min and the supernatant (S) was removed from the pellet (P) fraction. Pellets were suspended in TE buffer and glycerol then loaded alongside their corresponding supernatants on a 0.5% agarose gel stained with GelRed. Pellet fractions having DNA were later examined by electron microscopy. Arrow indicates the position of the well in the agarose gel. Asterisk indicates position of unbound SfAV1a gDNA.

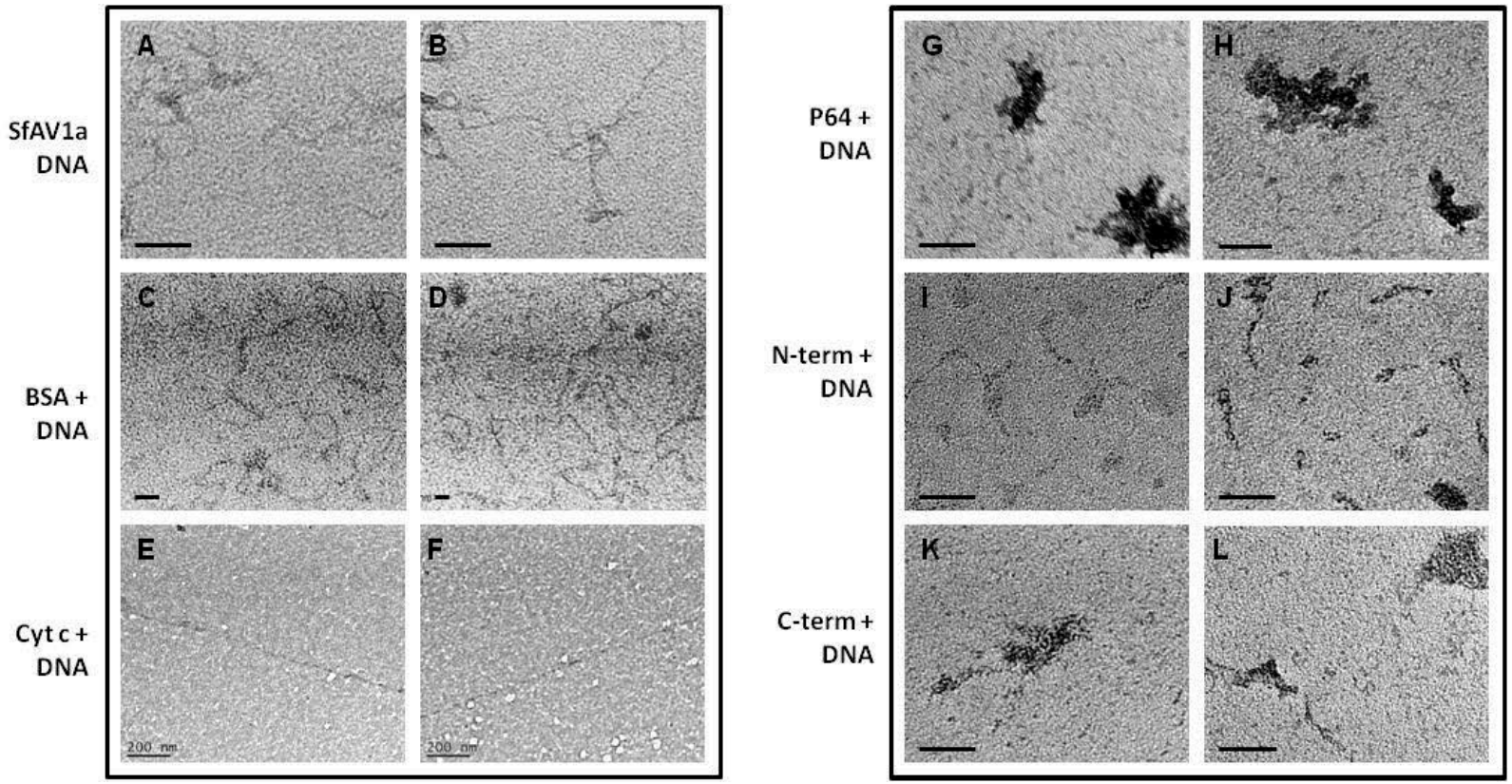

Figure 3.5 Electron micrographs demonstrating the effect of recombinant proteins on SfAV1a DNA. Viral DNA was incubated without protein (A, B), with BSA (C, D), with cytochrome C (E, F), or with the recombinant proteins derived from P64 (G, H), the N-terminal domain (I, J) and the C-terminal (K, L) in reactions as described for Figure 3.4. The pellets resulting from centrifugation of the DNA-cytochrome c complexes (E, F) and the DNA-recombinant protein complexes (G-L) were used for negative-stain electron microscopy. DNA alone and DNA-BSA mixtures were examined without centrifugation since centrifugation of these reactions did not induce the formation of DNA pellets (Figure 3.4). Bar = 50 nm for A, B, G-L; 20 nm for C and D; 200 nm for E and F.

Figure 3.6 Sequence homology of P64 and homologs. Putative homologs of P64 in other selected viruses showing the alignment of virus-specific 2-cysteine adaptor motif in the amino-terminal domain (A), and the basic motif (B) usually found downstream. Ascoviruses, SfAV1a, *Spodoptera frugiperda ascovirus 1a;* TnAV2c, *Trichoplusia ni ascovirus 2c*; HvAV3e, *Heliothis virescens ascovirus 3e*; DpAV4a, *Diadromus pulchellus ascovirus 4a*. Iridoviruses: CIV6, *Chilo* iridescent virus type 6; FV3, frog virus 3. Phycodnavirus: PBCV, *Paramecium bursaria* chlorella virus.

Figure 3.6

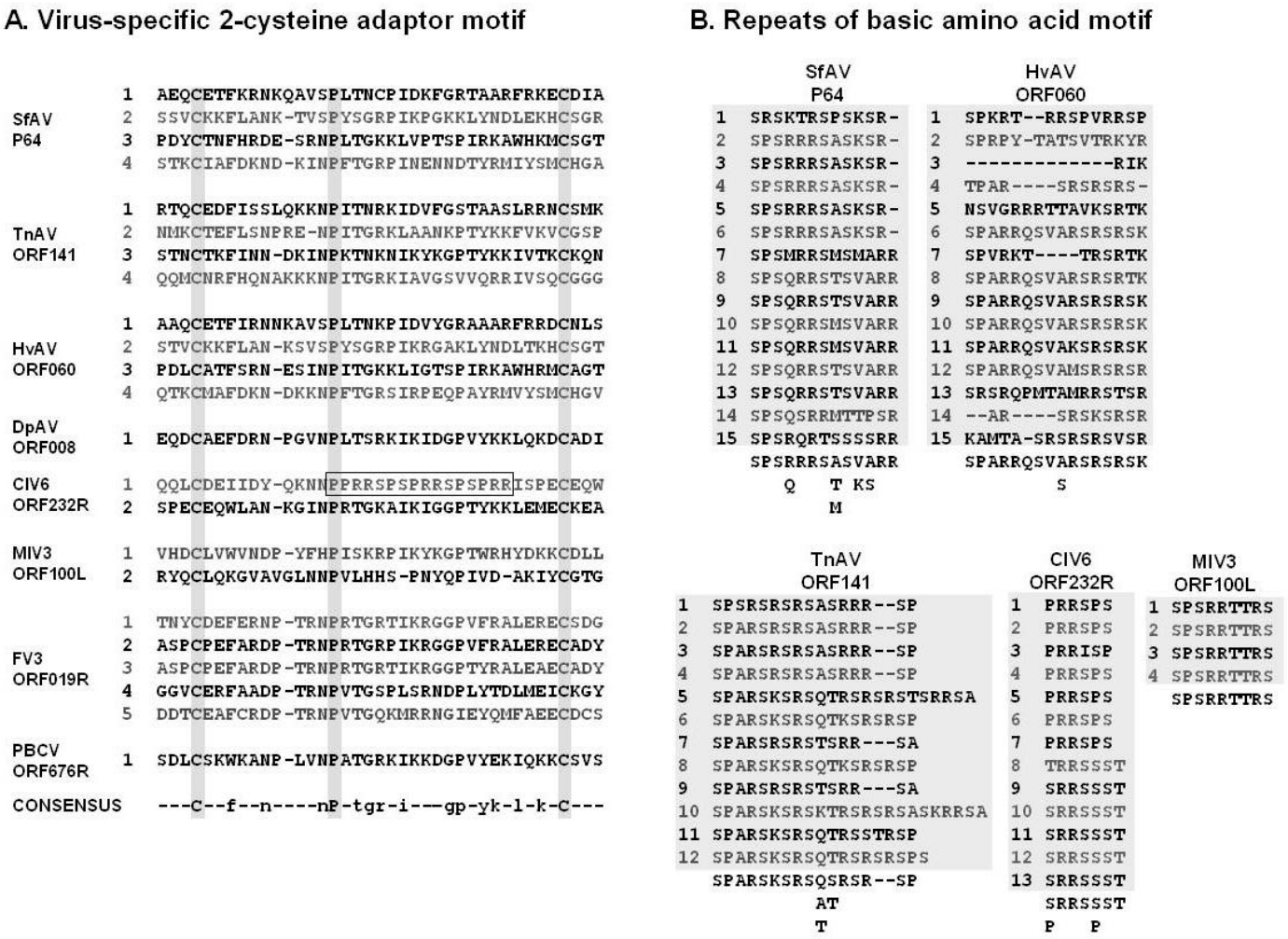
A. Virus-specific 2-cysteine adaptor motif
SfAV P64
TnAV ORF141
HvAV ORF060
DpAV ORF008
CIV6 ORF232R
MIV3 ORF100L
FV3 ORF019R
PBCV ORF676R
CONSENSUS
B. Repeats of basic amino acid motif
SfAV P64
HvAV ORF060
TnAV ORF141
CIV6 ORF232R
MIV3 ORF100L

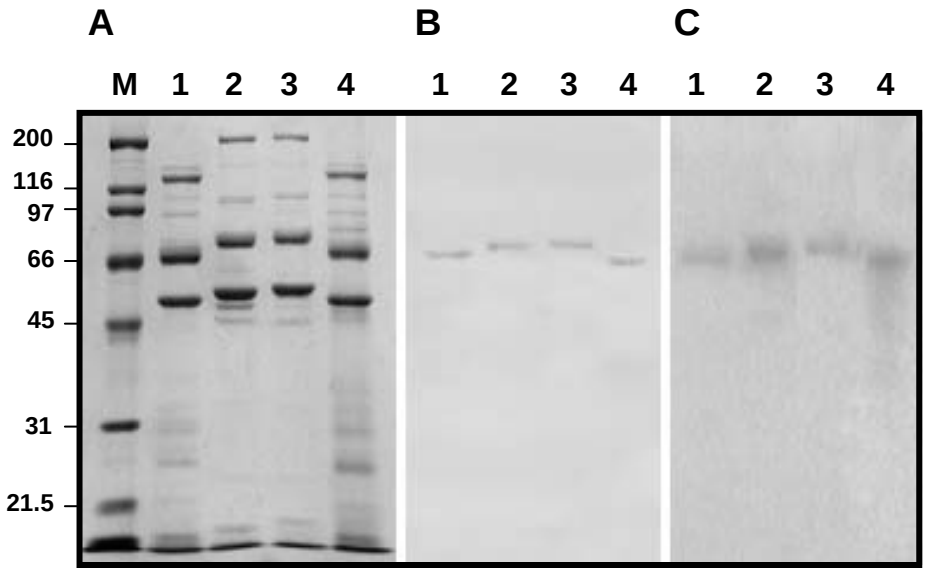

Figure 3.7 Ascovirus P64 homologs bind DNA. Western and Southwestern analyses suggest a similar genomic DNA-sequestering function for ascovirus basic virion P64 protein homologs. (A) Fractionation of purified ascovirus virion proteins by SDS PAGE in a 12% gel; (B) Western blot using an anti-P64 antibody showing antigenic relatedness of major basic proteins in ascovirus virions; (C) Southwestern analysis showing that ascovirus P64 homologs were the only ascovirus virion protein species that bound dsDNA. *Spodoptera frugiperda ascovirus 1a* (lane 1), H*eliothis virescens ascovirus 3e* (lane 2), *Trichoplusia ni ascovirus 2c* (lane 3), and *Spodoptera exigua ascovirus 7a* (lane 4); M, standard protein with molecular mass markers indicated in kilodaltons.

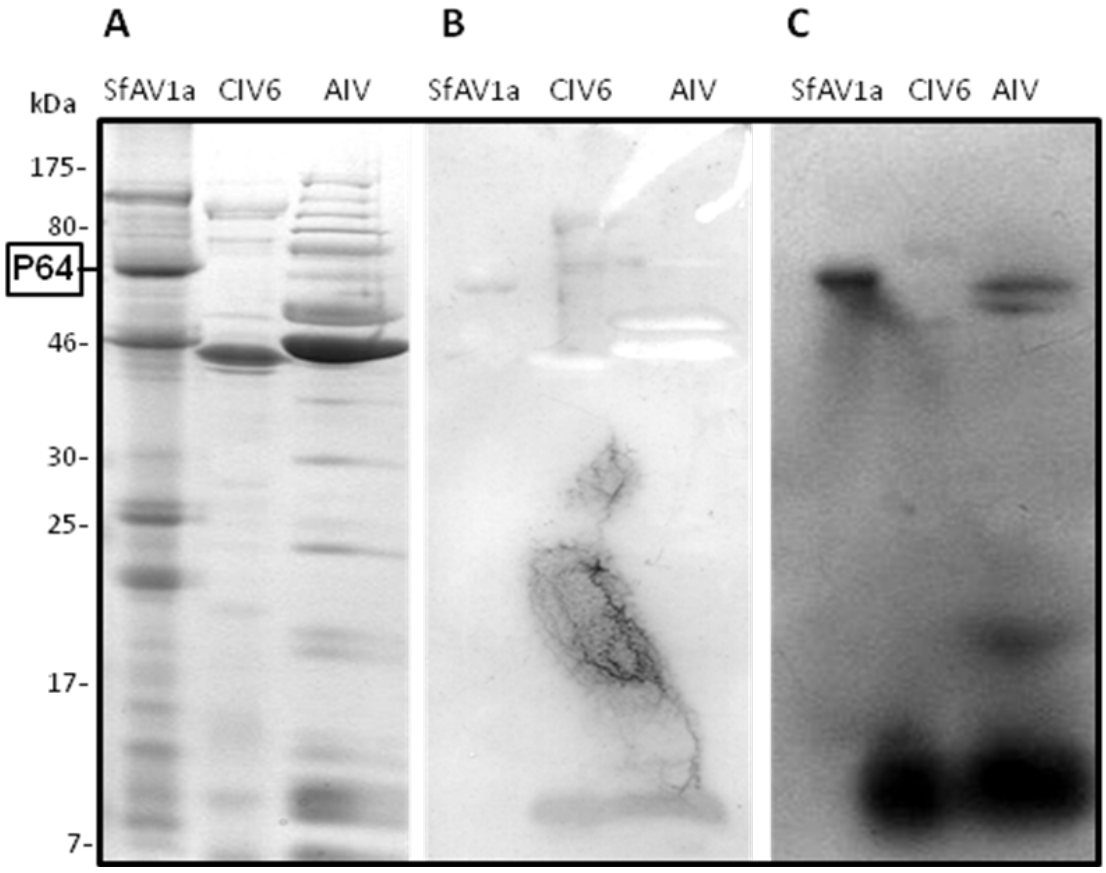

Figure 3.8 Comparison of DNA binding proteins in ascovirus and iridoviruses. Comparison of Western and Southwestern analysis provided evidence of similarities and differences between ascovirus and iridovirus DNA-binding proteins. (A) Purified virions (15-30 ng) from SfAV1a, *Chilo* iridescent virus 6, and an iridovirus purified from *Armadillidium vulgare* (AIV) were fractionated by running samples through a 12% SDS PAGE. Duplicate gels were blotted onto PVDF membranes which were used for Western blotting (B) with the primary antibody anti-P64 antibody or for Southwestern blotting (C) by incubating membrane with radiolabeled DNA. Stained SDS acrylamide gels and blotted membranes were compared to determine which of the proteins were most similar to P64 in antigenicity and which structural proteins bound DNA.

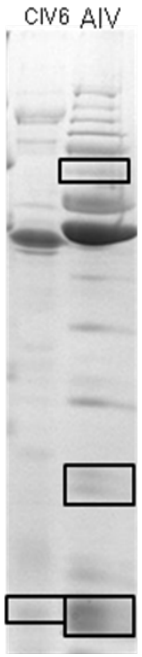

Table 3.1 Summary report on MALDI-TOF analysis of DNA binding proteins in Iridoviruses

Sample	Top Matches	Accession	Mass kDa	pI	# peptides/ unique	Score	Proteins similar to top match†
AIV top DNA binding protein	CIV6_ORF274L	AAK82135	51.3	6.7	8/6	376	Capsid_NCLDV CDD, major capsid proteins 78% of IRV9, IRV16, IRV22 72% of MIV014L
	CIV6_ORF443R	AAK82303	237.2	4.39	2/2	88	ORF216R 52% of 1357aa, ORF396L 43% of 919aa MIV091L 45% of 1027aa
	CIV6_ORF415R	AAK82275	26.7	4.9	3/2	79	See match below
AIV middle DNA binding protein	CIV6_ORF342R	AAK82203	9.3	8.7	3/2	157	MIV115R 58% of 60aa, CAJ53771 protein translocase TatC2 43% of 76aa
	CIV6_ORF415R	AAK82275	26.7	4.9	3/2	156	See match below
	Enterobacteria phage N4 virion RNA polymerase	AAO24831	382.5	5.7	8/4	62	phage virion RNA polymerase
AIV lower DNA binding protein	CIV6_ORF415R	AAK82275	26.7	4.9	21/6	500	See match above
	CIV6_ORF342R	AAK82203	9.3	8.7	2/1	82	See match above
	CIV6_ORF274L	AAK82135	51.3	6.7	2/2	52	See match above
CIV6 lower DNA binding protein	CIV6_ORF415R	AAK82275	26.7	4.9	14/10	759	MIV018L 61%, ACB27549 Transglutaminase domain-containing protein 37% of 159aa
	CIV6_ORF084L	AAB94426	18.4	9.6	4/3	170	EEN43086 46% of 88aa, AAK67236 Low density lipoprotein receptor 44% of 104aa
	CIV6_ORF312R	AAK82173	10.6	9.7	5/3	157	ABD82798 fibronectin 41% of 86aa
	CIV6_ORF234R	AAK82095	21.1	5.15	3/3	153	EFG81302 lincomycin resistance 52% of 74aa
	CIV6_ORF295L	AAK82156	156.5	6.86	3/2	138	MIV016R 46% of 314aa, HvAV3e ORF146 42% of 392aa
	CIV6_ORF466R	AAK82326	10.2	9.1	4/2	87	MIV112R 52% of 45aa

Table 3.1. Summary report on MALDI-TOF analysis of DNA binding proteins in Iridoviruses. An image with the proteins of interest used for MALDI-TOF analysis is provided for correlation between the virion and the mass spectrometry data. ORF matches in lighter font indicate that those were also identified in another band.

Figure 3.9 Phylogeny of P64 homologs and proteins containing either the vs2C-ad motif or basic repeats. Putative proteins of interest are noted with the ORF number if possible, the virus they come from and the GenBank reference number to the protein. (A) Amino acid sequences of P64 homologs which contained both the vs2C-ad motif and the basic repetitive motif were aligned for phylogenetic analysis. Numerical values at nodes of tree indicate bootstrap values based on 1000 trials. (B) A phylogeny was also obtained for proteins containing one or more vs2C-ad motifs without basic repeats. (C) Proteins from the family Iridoviridae and Phycodnaviridae that contained basic repetitive motifs were also compared. Of note are the highlighted large proteins (over 620 aa, highlighted) which contained conserved 2-cysteine motifs that did not match the canonical 2C-adaptor motif. There were also two types of small basic proteins (less than 300 aa): those that had sequence homology in the first 15 aa to non repetitive regions within the large basic proteins (asterisks) and those that did not. AtIV, *Aedes taeniorhynchus* iridescent virus; BohleIV, Bohle iridovirus; DpAV, *Diadromus pulchellus ascovirus*; ECFV, European catfish virus; EHNV, Epizootic haematopoietic necrosis virus; FV3, Frog virus 3; GIV, Grouper iridovirus; HvAV, *Heliothis virescens ascovirus*; IIV6, Invertebrate iridescent virus 6; ISKNV, Infectious spleen and kidney necrosis virus; LDV, Lymphocystis disease virus; PBCV, *Paramecium bursaria Chlorella* virus; PPIV, Pike perch iridovirus; REV, Rana esculenta iridovirus; SfAV, *Spodoptera frugiperda ascovirus*; SGIV, Singapore grouper iridovirus; sfERanavirus, Short-finned eel ranavirus; ssTIV, Soft-shelled turtle iridovirus; TnAV, *Trichoplusia ni ascovirus*.

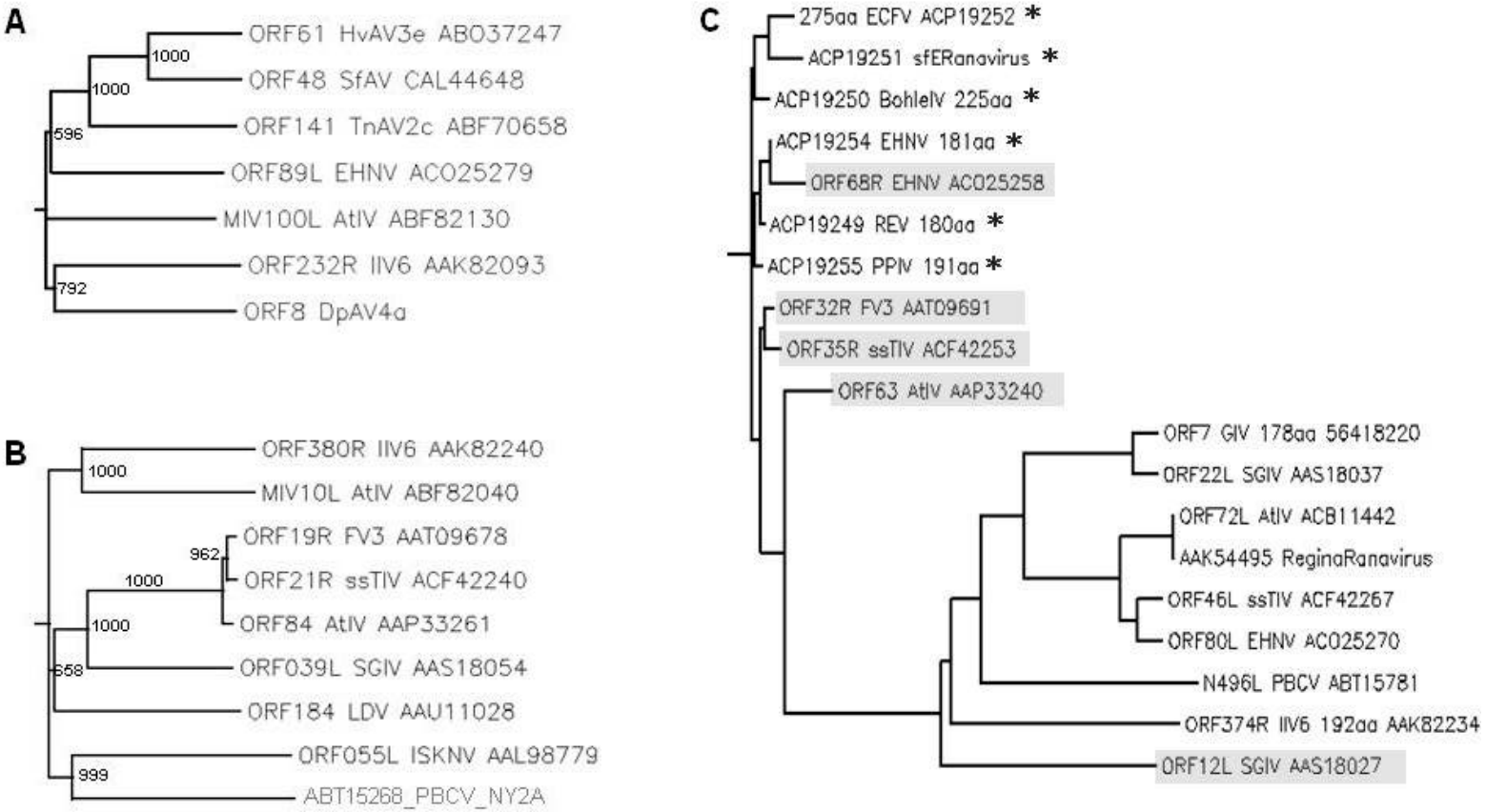
A
ORF61 HvAV3e ABO37247
ORF48 SfAV CAL44648
ORF141 TnAV2c ABF70658
ORF89L EHNV ACO25279
MIV100L AtIV ABF82130
ORF232R IIV6 AAK82093
ORF8 DpAV4a
1000
1000
596
792
B
ORF380R IIV6 AAK82240
MIV10L AtIV ABF82040
ORF19R FV3 AAT09678
ORF21R ssTIV ACF42240
ORF84 AtIV AAP33261
ORF039L SGIV AAS18054
ORF184 LDV AAU11028
ORF055L ISKNV AAL98779
ABT15268_PBCV_NY2A
1000
962
1000
1000
658
999
C
275aa ECFV ACP19252 *
ACP19251 sfERanavirus *
ACP19250 BohleIV 225aa *
ACP19254 EHNV 181aa *
ORF68R EHNV ACO25258
ACP19249 REV 180aa *
ACP19255 PPIV 191aa *
ORF32R FV3 AAT09691
ORF35R ssTIV ACF42253
ORF63 AtIV AAP33240
ORF7 GIV 178aa 56418220
ORF22L SGIV AAS18037
ORF72L AtIV ACB11442
AAK54495 ReginaRanavirus
ORF46L ssTIV ACF42267
ORF80L EHNV ACO25270
N496L PBCV ABT15781
ORF374R IIV6 192aa AAK82234
ORF12L SGIV AAS18027

CHAPTER 4

Characteristics of Virion-Containing Vesicle Membranes and Associated Proteins Produced During Ascovirus Infection

4.1 Abstract

Viruses are obligate intracellular parasites that require cellular components for synthesizing proteins and lipids necessary for virus replication, assembly, and release. All viruses have proteins incorporated into their structure but lipids may or may not be incorporated into mature virions depending on the type of virus. Lipids are a necessary for enveloped viruses. In some cases lipids are involved in the creation of membranes of subcellular compartments specializing in viral genome replication. Ascoviruses, particularly *Spodoptera frugiperda ascovirus* 1a (SfAV1a), manipulate lipid synthesis and cell and viral membranes in several ways during infection. Ascovirus cytopathology involves cellular hypertrophy, the rescue of apoptotic bodies for use as virion carrying vesicles, and the de novo synthesis of virion envelopes. Here I describe some SfAV1a derived proteins that may be involved in manipulating or creating these structures. Several SfAV1a ORFs were identified in vesicle membrane fractions by MALDI-TOF mass spectrometry and one of these (ORF43) was confirmed to be a plasma membrane associated protein. Previously, MALDI-TOF analysis was used to identify 21 SfAV1a virion associated proteins. In this study, six of those proteins (ORF36, 43, 54, 60, 91, and 109/61) were found to be part of the outer envelope, apparently synthesized *de novo*, and the intermediate tegument layer. Another four SfAV1a virion associated ORFs (ORF41,

46/47, 48, and 27/64) were located in the nucleocapsid core based on their association with the DNA condensing protein P64 which is known to occupy the virion core.

4.2 Introduction

A major characteristic of most viruses is to significantly manipulate normal cell functions. The changes induced are due primarily to redirection of host cell metabolic activity to replicate viral genomes and produce progeny virions (Shors, 2009; Watanabe *et al.*, 2007). Cellular alterations associated with infection can also be due to host responses that evolved to prevent virus infection from proceeding (Kaplan and Sieg, 1998; Shen and Shenk, 1995). Among the changes resulting from virus infection, it is well known that many viruses manipulate host plasma and intracellular membranes using host and virus encoded proteins (Chen and Lamb, 2008; Nayak *et al.*, 2009; McDonald and Martin-Serrano, 2009). In some viruses, small specialized membrane-bound compartments or vesicles are produced in which genome replication and assembly take place (Miller and Krijnse-Locker, 2008). Such compartments are derived from the endoplasmic reticulum, Golgi bodies, or lysosomes depending on the virus. For most enveloped viruses, virion structural proteins are targeted to specific membranes where they become concentrated in lipid rafts and interact with host proteins to promote membrane bending, budding and the eventual release of virions (Miller and Krijnse-Locker, 2008; Nayak *et al.*, 2009; Shors, 2009).

Among all viruses, the ascoviruses (family *Ascoviridae*) appear to manipulate cellular membranes more than any other known type of virus. Ascoviruses (AVs) are enveloped dsDNA viruses that produce large virions (130 x 400 nm) with a circular

genome ranging from 120-180 kbp, the specific size depending on the ascovirus species (Federici *et al*., 2005; Bigot *et al*., 2010). These viruses attack insects, primarily larvae of the lepidopteran family Noctuidae, and are transmitted by endoparasitic wasps. They begin replication in the nucleus, causing it to hypertrophy significantly (Federici, 1983). Subsequently, they induce apoptosis and then undergo most replication and virion assembly in large vesicles, 5 – 10 µm in diameter, formed by rescue of the developing apoptotic bodies (Federici *et al*., 2008). These vesicles, also referred to here as viral vesicles, contain mitochondria and other organelles such as ribosomes, along with fragments of the disrupted nucleus and nucleoli (Federici, 1983; Cheng *et al*., 2005). As the viral vesicles form, the cell also undergoes significant hypertrophy. Thus the cytopathology of ascovirus infection and virion assembly indicates several stages were cellular membranes are modified and manipulated by these viruses. These include (1) manipulation of cell membrane as the cell hypertrophies, (2) modification of the plasmalemma as the apoptotic bodies are rescued and converted into viral vesicles, a process that includes (3) the apparent de novo synthesis of numerous small vesicles throughout the cell that become part of the limiting membrane of the vesicles, and (4) the proliferation of membrane within the viral vesicles that subsequently becomes the source of the virion outer envelope.

The highly unique cytopathology caused by ascoviruses, especially the diverse ways summarized above by which membranes are manipulated during viral vesicle formation and virion assembly provides very strong evidence that these processes are encoded and controlled by the viruses. Thus, I hypothesize that these modifications result

from the insertion of proteins encoded by ascoviruses into cellular membranes, and also that some of these modifications likely involve the direct synthesis of membrane lipid components by lipid-metabolizing enzymes encoded by these viruses. With respect to the latter, annotation of the genome of the ascovirus type species, the *Spodoptera frugiperda ascovirus 1a* (SfAV1a), shows that this genome encodes nearly 25 proteins containing transmembrane helices (Bideshi *et al.*, 2006), at least some of which are likely involved in the modification and proliferation of host cell membranes. The research presented in this chapter is represents my initial attempts to address this hypothesis. To better understand how SfAV1a, and AVs by extension, manipulate host cell membranes I examined vesicle membranes to determine which viral components were significant components of this membrane. I also compared viral vesicle proteins with virion structural proteins that were sensitive to removal by detergent and salt treatments. Here, I report on proteins common to virion and viral vesicles membranes, as well as those that appear to be unique to each membrane type. In addition, I provide data to suggest which virion structural proteins are associated with the envelope, tegument, and core of the virion.

4.3 Materials and Methods

4.3.1 Biotinylation and identification of vesicles membrane proteins. The biotin labeling procedure from Florens *et al.* (2004) was adapted for use with virion-containing vesicles to identify surface proteins. These vesicles were obtained from 800 µL of infected hemolymph from *Spodoptera exigua* larvae that had been inoculated at the late 3rd to early 4th instar with SfAV1a nine days earlier. Hemolymph was harvested with

500 µL of 1% reduced glutathione (Sigma) in PBS pH 8.0. A vesicle suspension, 200 µL, was added to 1 mL PBS to wash and pellet. The volume of pelleted vesicles was approximately 50 µL. Vesicles were biotinylated with 20 mg/mL EZ-link Sulfo-NHS-LC-Biotin (Pierce), gyrating 5 hrs.

Biotinylated vesicles were washed in 100 mM glycine twice to remove excess biotin then vesicle membrane proteins were separated from virions. Biotinylated vesicles were lysed by suspending them in 50 mM Tris-HCl, pH 7.4 and adding lysis buffer for a final concentration of 7 M urea, 2 mM DTT, 1 mM PMSF, 0.1% SDS. Vesicles in lysis buffer were sonicated for 10 sec. Lysate was spun at 2000 x g for 10 min to remove large bodies then remaining supernatant was collected and spun at 18,300 x g, 1 hr, 4 °C to separate lipid membrane from virions in biotinylated-vesicle lysate. Supernatant derived from this procedure was considered enriched with vesicle membrane and membrane-associated proteins.

The enriched membrane fraction was added to streptavidin beads (Pierce) that had been equilibrated in PBS pH 8.0 and incubated for 1 hr at 4°C on a gyrator. Beads were then pelleted and the supernatant was removed. The beads were washed four times in PBS. Proteins were eluted from beads by adding Lamelli buffer to beads and boiling them for 5 min. Samples of biotinylated vesicles, enriched-membrane supernatant, and proteins eluted from beads incubated with enriched-membrane supernatant were fractionated by SDS PAGE and transferred to PVDF membrane for ligand blotting using the streptavidin conjugated alkaline phosphatase (Pierce) according to manufacturer's

instructions and detected with NBT and BCIP (Promega) according to the manufacturer's instructions.

Protein profiles from each sample were compared to determine which proteins were significant components of vesicle membranes. Those chosen were sent for MALDI-TOF analysis as described in Tan *et al.* (2009a).

4.3.2 GFP-fusion construct design and expression. First an expression vector capable of expressing proteins in Sf9 insect cells had to be created. A large fragment from pIZT/V5-His (Invitrogen) including the OpIE2 promoter, the multiple cloning site, and the OpIE2 polyadenylation sequence and having Sma*I* blunted ends was ligated to the blunt ends of pUC19 that had been cleaved with Hind*III* and Eco*RI*; this new plasmid was called pUCIE2. The fragment from pIZT/V5-His was obtained using the primers pProIE2-F and pPIE2pA-R (see Table 4.1 for primer sequences). Next, a GFP fragment (also derived from pIZT/V5-His) having a Nar*I*-cleaved 5' end and a Age*I* 3' end and a putative cathepsin sequence (Sac*I* 5', Nar*I* 3') from SfAV1a were ligated into pUC19 (cleaved with Sac*I* and Age*I*) in a three way ligation to create pCathGFP. The primers are listed in Table 4.1.

Using the pCathGFP cloning vector, other SfAV1a ORFs of interest were used to replace the cathepsin gene fused to the GFP sequence. SfAV1a ORFs were designed with Sac*I* 5' and Nhe*I* 3' cleavage sites for insertion into the vector. The GFP sequence was ligated to the 3' end of the SfAV1a ORF at the Nhe*I* site in GFP, four nucleotides from the adenosine of the original GFP start codon. The primers for the SfAV1a ORFs are listed in Table 4.1.

Table 4.1 List of primers for GFP-fusion construction

Primer name	*Sequence*	*Target source*
pProIE2-F	5'- TCCCCCGGGGGATCATGATGATAAACAATGTAT -3'	pIZT/V5-His (Invitrogen)
pPIE2pA-R	5'- TCCCCCGGGCCTTTGAGTGAGCATCGATCCCAC -3'	
GFP-F	5'- GGCGCCATGGCTAGCAAAGGAGAAGAACTT -3'	pIZT/V5-His
pGFP(orf)-R	5'- ACCGGTTAATCCATGCCATGTGTAATCCCAGC -3'	
DBCath-F	5'- CGAGCTCATGGACGGTATGATATACAATAC -3'	SfAV1a
pCathGFP-R	5'- GGCGCCCGCGCCCAACATTTGCAGCAATTC -3'	
TSorf43F	5'- GAGCTCCGAAGTAAATGTCGCACACTGAAAGAA -3'	SfAV1a
TSorf43NheR	5'- CTAGCTAGCAATGGAATTTCTAAAAATTGGATCG -3'	
TSorf55F	5'- GAGCTCCGTACGTGATGGCTGTACGCGAGTACGC -3'	SfAV1a
TSorf55NheR	5'- CTAGCTAGCAAAGTCTACAACTACAGTGCCGGAT -3'	
TSorf60F	5'-GAGCTCTTGATCTGATCATGATAAAACGTATAC -3'	SfAV1a
TSorf60NheR	5'- CTAGCTAGCGTTGGATAAAACTTTGTTCAGAGCC -3'	

Underlined sequence indicates cleavage site used for cloning/ligation

To express the GFP-fusion constructs, Sf9 cells were first grown to 50-60% confluence in 4-well Lab-Tek chamber slides (Nalge Nunc). The transfection mix included 1 µg of plasmid, *Trans*IT-LT1 transfection reagent (Mirus) and Grace's insect media with L-glutamine (Lonza-BioWhittaker) in a volume of 100 µL and incubated for 2 h before applying to Sf9 cells that had previously been rinsed with Grace's insect media. Transfection proceeded for 5h in a total volume of 350 µL. Transfection mix was replaced with TC Grace and cells were incubated at 27° C for 2 days. For a GFP expression control, pIZT/V5-His was used to transfect cells to expresses GFP without being fused to another protein. Cells were examined using the Leica DMRE light microscope. Images were captured using the filters L5 (for DAPI signal) and N3 (for GFP signal) and the SPOT RT-color (Diagnostic Instruments Inc.) camera system.

4.3.3 Removal of structural proteins from SfAV1a virion by detergent-salt treatments and identification. SfAV1a was purified as described previously (Federici *et*

al., 1990) except that virions were suspended in PBS after purification by sucrose gradients. The procedure from Tsai *et al.* (2006), with some modifications, was used to separate envelope proteins from the virion core. Separate samples of virus were treated with the indicated amounts of Triton X 100 detergent and NaCl for 45 min, thereafter, samples were loaded in 2 ml microfuge tubes on top of 1.8 mL of 28% sucrose. These were spun at 23,500 x g for 1 h at 4°C using the Beckman Allegra 25R centri fuge with the TA-15-1.5 rotor. The first 120 µL from the top was saved as supernatant. The remaining sucrose was removed and the pellet was suspended in 50 mM Tris buffer and 2% SDS. Lamelli buffer was added to all samples before resolving the proteins by SDS PAGE.

To identify the proteins that were dislocated from the virus pellet to the supernatant, proteins were compared to the virion structural proteins that had been identified by Tan *et al.* (2009). Based on their location in the virion protein profile, the detergent/salt susceptible proteins in the supernatant were attributed to the predetermined ORFs of SfAV1a virions.

4.3.4 Biotinylation of Bacmid-recombinant proteins. Recombinant 6-histidine-tagged P64 (rP64) was produced using the Bac-to-Bac (Invitrogen) expression kit as previously described (Tan *et al.* 2009b). Recombinants of the vs2C-ad domain in the amino-terminal (rN-term) and the basic repeats in carboxyl-terminal (rC-term) were expressed with the histidine tag on the amino-terminus of each recombinant and purified in a similar manner as rP64 (Fig. 3.1A). SfAV1a genomic (g) DNA was purified with DNAzol (Invitrogen) according to the manufacturer's instructions and used for PCR. The

rN-term included the first 219 amino acids of P64 (SfAV1a048) and was amplified by PCR using the primer pair P64forward 5'-CGCGGATCCATGGCGTCAAAACGTAAA-3' and N1reverse 5'-ATACTCGAGGGCGCCGTGACACATGCT-3'. Amino acids 265 to 565 of P64 were included in the rC-term and amplified by PCR using the primer pair Cforward 5'- AGAGGATCCAGCACGAGTCGTTCCAAG-3' and P64reverse 5'-CCGCTCGAGATCCTTCGACGATCAGGT-3'.

To label purified recombinants, 10-15 µg of protein was incubated with EZ-link Sulfo-NHS-Biotin and applied to a spin column for removal of free biotin according to the directions in the EZ-link Sulfo-NHS-Biotinylation kit (Thermo Scientific).

4.3.5 Ligand blotting to detect protein-protein interaction. Virion proteins from SfAV1a and other viruses were separated by SDS PAGE and blotted onto nitrocellulose membranes in PBS 0.5% Tween. Blots were incubated with 1% BSA in PBS 0.5% Tween for 1hr. Biotinylated recombinant proteins diluted 40-fold in PBS having either 0.5% or 0.05% Tween then incubated with the nitrocellulose blot for 4 hr. The membrane was washed 3X in the PBS 0.5% or 0.05% Tween to correspond to the Tween concentration of the biotinylated-recombinant-protein suspension. Streptavidin conjugated to horse radish peroxidase (Thermo Scientific) was suspended in PBS-Tween (0.5% or 0.05%) in a 1:12,500 dilution and incubated with the blots for 1 hr. Blots were washed again 3X. Bound proteins were detected using a 1:1 dilution of TMB stabilized substrate for HRP (Promega) in PBS-Tween.

4.4 Results

4.4.1 Identification of proteins derived from virion-vesicle. Comparison of protein profiles of *S. exigua* healthy hemolymph, purified SfAV1a virions and virion-containing vesicles from infected *S. exigua* hemolymph were compared to observe general differences in the number and size of proteins (Fig. 4.1A). In an attempt to isolate virus encoded proteins from vesicle membranes, whole viral vesicles were labeled with EZ-link Sulfo-NHS biotin which targets primary amines. Biotin-labeled proteins from viral vesicles were pulled down with streptavidin beads then eluted and resolved by SDS PAGE (Fig. 4.1B). Biotin-labeled vesicles were also lysed and resolved by SDS-PAGE before blotting and detecting biotin-labeled proteins (Fig. 4.1C). Samples of biotin-labeled vesicles were manipulated further after lysis by centrifugation in order to separate the denser virus particles from the lighter fraction of vesicle membranes. The resulting sample, enriched membrane supernatant, was also resolved by SDS-PAGE and blotted for detection of biotin labeled proteins (Fig. 4.1C). In addition, the profile of biotin-labeled proteins pulled down by streptavidin beads (Fig. 4.1B) correlated to some of the major biotin-labeled proteins in the whole vesicles and supernatant (Fig. 4.1C). Proteins were chosen for MALDI-TOF analysis based on whether they were labeled with biotin and their appearance of being more abundant in the enriched-vesicle-membrane fraction as compared to SfAV1a virions or *S. exigua* hemolymph (numbers 1-5, Fig 4.1 B-C).

Protein bands 1-5 indicated in Fig. 4.1 B-C correspond to samples submitted for MALDI-TOF analysis had numerous SfAV1a virion structural proteins identified within each of these (Table 4.2). Ion scores for the proteins enriched-vesicle-membrane samples

were compared to those of proteins identified in the SfAV1a virion structural protein study by Tan *et al.* (2009a). The goal was to compare MALDI-TOF data from vesicle membrane proteins to the MALDI-TOF data of SfAV1a virion structural proteins (Tan *et al.*, 2009a) to find vesicle membrane proteins that had higher scores in the enriched-vesicle-membrane samples than in the SfAV1a virion structural protein data. There were many SfAV1a proteins that had high scores in both the vesicle membrane protein samples and the SfAV1a virion protein. This indicated that many virion structural proteins contributed to the making of the vesicle membrane or else there was a great deal of contamination from the virions within the vesicle. SfAV1a ORF013, ORF043, ORF055, ORF060 and ORF061 (in bold, Table 4.2) were chosen for further analysis because they did not have high scores in the SfAV1a structural protein data collected by Tan *et al.*, (2009a) or they had a transmembrane helix suggesting an association with membranes.

4.4.2 Localization of virion vesicle proteins. SfAV1a ORF043, ORF055, and ORF060 were the first of the group of proteins of interest that were fused to GFP and expressed in Sf9 cells. None of those proteins have any recognizable domain that could help to classify them (Bideshi *et al.*, 2006). ORF043 and ORF060 did, however, contain one and two transmembrane helices respectively. Fluorescent microscopy revealed plasma membrane localization for ORF043-GFP (Fig. 4.2A). ORF55-GFP was expressed in a punctuate manner within the nuclei of transfected cells (Fig. 4.2B). ORF060-GFP had uneven distribution within the cytosol. The control, expression of GFP from

pIZT/V5-His that was not fused to another protein, showed an even distribution of the GFP signal in the cytoplasm of transfected cells (not shown).

4.4.3 Identification of virion structural proteins in the SfAV1a envelope. The detergent Triton X 100 was used in combination with increasing concentrations of NaCl to remove different layers of SfAV1a virions; this method was adapted from studies by Tsai *et al.* (2007) with a different type of virus. Detergent alone (1% TX 100, Fig 4.3) was able to remove five to six proteins from the virus particle (in pellet fraction) into the supernatant. The addition of 0.5M NaCl to the detergent removed two more structural proteins. Higher concentrations of NaCl, up to 1.5 M, did not appear to remove any additional structural proteins from virus particles (Fig. 4.3). The location of the displaced virion proteins was correlated to the location and identity of SfAV1a virion structural proteins analyzed in Tan *et al.* (2009a). Table 4.3 shows the SfAV1a ORF identities and descriptions assigned to proteins displaced from virus particles, the majority having a transmembrane helix identified in some portion of the protein.

4.4.4 Identification of virion structural proteins that bind to P64. The previous results gave an idea of the structural proteins associated with the outside layers of SfAV1a virions. The goal of the next study was to "build" the virus from the inside towards the outside by finding out which virion structural proteins comprise the nucleoprotein core. P64 is part of the virion structure. P64 has been shown to bind and condense viral genomic DNA for packaging-making it one of the core proteins. However, it was not known what other proteins P64 bound to during these processes. Ligand blotting was used to determine which other virion structural proteins P64 interacts with.

The ligands were biotin-labeled, purified recombinant proteins rP64, rN-term, and rC-term; these were incubated with a blot of resolved virion structural proteins [SfAV1a, other AVs, *Chilo* iridescent virus (CIV6), *Armadillidum vulgare* iridescent virus (AIV)]. The location of the ligand on the blot was detected at discreet protein bands with the aid of a horseradish peroxidase chromogenic reaction. Although Fig. 4.5 is in black and white, it is important to note that the chromogenic reaction of the streptavidin-horseradish peroxidase and substrate produced a distinctly different color on the blot than that of the color of the prestained marker (M, Fig. 4.4 A-C) making it easily distinguishable from the marker stain. The location of those ligand-bound protein bands was correlated to the location and identity of SfAV1a virion structural proteins that had already been identified by Tan *et al.* (2009a). The results are shown in Table 4.4. The extent of ligand binding depended on the concentration of Tween 20 and the type of membrane (nitrocellulose or PVDF) used. Biotin-labeled rP64 appeared to have the most specific binding character; it bound the fewest proteins under the more permissive conditions (Fig. 4.4A). The rP64 ligand bound to the major capsid proteins of other viruses more than to the one from SfAV1a (Fig. 4.4A). Biotin-labeled rN-term bound mostly large proteins (46 kDa and above, Fig. 4.4B) whereas rC-term showed bound more of the smaller virion proteins (below 46 kDa, Fig. 4.4C). The proteins identified as binding partners of rN-term were more similar to rP64 binding partners than were those of rC-term (Table 4.4).

4.5 Discussion

There were a number of virion structural proteins identified in the enriched-membrane samples derived from vesicles. It is possible that AVs use some of the same proteins to create mature virions as it does to construct a durable membrane for virion-containing vesicles. In this study, I focused on those ORFs that seemed to be unique to or more abundant in virion-containing vesicles as compared to SfAV1a virions. Of the five ORFs chosen for further study, three of them have one or two transmembrane helices (Table 4.2; ORF013, ORF043, and ORF060). Beyond this, nothing is known of the actual function of these proteins. Of the vesicle membrane associated proteins, ORF043 was the only one thus far confirmed to be a membrane associated protein since it localized to the plasma membrane; ORF013 and ORF061 still need to be analyzed. ORF060 has two transmembrane helices but was seen in the cytoplasm with a non uniform localization rather than even dispersal in the cell. This does not preclude ORF060 from being a membrane protein as it could associate with the membranes of certain organelles (lysosomes, endoplasmic reticulum, etc.). ORF055 clearly localized to the nuclei of transfected cells but appeared to concentrate in rounded substructures within nuclei, possibly nucleoli. To confirm this, further studies would need to compare nucleoli specific fluorescent staining patterns with that of ORF55-GFP expression to see if they co-localize. Many SfAV1a ORFs have no known function or identifiable domain. These data can provide clues and a basis for further study of AV cytopathology and the specific role of the above mentioned proteins. It would be interesting to see if the localization of the above mention ORFs changes during AV infection.

Data sets from the virion envelope removal (Table 4.3) and ligand binding studies (Fig. 4.4 and Table 4.4) complemented each other well in that there was little overlap. Proteins subject to removal by detergent and salt treatments were assigned to the outer membrane and tegumental space just underneath the outer membrane (Fig. 4.5). Those envelope/tegument proteins did not get bound by the rP64 ligand (compare Fig 4.1 to Fig 4.4A). It appeared that P64 bound itself (ORF048) or ORF015 (which was identified in the same position as P64/ORF048 (Tan *et al.* 2009a), the major capsid protein (MCP/ ORF041) and a 100 kDa protein (ORF027/ORF064). Those proteins identified as targets of the rP64 ligand were assigned to the nucleoprotein core (Fig. 4.5). MCP was not completely removed by detergent/salt treatments but some protein in the same position as MCP did go to the supernatant (Fig 4.1). This suggests that the MCP may be subject to disturbance by detergent/salt treatment because it is part of the next layer underneath the outer envelope and tegument space. The rN-term ligand binding pattern corresponded to the rP64 ligand binding pattern better than the rC-term ligand. Many of the proteins that rC-term bound were susceptible to detergent/salt removal. These results suggest that the N-terminal half of P64 may be the domain responsible for the protein-protein interactions of P64 rather than the C-terminal half. It is important to note that many proteins can be incorporated into virions but some of these could have a special role in the activation of replication and the start of early transcription. Some virion associated proteins could have a catalytic function that serves to inhibit cellular transcription or translation. For this reason, some of the gene products identified in SfAV1a virions here may not serve a structural purpose but an enzymatic one. These data and previous studies point to

significant differences between AVs and iridoviruses. The detergent/salt treatments indicated the proteins exposed on the surface were likely embedded in an outer lipid membrane. Members of the family *Iridoviridae* have a capsid protein layer on the surface with the lipid membrane just underneath which covers the nucleoprotein core (Chinchar *et al.*, 2009). AVs have one DNA binding protein in their virion while members of the *Iridoviridae* have at least two DNA-binding proteins. Another, more obvious difference is that AVs are bacilliform in shape whereas iridoviruses are icosahedral.

Bigot *et al.* (2009) noted that 28 genes were common to species of iridoviruses and ascoviruses: *Chilo* iridescent virus 6, mosquito iridescent virus 3, SfAV1a, TnAV2c, HvAV3e and DpAV4a. Comparison of the four AV genomes shows they have 34 genes in common. Bigot's *et al.* (2009) study also noted that of the 21 SfAV1a structural proteins described (Tan *et al.*, 2009a), 11 have homologs in all the AVs including DpAV4a and 10 of those are also seen in iridoviruses. In other words nearly 36% (10 out of 28) core genes of AVs and iridoviruses are likely to have a role in virion structure. Of the SfAV1a virion-associated proteins noted in this study, six (SfAV1a ORF64, ORF48, ORF41, ORF54, ORF91, and ORF109) of those have been confirmed as Chilo iridescent virus virion-associated proteins (CIV209R, 232R, 274L, 337L, 401L, and 355R respectively) (Ince *et al.*, 2010). The function of most of these gene products has not been investigated. Here, I shed light on where the major structural proteins reside within the mature virion (Fig. 4.5). Of the ORFs identified as playing a role in viral vesicle membranes (ORF013, ORF043, ORF055, ORF060, ORF61), three of them (ORF043,

ORF060, and ORF061) had already been identified as virion structural proteins (Tan *et al.*, 2009a); ORF055 and ORF061 have homologs in other AVs and an iridovirus.

The fact that most of the gene products of interest in enriched-vesicle-membrane samples were not specific to AVs suggests that they are not responsible for the formation of vesicle membranes, a feature unique to AV cytopathology. If this is the case, the other proteins identified by MALDI-TOF analysis in Table 4.2 require further study. It could be that most of the proteins that occupy the vesicle membrane are the same as those in the outer envelope of the AV which would explain why many of the proteins identified had high scores in the data presented here and in the data concerning the identification of virion structural proteins (Tan *et al.*, 2009a). The data concerning vesicle-membrane proteins was biased towards SfAV1a derived proteins. It could be that certain host proteins play a role in vesicle membrane integrity and the approach used here was not sensitive enough to detect them. There could have been an up regulation of *S. exigua* host proteins that would have been difficult to detect because the database used for identifying peptides though MALDI-TOF lacks the *S. exigua* annotated genome with which to compare peptides.

AVs have a mechanism for lipid synthesis to accommodate the extra surface area of the hypertrophied cell. This process could be driven solely by AV proteins because they encode lipid metabolizing enzymes, i.e. carboxyl esterase, fatty acid elongase, and phosphate acyltransferase (Bideshi *et al.*, 2006; Bigot *et al.*, 2009). On the other hand, lipid synthesis could occur with the help of host proteins. During AV infection, it has been noted that empty vacuoles 400-700 nm wide form and assemble along planes

accompanied by mitochondria (Federici, 1983). At some point the plasma membrane invaginations that develop during AV infection have to join in order to create the signature virion-containing vesicles. It is possible that the small vacuoles align and connect opposing plasma membrane invaginations. The vacuoles could be synthesized *de novo* or be recruited from other cellular compartments. There are examples of Enteroviruses, Flaviviruses and others recruiting or inducing the formation of intracellular vesicles, but for the purpose of genome replication (Miller and Krijnse-Locker, 2008). During cytokinesis/abscission, endosomal sorting complexes required for transport (ESCRT) are recruited to the membranes to encourage bending, budding, and joining of membranes (Raiborg and Stenmark, 2009). A model has even been proposed where endosomes or Golgi-derived vesicles align across the midbody between the two joined daughter cells and become fused to each other and the plasma membrane to separate the two daughter cells (McDonald and Marin-Serrano, 2009). ESCRT proteins are intimately involved in this process and also in the budding of HIV, HBV, and Influenza virus from cell membranes (McDonald and Martin-Serrano, 2009; Nayak *et al.*, 2009; Watanabe *et al.*, 2007). ESCRT proteins may, therefore, play a role in vesicle formation during AV infection. Each of these aspects of AV manipulation of membranes requires further study.

Many ascovirus gene products have homologs in viruses from the family *Iridoviridae*. Iridoviruses have become pathogens of increasing importance because of their negative impact on fresh and salt water fish and commercial fish farms (Chen *et al.*, 2006; Dong *et al.*, 2010). A great deal of data in bioinformatics, proteomics, and

molecular biology has been accumulating about iridovirus. Advances made in understanding the pathobiology of one family and the specific function virion structural proteins could provide insight and a basis from which to study of the other family. Future studies of AVs should take advantage of similarities between AVs and iridoviruses by using the molecular, proteomic, and bioinformatic data being produced. In addition, a focus on those gene products that are unique to AVs would further advance the understanding of AV specific manipulation of membranes that leads to vesicle formation and *de novo* virion-envelope synthesis.

4.6 References

Bideshi, D. K., M. V. Demattei, F. Rouleux-Bonnin, K. Stasiak, Y. Tan, S. Bigot, Y. Bigot, and B. A. Federici. 2006. Genomic sequence of *Spodoptera frugiperda ascovirus 1a*, an enveloped, double-stranded DNA insect virus that manipulates apoptosis for viral reproduction. J. Virol. **80:**11791-805.

Bigot, Y., S. Renault, J. Nicolas, C. Moundras, M. V. Demattei, S. Samain, D. K. Bideshi, and B. A. Federici. 2009. Symbiotic virus at the evolutionary intersection of three types of large DNA viruses; iridoviruses, ascoviruses, and ichnoviruses. PLoS One. **4:**e6397.

Carner, G. R. and J. S. Hudson. 1983. Histopathology of virus-like particles in *Heliothis* spp. J. Invertebr. Pathol. **41:**238-249.

Chen, B. J. and R. A. Lamb. 2008. Mechanisms for enveloped virus budding: Can some viruses do without ESCRT? Virology. **372:**221-232.

Chen, L. M., F. Wang, W. Song, and C. L. Hew. 2006. Temporal and differential gene expression of Singapore grouper iridovirus. J. Gen. Virol. **87:**2907-2915.

Cheng, X. W., L. Wang, G. R. Carner, and B. M. Arif. 2005. Characterization of three ascovirus isolates from cotton insects. J. Invertebr. Pathol. **89:**193-202.

Dong, C., S. Weng, Y. Luo, M. Huang, H. Ai, Z. Yin, and J. He. 2010. A new marine megalocytivirus from spotted knifejaw, *Oplegnathus punctatus*, and its pathogenicity to freshwater mandarinfish, *Siniperca chautsi*. Virus Res.**147:**98-106.

Federici, B. A. 1982. A new type of insect pathogen in larvae of the clover cutworm, *Scotogramma trifolii*. J. Invertebr. Pathol. **40:**41-54.

Federici, B. A. 1983. Enveloped double-stranded DNA insect virus with novel structure and cytopathology. Proc. Natl. Acad. Sci. USA. **80:**7664-7668

Federici, B. A., D. K. Bideshi, Y. Tan, T. Spears, and Y. Bigot. 2009. Ascoviruses: superb manipulators of apoptosis for viral replication and transmission. Curr. Top Microbiol. Immunol. **328:**171-96

Federici, B. A., and R. Govindarajan. 1990. Comparative histopathology of three ascovirus isolates in larval noctuids. J. Invertebr. Pathol. **56:**300-11.

Florens, L.,X. Liu, Y. Wang, S. Yang, O. Schwartz, M. Peglar, D. J. Carucci, J. R. Yates, Y. Wub. 2004. Proteomics approach reveals novel proteins on the surface of malaria-infected erythrocytes. Mol. Biochem. Parasitol. **135:**1-11.

Hamm, J. J., Pair, S. D., Marti, O. G. 1986. Incidence and host range of a new ascovirus isolated from fall armyworm, *Spodoptera frugiperda* (Lepidoptera: Noctuidae). Fla. Entomol. **69:**524-531.

Hamm, J. J., E. L. Styer, and B. A. Federici. 1998. Comparison of field-collected ascovirus isolates by DNA hybridization, host range, and histopathology. J. Invertebr. Pathol. **72:**138-46.

Kaplan, D., and S. Sieg. 1998. Role of the Fas/Fas ligand apoptotic pathway in human immunodeficiency virus type 1 disease. J. Virol. **72:**6279-82.

McDonald, B., and J. Martin-Serrano. 2009. No strings attached: the ESCRT machinery in viral budding and cytokinesis. J Cell Sci. **122:**2167-2177.

Miller, S. and J. Krijnse-Locker. 2008. Modification of intracellular membrane structures for virus replication. Nat. Rev. Microbiol. **6:**363-374.

Nayak, D. P., R. A. Balogun, H. Yamada, Z. H. Zhou, S. Barman. 2009. Influenza virus morphogenesis and budding. Virus Res. **143:**147-161.

Raiborg, C. and H. Stenmark. 2009. The ESCRT machinery in endosomal sorting of ubiquitinylated membrane proteins. Nature. **458:**445-452.

Shen, Y., and T. E. Shenk. 1995. Viruses and apoptosis. Curr. Opin. Genet. Dev. **5:**105-111.

Shors, T. 2009. Understanding viruses. Sudbury: Jones and Bartlett Publishers. pp. 31-69.

Tan, Y., D. K. B. Bideshi, J. J. Johnson, Y. Bigot, and B. A. Federici. 2009. Proteomic analysis of the *Spodoptera frugiperda ascovirus 1a* virion reveals 21 proteins. J. Gen. Virol. **90:**359-365.

Tan, Y., T. Spears, D. K. Bideshi, J. J. Johnson, R. Hice, Y. Bigot, and B. A. Federici. 2009(b). P64, a novel major virion structural protein potentially involved in condensing the *Spodoptera frugiperda ascovirus 1a* genome. J. Virol. **83:**2708-2714.

Tillman, P. G., Styer, E. I., Hamm, J. J. 2004. Transmission of Ascovirus from *Heliothis virescens* (Lepidoptera: Noctuidae) by three parasitoids and effects of virus on survival of parasitoid *Cardiochiles nigriceps* (Hymenoptera: Braconidae). Environ. Entomol. **33:**633-643.

Tsai J. M., H. C. Wang, J. H. Leu, A. H. Wang, Y. Zhuang, P. J. Walker, G. H. Kou, and C. F. Lo. 2007. Identification of the nucleocapsid, tegument and envelope proteins of the shrimp white spot syndrome virus virion. J. Virol. **80:**3021-3029.

Watanabe, T, E. M. Sorensen, A. Naito, M. Schott, S. Kim, and P. Ahlquist. 2007. Involvement of host cellular multivesicular body functions in hepatitis B virus budding. Proc. Natl. Acad. Sci. U. S. A. **104:**10205-10210.

4.7 Figures and tables

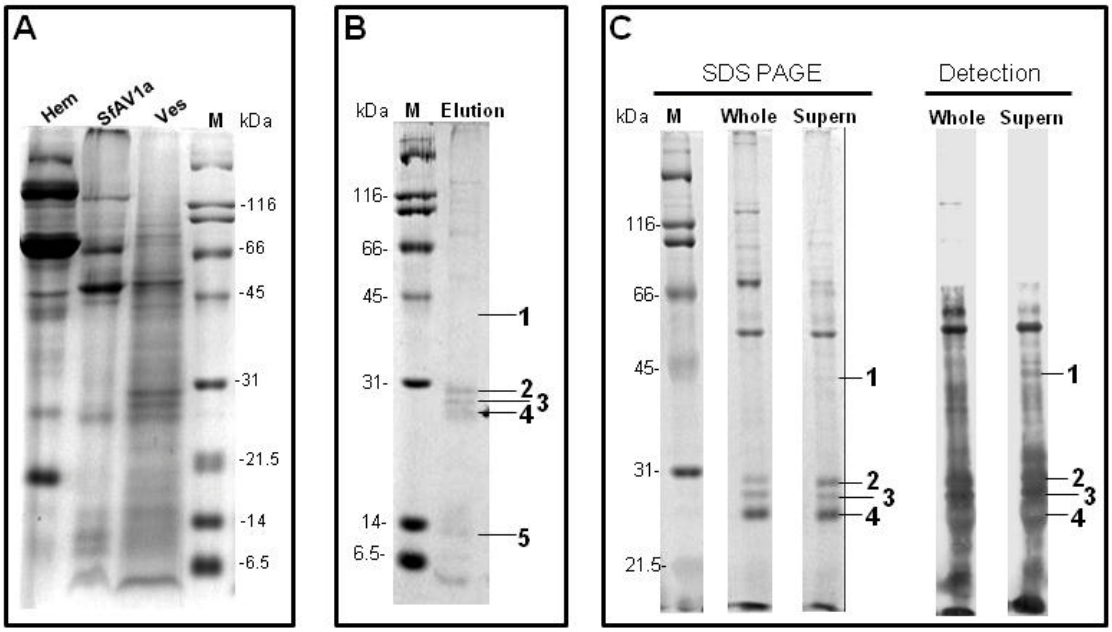

Figure 4.1 Identification of viral vesicle membrane proteins by labeling with biotin. (A) Hemolymph was collected from healthy *Spodoptera exigua* larvae, SfAV1a virions were purified from infected *S. exigua* larvae, and viral vesicles were harvested from *S. exigua* larvae 9 days post infection with SfAV1a. (B) Biotin-labeled vesicles were lysed and applied to a streptavidin bead column to pull down any biotin labeled proteins. Beads were suspended in buffer for SDS PAGE and boiled before loading into gel. (C) Samples were collected at various steps in the procedure for biotin labeling membrane proteins. Those shown here were collected from intact vesicles that had been labeled with biotin (2nd lane) and from supernatant left over after disrupted biotin labeled vesicles were centrifuged at 14,000 rpm for 45 min (3rd lane). The ligand blot procedure was performed against samples described in the second and third lanes of (C) using streptavidin conjugated to alkaline phosphatase. Lines with numbers point to samples of interest submitted for MALDI-TOF analysis.

Table 4.2 Summary of MALDI-TOF analysis of vesicle membrane proteins

Vesicle Membrane Samples	SfAV1a ORFs	*Mass (kDa)*	# Peptide matches	Ion Score	Putative function/domain	Homologs
Sample 1	**60**	***8.6***	**2 matches**	**59**	**•Two TM * helices**	•HvAV071
	55	***35.1***	**1 match**	**61**	**•Unknown**	•HvAV065, TnAV126, CIV254
	41, 64	*50.9, 90.0*	10, 14	636, 573	•MCP, kinase,	
	84	*119.3*	9	52	dynein-like beta chain	
Sample 2	**43**	***26.0***	**9 matches**	**119**	**•One TM helix**	•HvAV057, TnAV149
	33, 38	*27.5, 22.2*	1, 1	158, 41	•Unknown, Unknown,	
	56	*37.6*	2	25	Unknown	
Sample 3	**61**	***25.3***	**2 matches**	**62**	**•Thiol oxidoreductase-like**	•HvAV073, TnAV118, CIV347, TFV094, EHNV016
	109, 64	*22.4, 90.0*	7, 5	376, 123	•Phosphatase, Kinase,	
	123, 36	*28.6, 26.2*	2, 1	30, 28	Unknown, One TM helix,	
	58	*37.0*	1	25	Unknown	
Sample 4	38	*22.2*	8	315	•RNA pol I subunit,	
	8	*98.4*	3	42	Unknown	
Sample 5	**13**	***67.3***	**2 matches**	**50**	**•Carboxyl esterase with TM helix**	•HvAV018
	91	*14.4*	5	106	•Transcription factor	

*TM-transmembrane. ORFs in bold indicate gene products of interest chosen for further study. HvAV, Heliothis virescens ascovirus 3e; TnAV, Trichoplusia ni ascovirus 2c; CIV, Chilo iridescent virus 6; TFV, Tiger frog virus; EHNV, epizootic haematopoietic necrosis virus

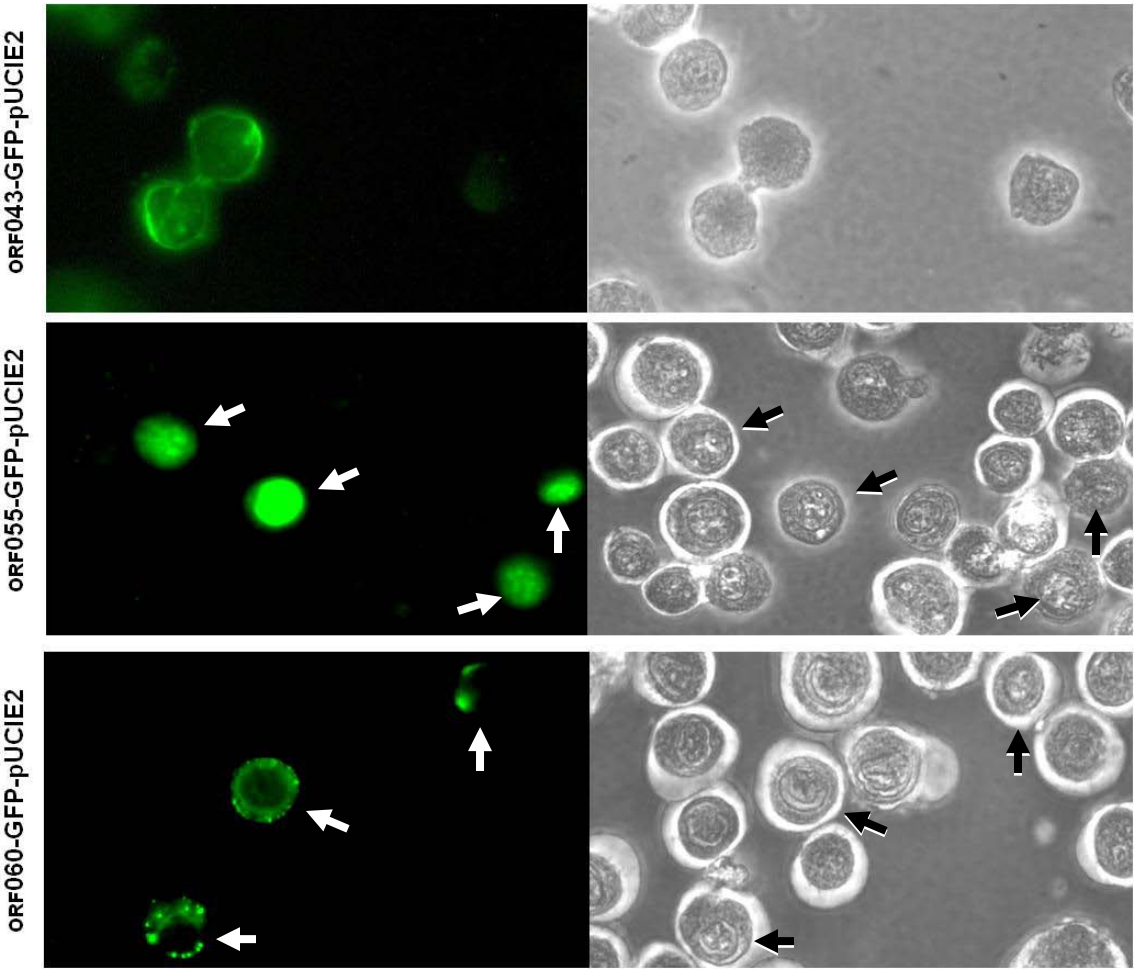

Figure 4.2 Localization of GFP-fusion proteins identified by MALDI-TOF. To determine whether the proteins identified though biotin labeling and detection were membrane bound proteins, genes of interest were fused with GFP at the C-terminus and expressed under an OpIE2 promoter that works well in lepidopteran cell lines. Sf9 cells were transfected with the individual constructs.

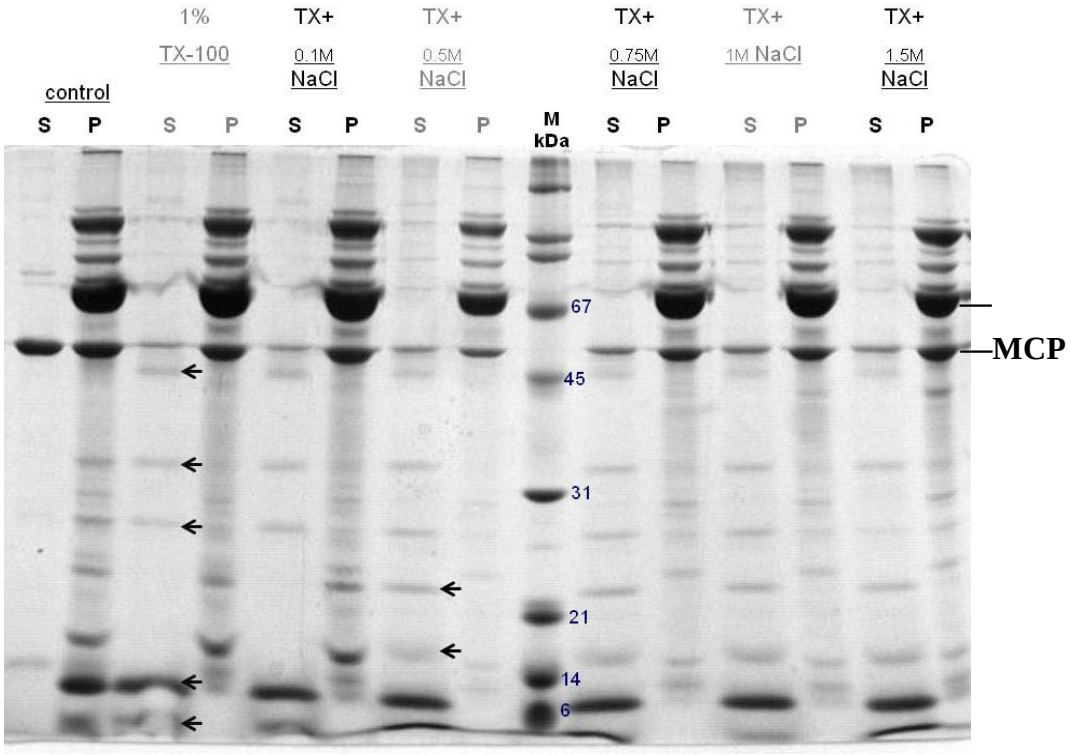

Figure 4.3. Removal of SfAV1a virion structural proteins by treatment of virions with detergent and salt. Separate samples of virus were treated with the indicated amounts of Triton X 100 detergent and NaCl for 45 min after which samples were loaded in 2 ml microfuge tubes on top of 28% sucrose. The first 120 µL from the top was saved as supernatant (S). The remaining sucrose was removed and the pellet (P) was suspended in 50 mM Tris buffer and 2% SDS. The supernatant and pellets were combined with 5x SDS loading buffer and resolved by SDS PAGE. The first column of arrows indicate the first proteins to be displaced from the virion into the supernatant with detergent alone while the second set of arrows indicate the proteins that were displaced upon addition of a high enough concentration of salt. The positions of P64 and major capsid protein (MCP) are indicated.

Table 4.3 SfAV1a structural proteins displaced by detergent/salt treatment

Treatment for SfAV1a virions	Identity of displaced virion structural proteins	Description	Homologs
1% Triton X 100	ORF 36	▪One TM* helix at the C terminus	▪HvAV051, TnAV038
	ORF 54	▪Myristylated membrane protein	▪TnAV129, CIV337, EHNV001
	ORF 109/61	▪CTD phosphatase with transcription factor/ Thiol oxidoreductase-like protein	▪HvAV108, TnAV093, CIV355/ HvAV073, TnAV118, CIV347, EHNV016
	ORF 43	▪One TM helix at the C-terminus	▪HvAV057, TnAV149
	ORF 60	▪Two TM helices in the middle and C terminus	▪HvAV071
1% Triton X 100 and 0.5 M NaCl	ORF 2	▪Cytochrome oxidase assembly factor- one TM helix at C terminus	▪HvAV003
	ORF 91	▪Yabby-like transcription factor	▪HvAV128, TnAV059, CIV401

**TM-transmembrane*

HvAV, Heliothis virescens ascovirus 3e; TnAV, Trichoplusia ni ascovirus 2c; CIV, Chilo iridescent virus 6; EHNV, epizootic haematopoietic necrosis virus

Figure 4.4. Structural proteins in the virion core that may bind P64 as revealed by ligand blotting. Virion proteins were resolved by SDS PAGE then blotted onto nitrocellulose membranes (or PVDF membrane for the rP64 ligand in 0.5% Tween). Biotin-labeled rP64 (A), rN-terminal (B), or rC-terminal (C) was incubated with the blots under varying stringencies (0.05% or 0.5% Tween). M indicates the prestained marker that appeared blue on the blots. The color of the prestained marker was different from that produced by the chromogenic substrate in the detection step and does not indicate that biotin labeled protein bound. M_2, a non stained broad range protein marker; 1-SfAV1a; 2-CIV6; 3-TnAV2c; 4-HvAV2c; 5-SeAV; 6-AIV

Figure 4.4

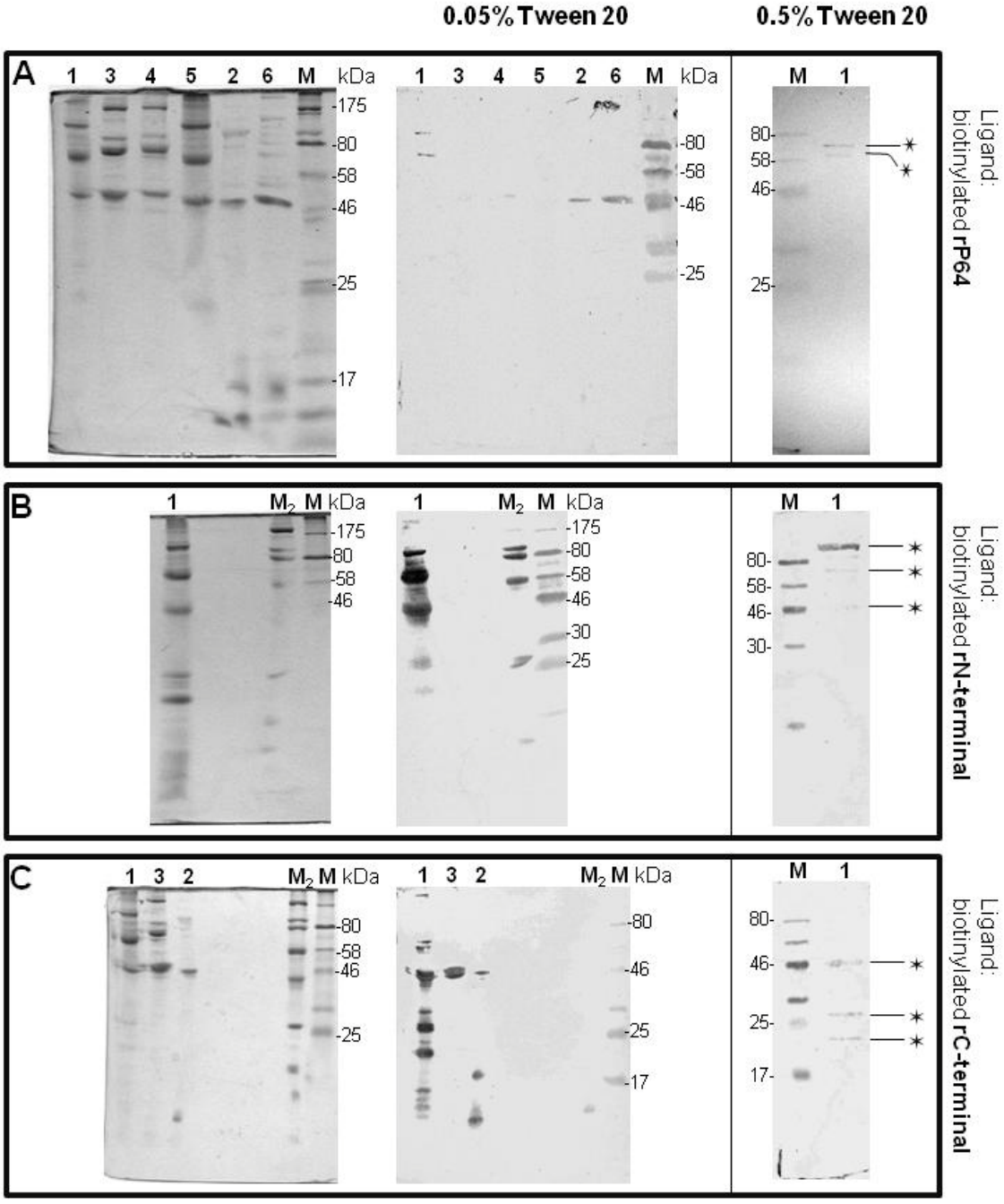
0.05% Tween 20
0.5% Tween 20
A
1 3 4 5 2 6 M kDa
175
80
58
46
25
17
1 3 4 5 2 6 M kDa
80
58
46
25
M 1
80
58
46
25
Ligand: biotinylated rP64
B
1 M2 M kDa
175
80
58
46
1 M2 M kDa
175
80
58
46
30
25
M 1
80
58
46
30
Ligand: biotinylated rN-terminal
C
1 3 2 M2 M kDa
80
58
46
25
1 3 2 M2 M kDa
80
46
25
17
M 1
80
46
25
17
Ligand: biotinylated rC-terminal

Table 4.4 Ligand binding indicates SfAV1a structural proteins in the core

Recombinant Protein	Possible binding partners based on ligand blot	Corresponds to proteins that leave virus particle with Triton X 100/NaCl treatment	Homologs in iridoviruses
rP64	ORF46-47	No	-/-
	ORF27/ORF 64	No	-/CIV209R
	ORF48 (P64)/ORF15	No	CIV232R, EHNV89L/-
	ORF41 (MCP)	No	FV3-90R, LCDVic043, MIV14
rN-term	ORF46-47	No	See above
	ORF27/ORF64	No	See above
	ORF41 (MCP)	No	See above
rC-term	ORF41 (MCP)	No	See above
	ORF54	Yes	CIV337L, FV3-2L, SGIV19
	ORF109/ORF61	Yes	CIV355L, SGIV61R/CIV337L, SGIV70R

CIV- *Chilo* iridescent virus 6, EHNV- epizootic haematopoietic necrosis virus, FV3- Frog virus 3, LCDVic- lymphocystis disease virus isolate China, SGIV- Singapore grouper iridovirus

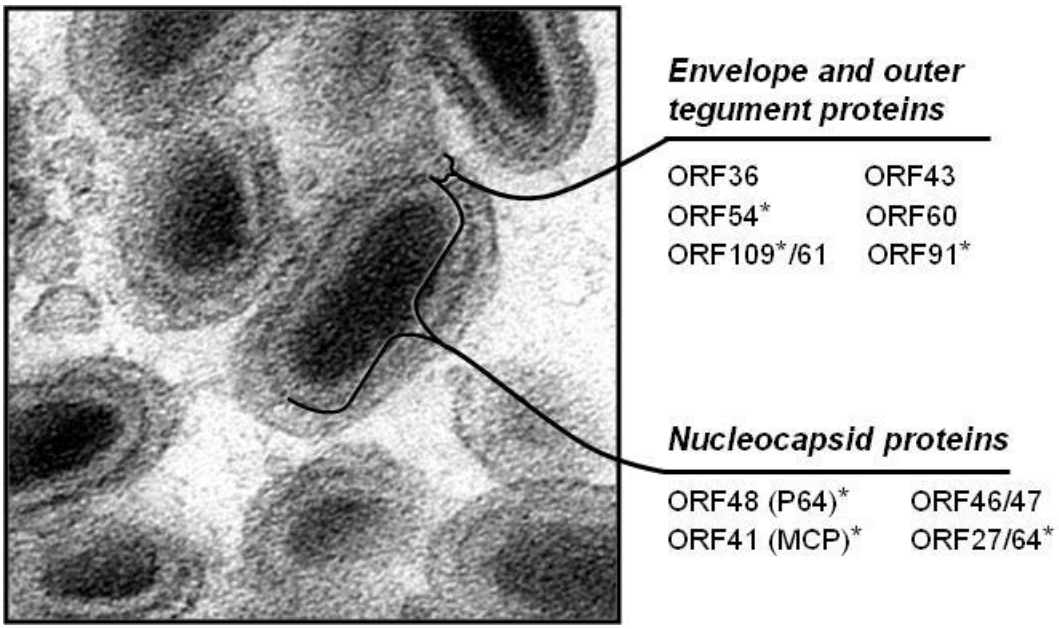

Figure 4.5 Assignment of SfAV1a virion structural proteins to substructures within the virion. The proteins susceptible to removal by detergent and salt treatments were assigned to the outer envelope and the space just underneath that envelope. Those proteins that remained with the virus particle after detergent/salt treatment and appeared to interact with the rP64 and rN-terminal ligands were assigned to the capsid and nucleoprotein layers in the interior of the virion. The major capsid protein (MCP) may be a significant component of the electron dense layer just underneath the outer envelope and tegument space. Studies here support the immunoelectron microscopy work done previously (Tan et al. 2009b) showing P64 localization to the electron dense core of the virion. Asterisks indicate that homologs of these ORFs were found in *Chilo* iridescent virus virions according to Ince *et al.*, 2010.

CHAPTER 5

Summary and Conclusions

5.1 Introduction

Ascoviruses (AVs) are members of the diverse group of large nuclear and cytoplasmic DNA viruses (LNCDV). LNCDVs typically have large dsDNA genomes and can start replication in the nucleus and complete it in the cytoplasm or simply remain in the cytoplasm throughout viral replication. Genomic comparisons have shown that the six viral families (*Poxviridae*, *Mimiviridae*, *Asfaviridae*, *Iridoviridae*, *Ascoviridae*, and *Phycodnaviridae*) that compose this group originated from an icosahedral LNCDV ancestor that encoded over 40 genes that function in DNA and RNA metabolism, DNA packaging, and virion structure (Iyer et al., 2006). Many of the current LNCDVs have well over 100 ORFs and are extremely diverse in gene composition, host range, transmission, and pathology. Genes these viruses do not share in common were likely acquired from the specific hosts in which they replicate and likely facilitate their replication in these hosts (Filée, *et al.*, 2008). In the case of ascoviruses (AVs), the genes that make them a separate family of viruses probably originated from insects, specifically the lepidopteran hosts in which they replicate. Many of the ORFs identified in AV's have no known function or are homologs of iridovirus (family *Iridoviridae*) genes that have no known function. In general, many genes from LNCDV members have no recognizable domain or function. This lack of detail points to the need for molecular analyses (RNAi, qPCR) and bioinformatic studies of specific viral genes and the sequencing and

annotation of lepidopteran genomes, which would help clarify whether AVs acquired significant genetic material from their hosts. What is clear is that AV specific genes drive a unique process of vesicle formation for the purposes virion assembly and transmission to the next host via the ovipositor of endoparasitic wasps.

In my dissertation, I used the ascovirus type species, the *Spodoptera frugiperda ascovirus* 1a (SfAV1a), to address four objectives aimed at identifying ascovirus structural proteins and their role in ascovirus biology, with specific emphasis on how these proteins were involved in packaging the ascovirus genome into the virion, and their relatedness to proteins in other LNCDV viruses, especially iridoviruses. Objectives 1 and 2 addressed, respectively, the localization and function during replication of a major virion structural protein, P64. The results of these studies are reported in Chapter 2. Part of Objective 2 was also addressed in Chapter 3 but went further in the latter chapter to explore the functional domains of P4 and their interaction with DNA. Results for Objective 3—the identification of P64 homologs or other DNA binding proteins in AVs and iridoviruses—were addressed in Chapter 3. Objective 4 involved assigning SfAV1a virion structural proteins to specific substructures within the virion and have been addressed in Chapter 4. The data gathered here contribute new information and provides a basis for better understanding the proteins important for AV assembly. Below I summarize the specific results of my research obtained through pursuit of the above objectives.

5.2 Summary of results for Objective 1 and Objective 2

To address Objective 1 (in Chapter 2), I used immunoelectron microscopy to show how the virion structural protein P64 progressively localized from the region of viral DNA replication, to electron dense bodies, then on to pre- and post-enveloped viral cores during SfAV1a virogenesis. This along with P64's basic character and its ability to bind DNA (Southwestern blots) led to the hypothesis that P64 was responsible for packaging the dsDNA genome into SfAV1a virions. Evidence was needed to show that P64 could condense rather than simply bind DNA. Using transmission electron microscopy as reported in Chapter 3, I demonstrated that P64 changed the conformation of DNA from a linear to a globular form. I showed that P64 caused DNA to aggregate, and more specifically that each of its domains aggregated DNA separately. The first domain, the N-terminal half of P64, is comprised of four 2-cysteine adaptors, motifs specific to ascoviruses, iridoviruses, and phycodnaviruses. The second domain, the C-terminal half of the molecule, includes 14 basic tandem repeats of 13 amino acids, with the whole repetitive stretch being rich in arginine and serine. The many serines in the basic repetitive region also happened to be in sites recognizable by the serine/threonine kinase PKC. I demonstrated that P64 was phosphorylated when expressed using the Bac-to-Bac expression system, but was unphosphorylated in mature virions. The phosphorylation status of P64 could provide the means for modulating P64-DNA association for DNA release at initial infection and packaging during virogenesis.

5.3 Summary of results for Objective 3

Data for Objective 3 (in Chapter 3) was obtained through Southwestern and Western blot analyses. I showed that among AVs, only P64 homologs bound DNA. No small DNA binding proteins typical of other viruses and eukaryotes identified using these methods or bioinformatic analyses. Through these methods I also showed one way by which AVs diverged from the family *Iridoviridae*: AVs use one protein for DNA binding and packaging whereas iridoviruses use at least two proteins. Examination of two species of iridoviruses showed large and small DNA binding proteins: the large proteins are likely homologs of P64 and the functions of the small one(s) are as yet unknown. Proteins containing the virus-specific 2-cysteine adaptor, like those found in P64, have also been identified as virion structural proteins in the *Chilo* iridescent virus, Singapore grouper iridovirus, and a megalocytivirus, all members of the family *Iridoviridae* (Dong *et al.*, 2010; Ince *et al.*, 2010; Song *et al.*, 2006). These results suggest that P64 and its homologs in AVs and iridoviruses containing both the virus-specific 2-cysteine adaptor motif and the basic repetitive motifs together represent a novel family of DNA packaging proteins.

5.4 Summary of results for Objective 4

Objective 4 dealt with SfAV1a infection-associated membranes, specifically the viral proteins embedded in those membranes. Two types of membranes were analyzed: the delimiting membrane of virion-filled vesicles and the outer envelope of SfAV1a virions. Membranes obtained from virion-containing vesicles (also referred to as viral vesicles) were analyzed by MALDI-TOF for the presence of SfAV1a encoded proteins to

understand how the virus modified cellular membranes for vesicle formation. With GFP-fusion constructs, I confirmed one SfAV1a protein, ORF43, was a component of viral vesicles, as it initially was detected in cell's plasma membrane. Additional GFP-fusion constructs need to be analyzed for cellular localization of other SfAV1a proteins identified in vesicle membrane samples. Detergent/salt treatments of SfAV1a purified virions were helpful in removing the virion envelope and associated proteins. The SDS-PAGE profile of displaced proteins and remaining virus particles were compared to the intact virion profile. In these experiments, proteins displaced by detergent/salt treatments were identified by matching their migration in SDS-PA gels to that of virion structural proteins identified previously (Tan *et al.*, 2009). Envelope associated proteins included ORF36, ORF54, ORF109/61, ORF43, ORF60, ORF2, and ORF91. Most of the proteins ascribed to the virion envelope did not appear to associate with the P64 ligand (ligand blotting method), as expected. P64 is considered part of the electron dense nucleoprotein core and therefore would not associate with the proteins in the outer layer(s). Virion proteins that did bind to the P64 ligand were considered nucleocapsid proteins: ORF46-47, ORF27/64, ORF48 (P64), and ORF41 (major capsid protein). In this way I was able to deconstruct the different substructures of the SfAV1a virion. Importantly, from an evolutionary perspective, half of the SfAV1a virion structural proteins identified have homologs in species of the family *Iridoviridae*. Understanding the role and location of virion structural proteins in one family could shed light on those of the other, as information remains lacking on gene/protein functions for both families of viruses. Ten SfAV1a structural proteins are shared among AVs and certain species belonging to the

Iridoviridae, yet their morphologies are completely different - AVs are bacilliform and iridoviruses are icosahedral. The differences in the protein composition may explain how AV virions evolved a different shape from the icosahedral symmetry of iridoviruses. For example a phycodnavirus (the evolutionary ancestor of asfarviruses, iridoviruses, and ascoviruses) structural protein Vp260 (ORFA122R) has homologs in iridoviruses but not AVs (Bigot *et al.*, 2009). There is also an example of a protein found in ascoviruses (homologs of SfAV1a ORF38), but which is absent from the other viral families (Bigot *et al.*, 2009). It remains to be determined whether the gain or loss of the above mentioned proteins contributes to virion morphology.

5.5 Potential future studies

The above studies provided important information about P64 and its homologs. Further investigations could advance our understanding of P64's ability to package DNA into virions. Future analysis of P64 and its domains could include studies with single-stranded DNA and RNA and double stranded RNA to see how well they can associate with the various nucleotides. Furthermore, my preliminary analysis of the effects of pH 4, 7, and 11 and the presence or absence of zinc and magnesium ions on P64 showed that it was able to maintain its association with DNA under all these conditions to varying degrees (not shown). These studies would have to be repeated and quantified, but they suggest that P64 could provide alternative peptide sequences that could be used for studying stable gene delivery to cells. Further studies of P64 could also include mutation analyses-substituting serines for alanines-to see how the lack of phosphorylation sites affects P64-DNA interaction. Since P64 is a virion structural protein, it is probably a late-

expressed gene. Expression analyses distinguishing AV early, intermediate, and late gene expressions have not been done. Quantitative-PCR studies over time and analysis of the P64 promoter region could aid our understanding of what other genes are expressed late in SfAV1a infection and help distinguish late genes from early and intermediate gene expression. This would significantly advance our understanding of AV pathobiology and the role of various genes.

It would also be interesting to see what roles the novel lipid-metabolizing genes encoded by SfAV1a play in cell membrane enlargement, cellular division into vesicles, and virion envelopment. Emphasis should be placed on those lipid-metabolizing genes that are common to all the ascoviruses because all AVs induce the formation of virion-filled vesicles. The quantitative-PCR analysis for early, intermediate, and late genes, mentioned above would be ideal studies from which to begin understanding those common genes and how those genes and others help AVs occupy their specific niche. The data presented here sheds light on how AV genomes are condensed and packaged into virions by the novel P64 protein and what proteins are associated with the core versus the outer envelope. These data provides the basis for understanding which virion associated proteins are used for cell entry by the virus and which of those participate in the initial disruption of lepidopteran cell biology in novel and traditional ways.

5.6 References

Bigot, Y., S. Renault, J. Nicolas, C. Moundras, M. V. Demattei, S. Samain, D. K. Bideshi, and B. A. Federici. 2009. Symbiotic virus at the evolutionary intersection of three types of large DNA viruses; iridoviruses, ascoviruses, and ichnoviruses. PLoS One. **4:**e6397.

Dong, C., S. Weng, Y. Luo, M. Huang, H. Ai, Z. Yin, and J. He. 2010. A new marine megalocytivirus from spotted knifejaw, *Oplegnathus punctatus*, and its pathogenicity to freshwater mandarinfish, *Siniperca chautsi*. Virus Res. **147:**98-106.

Filée, J., N. Pouget, and M. Chandler. 2008. Phylogenetic evidence for extensive lateral acquisition of cellular genes by Nucleocytoplasmic large DNA viruses. BMC Evol. Biol. **8:**320-331.

Ince, I. A., S. A. Boeren, M. M. van Oers, J. J. M. Vervoot, and J. M. Vlak. 2010. Proteomic analysis of Chilo iridescent virus. Virology. In press.

Iyer, L., S. Balaji, E. V. Koonin, and L. Aravind. 2006. Evolutionary genomics of nucleo-cytoplasmic large DNA viruses. Vir. Res. **117:**156-184.

Song, W. J., Q. Lin, S. B. Joshi, T. K. Lim, and C. L. Hew. 2006. Proteomic studies of the Singapore grouper iridovirus. Mol. Cell. Proteomics. **5:**256-264.

Tan, Y., D. K. B. Bideshi, J. J. Johnson, Y. Bigot, and B. A. Federici. 2009. Proteomic analysis of the *Spodoptera frugiperda ascovirus 1a* virion reveals 21 proteins. J. Gen. Virol. **90:**359-365.